METALS AND THE CONFORMATION OF FIBRIN

By

Dhesigen P Naidoo B.Sc.(Hons) (UDW)

Thesis submitted for the Degree

Master of Science (Medicine)

University of Cape Town

February 1992

Kaalangh chendra thirumathie Panjalai avargalin nennavuk-kaga

Dedicated to Sam and Saga Sommayya.

ACKNOWLEDGEMENTS

This study was carried out in the Department of Chemical Pathology, Red Cross Children's Hospital, University of Cape Town and Provincial Administration of the Cape Province. Funding for this work was provided by the MRC and UCT research funds. I thank my supervisor, Dr Langley R Purves, for the opportunity to study for this degree and for the many invaluable discussions. I also thank my colleagues, Dave Ross, Fahri Hassan, George Fisher and Sue Lindsey for encouragement and support, and especially Tim Egan, whose guidance has proved invaluable in the completion of this work. I am grateful to Lesmaine De Vries for her generous assistance in preparing the manuscript. I also thank George Lindsey for the use of the fluorescence spectrophotometer and useful discussion. For amazing patience and endurance thank you Rucksana.

Parts of this work have been submitted for publication

i) Zinc binding by fibrin facilitates proteolysis by a snake (Puffadder) venom protease.
Accepted by Thrombosis & Haemostasis

ii) Fibrin-D-dimer as a zinc potentiated substrate for a puffadder venom protease.
Submitted to Biochemistry.

I, DHESIGEN P. NAIDOO, hereby declare that the work on which this thesis is based is my original work (except where acknowledgements indicate otherwise) and that neither the whole work nor any part of it has been, is being, or is to be submitted for another degree in this or any other University.

I empower the University to reproduce for the purpose of research either the whole or any portion of the contents in any manner whatsoever.

Signed by candidate

SIGNATURE

18/02/1992

DATE

TABLE OF CONTENTS

TABLE OF FIGURES

ABSTRACT

The carboxy terminal of the γ–chain of human fibrinogen contains at least three biologically important functional domains:

(i) the fibrinogen γ-chain polymerisation centre,

(ii) the platelet receptor domain and

(iii) the site for staphyloccocal clumping.

The nature of the site specificity of these interactions necessitates the existence of a preferred conformation for this region, the nature of which has yet to be clearly established.

A novel zinc metalloproteinase isolated from puff adder venom (PAV protease) capable of specifically cleaving the di-γ-chain of transglutaminase (Factor XIIIa) catalysed crosslinked plasmin derived D-dimer into apparently symmetrical monomers has been described. The activity is fibrin specific and displays an unusual site specificity for the γ-carboxy terminal domains within the crosslink region. The activity was reported to be potentiated by zinc.

The effect of zinc on the digestion of D-dimer by PAV protease was evaluated by SDS-PAGE and by a fluorimetric technique utilising a fluorescent dansylcadaverine conjugate of the substrate (f-D-dimer). A differential zinc binding study determined that the potentiation of activity by zinc was due to a zinc-substrate rather than a zinc-enzyme interaction. The binding constant for zinc to D-dimer was determined by Scatchard analysis of zinc titration data. The interaction of zinc and f-D-dimer was confirmed by fluorescence anisotropy determinations. The nature of the coordination capsule around the metal cation was determined by examining a cobalt-fibrin-D-dimer complex and characterising the difference visible absorption spectrum thereof. The donor ligands from the D-dimer fragment for the

metal ion were determined as histidines by examining zinc(II) and cobalt(II) binding to diethylpyrocarbonate modified fibrin-D-dimer and hydroxylamine treated DEPC-fibrin-D-dimer.

Through this study it has been established that the PAV protease cleavage of the di-γ-chain of the plasmin derived D-dimer fragment is potentiated by zinc(II) ions through the formation of a novel zinc determined conformation of fibrin-D-dimer. This presents the possibility of a fibrin-specific neo-epitope being manifested in the presence of zinc ions that could provide a means to determine fibrin degradation products more specifically.

A model for the neo-epitope has been proposed.

1. INTRODUCTION

The interaction of metal ions with proteins is an interesting consideration when contemplating the biology of evolution. The cooperative interaction of metal and protein results in a change in the conformation or the electrical state of the protein. These modifications in turn confer on the protein more efficient catalytic properties as an enzyme or result in a potentiation of the substrate. This thesis discusses the role of zinc(II) in the digestion of a plasmin derived fragment of polymerised fibrinogen by a snake venom protease. To this end the following points are discussed in the Introduction:

1.1 Zinc protein interactions.

1.2 Structure of fibrinogen

1.3 The polymerisation of fibrinogen and fibrino(geno)lysis

1.4 Fibrinogen and fibrin interactions

1.5 Assaying the degradation products of fibrinogen and fibrin

1.6 Snake venom enzymes and fibrinogen

The introductory discussion of each category now follows -

1.1. Zinc-Protein Interactions

Zinc has been known as a biologically important metal for a long time. Adult human beings contain approximately 2g of zinc, most of which is bound to zinc enzymes and zinc proteins, and the free zinc concentration in plasma is low (Prince, 1979). The other two metals that share group IIB with zinc, ie. cadmium and mercury, have no known biological role and are among the most toxic of metals. What is it then about zinc chemistry that affords the metal its outstanding biological significance ?

Zinc has the electron configuration [Ar] $3d^{10}4S^2$ and therefore has a highly stable divalent state, [Ar] $3d^{10}$, due to the completely filled outermost (d) shell compared with the higher oxidation states. This is important in a biological medium that has a dynamic oxidative potential in continual flux.

Zinc is relatively inert with respect to oxidoreduction susceptibility that is characteristic of the other transition elements. Oxidoreduction is a major factor in changes in coordination geometry and in determining rates of ligand substitution. Zinc(II) tends to favour a tetrahedral geometry when bound to organic ligands, however, the coordination spheres of zinc complexes exhibit flexibility and stereochemical adaptability. Vallee and Auld (1990a) conclude that the multiplicity of geometry and coördination numbers denote that zinc readily submits to the demands of its ligands and these properties provide a mechanism for the translation of chemical structure into biological functions.

Zinc, through coordination to biological molecules, may have a structural or catalytic role and even exhibit both functions. The zinc structures in biological systems may be broadly divided into three groups:

1.1.1 The 'zinc fingers' - a conserved class of eukaryotic nucleic binding proteins involved in the regulation of gene expression and specification of cell fate (Klug & Rhodes, 1987, Berg, 1986a,b);

1.2.1 The zinc enzymes and

1.3.1 The zinc proteins.

1.1.1 The 'Zinc-fingers'

The last decade has seen an entirely new group of zinc proteins attracting a great deal of interest in the literature. An important part of gene expression and regulation is the binding of a regulatory protein to the recognition sequence of an appropriate gene. Such proteins would need to be structurally suited for binding to the DNA helix and therefore would have to contain a domain or motif to serve for such binding. Several bacterial proteins (regulatory) possess helix-turn-helix motifs, as observed in their crystal structures, for this purpose (Klug & Rhodes, 1987). Eukaryotic systems solve this problem via the formation of 'zinc fingers' which provide the structural motif for binding to the DNA helix. The 'zinc fingers' are in fact peptide loops with a single zinc atom coordinated to two cystine and two histidine residues at the base forming a finger (Berg, 1986b).

It has been suggested that since the redox state intracellularly does not favour cysteine disulphide bridges an alternative mechanism to stabilise peptide loop structures requires zinc coordination .

There are two types of 'zinc fingers' corresponding to two models of interaction with the DNA helix (Fairall, 1986; Berg, 1988).

The first model has the regulatory protein with its 'zinc fingers' following the helical path of the major groove with consecutive 'zinc fingers' equivalently orientated with respect to the DNA double stranded helix and so each repeat is one finger as is illustrated in Transcription factors IIIA and Spl (Fairall, 1986, Berg, 1988, Kuwahara, 1990, Frankel, 1987).

In the second model, the regulatory nucleic acid binding protein lies

on one face of the double helix, alternate 'fingers' make non-equivalent DNA contacts in accordance with a two finger repeat. Some illustrative examples are the 'zinc finger' motifs in human male-associated protein ZFY (Weis et al, 1990), the Kruppel-related sequence in Xenopus laevis (Nietfield et al, 1989) and the human DNA-binding nucleocaspid protein that recognises the HIV-I enhanced sequence (South et al 1990). The latter finding may have dynamic implications in the long road to the development of vaccines for the prevention of AIDS.

1.1.2 The Zinc Enzymes

The first metalloenzyme to be discovered (1940) was carbonic anhydrase (EC 4.2.1.1) which catalyses the reaction

$$CO_2 + H_2O \rightleftharpoons HCO_3^- + H^+$$

to complete the transfer of carbon dioxide from the tissues into the blood and finally into the alveolor air. The enzyme catalyses the reaction 10^6-fold. The zinc cation in carbonic anhydrase is contained in a deep protein pocket which also contains water molecules arranged in an ice like order. Zinc is coordinated to three imidazole ε nitrogens and an 'activated' H_2O molecule (Vallee & Auld, 1990b). It seems possible that the coordinated H_2O molecule converts zinc to zincate $Zn(OH)^+$, the zinc ion donates a hydroxide ligand to carbon dioxide, which is attracted to the hydrophobic cavity on the enzyme. The nucleophilic hydroxide interacts with the carbon dioxide to form the bicarbonate ion. This is equivalent to replacing the 10^6 slower uncatalysed reaction.

$$H_2O + CO_2 \rightleftharpoons HCO_3$$

Only the forward reaction is favoured at high pHs. The enzyme with its zinc plays a Lewis base role allows the conversion to occur at physiological pH (Fisher, 1975).

The other traditionally cited zinc enzyme is carboxypeptidase A (EC 3.4.17.1), a digestive protease that hydrolyses the carboxyterminal peptide bond in polypeptide chains. The enzyme coordinates zinc through the imidazole rings of two histidines, the side chain of one glutamic acid and one 'activated' water molecule (Blow & Steitz, 1970). The enzyme's zinc together with other groups at the active site induce rearrangements in the electronic distribution of the substrate, thereby rendering it more susceptible to hydrolysis.

Vallee and Auld (1990a) on examination of the sequences of twelve zinc enzymes whose crystal structures are known deduce that catalytic zinc cations coordinate with the enzyme through three amino acids, cysteine, histidine or glutamic acid, and one 'activated' water molecule. The structural zinc atoms seem to coordinate almost exclusively to cysteine residues through the sulphur atoms. An example is the class I enzyme alcohol dehydrogenase (EC 1.1.1.1) whose structural zinc atom is tetrahedrally bound to the four sulphur atoms of C-97, C-100, C-103 and C-111. The functional or active-site zinc has to co-operate with the coenzyme NADH. This catalytic zinc is coordinated to two cysteine residues, one histidine and one water molecule (Eklund & Branden, 1983).

Aspartate transcarbamyolase, a class II enzyme (EC 2.1.3.2) possesses a single structural zinc coordinated to C-109, C-114, C-137 and C-140 in a tetrahedral fashion where the zinc holds together two loops formed in this region of the polypeptide chain which forms part

of the interface between the regulatory and catalytic subunits, the zinc stabilisation of the loops is thought to be responsible for stabilising the quaternary structure. There exists a strong likelihood that the zinc induced local conformational and structural change lends itself to the fine tuning of its interaction with the catalytic subunit due to the entropic contribution to the energy of activation of zinc binding at such sites (Keating, 1985). Recent work on the enzyme has focussed on an examination of Zinc(II) interactions with ATCase and with the isolated regulatory subunits of ATCase with a view to gaining information on the structural roles of zinc in the intact enzyme and in the assembly of the enzyme (Jefferson et al, 1990).

The class III hydrolases consist of the metallo exo- and endo-peptidases. A notable example of a metalloendopeptidase, thermolysin (EC 3.4.24.4) contains one catalytic zinc liganded to H-142, H-146 and E-166 and a distorted tetrahedron is completed by a water molecule, in addition to several structural calcium atoms (Monzingo & Matthews, 1982). A representative example of a class IV enzyme that coordinates zinc is 5-aminolevulinate dehydratase (Dent et al, 1990).

1.1.3 The Zinc Proteins

Zinc is also structurally bound to a variety of non-enzyme proteins. The most abundant zinc protein in plasma is albumin (Failla et al, 1982, Parisi & Vallee, 1970). Albumin binds zinc(II) with a dissociation constant of pK = 6.98, binding sites n = 1 (Marx, 1988). The iron transport protein transferrin can transport zinc in the absence of iron. The equilibrium constants for zinc(II) binding to the

two available binding sites have been determined at $pK_1 = 7.8$ and $pK_2 = 6.4$, K_1 corresponds to zinc binding the C-terminal site and K_2 for the
N-terminal site at pH 7.4. These results indicate that at serum bicarbonate concentrations, transferrin should have a higher affinity for zinc(II) than serum albumin indicating a possible role in zinc transport (Harris, 1983).

Zinc has been shown to play an interesting structural role in the oligomerisation of human growth hormone (hGH) to hGH dimers. The dimer binds two zinc atoms per dimer molecule in a cooperative fashion with each zinc liganding in a tetrahedral configuration to H-18, H-21 and E-174 bridging two hGH molecules into a more stable hGH dimer which has been proposed as the major storage form of the protein (Cunningham et al, 1991a, b, c).

1.1.4 Zinc and Fibrinogen and Fibrin

Marx (1988) studied the non-specific binding of zinc to fibrinogen and the zinc content of 'collapsed' fibrin gel supernatant by means of ultrafiltration and atomic absorption techniques. Essentially, the linear polymerisation of fibrin monomers into protofibrils is not a cation sensitive process, however, calcium(II) and zinc(II) independently of each other are both capable of inducing the formation of gel by augmenting the lateral association of the protofibrils. The gelation is modulated by physiologic levels of calcium(II) and zinc(II). Marx calculated that zinc binds to fibrinogen with dissociation constant $K_D = 18\mu M \pm 3\mu M$ and $n = 6$. It is also important to note that zinc(II) does not compete with calcium (II) for binding to fibrin.

Scully & Kakkar (1982) reported the adsorption of fibrinogen to zinc chelate colums at pH 7.8. The fibrinogen eluted sharply with a pK_a of 5.8. Although the binding was (highly) non-specific, the pK_a of 5.8 implies the involvement of histidine residues.

1.1.5 Zinc as a Micronutrient

Zinc was first shown to be an essential trace element in living systems as early as 1869, when Ranlin showed the trace element as a basic nutrient for Apergillus niger. Zinc distribution in biological fluids and tissues has been studied in detail by various groups (Fisher, 1975). The total zinc concentration in human beings is approximately 2.0g/70kg (Underwood, 1971). This is about half that of iron and 10-15 times that of copper. Zinc is not distributed uniformly in the body. Those tissues with high zinc concentrations include the prostrate, skin and appendages, choroid, liver, pancreas, bone and blood. Zinc is found in high concentrations in keratins with 20% of the total body zinc in the skin (Fisher, 1975, Underwood, 1971).

Zinc in human blood is distributed 75-88% in erythrocytes, 12-22% in plasma and 3% in leukocytes. The normal plasma content of zinc in healthy individuals is within the range 10.7-16.9 μM (Failla et al, 1982). Serum zinc is higher than plasma levels by about 16%. This is due primarily to the platelet disintegration during clotting and the greater dilution in plasma. Hemolysis contributes 4% to the serum-plasma difference. Plasma zinc is bound approximately one third to albumin and 35% to α-macroglobulin (Parisi & Vallee, 1970). Research in the last decade has implicated serum transferrin as a possible major zinc transporter as well (Harris, 1983, Chesters & Wile, 1981).

1.2. Structure of Fibrinogen

Fibrinogen crystallisation has proved to be difficult enough to the extent of there being no X-ray structure available at this time. In the absence of such data, a low resolution model for the structure of fibrinogen has had to be postulated from electron microscopy and chemical studies. The fibrinogen molecule, M_r 340 000 is dimeric, each monomer consisting of three non-identical but genetically-related polypeptide chains designated Aα, Bβ and γ. The molecule is arranged in a trinodular structure (Hall & Slayter, 1959, Doolittle, 1975, Doolittle, 1984). The central region, the E domain - also called the N-terminal disulphide knot (NDSK) - is dimeric containing the amino terminals of all six constituent chains. The two sets of chains extend away from the E domain to end in two carboxyterminal domains designated the D-domains, thus the trinodular structure (Fig.1). The three chains form three-stranded ropes arranged in coiled coils between the D-domains and the central E-domain and are joined together by a series of disulphide linkages (Hoeprich and Doolittle, 1983) (Fig.2). In the N-terminal disulphide knot, the two halves of the molecule are linked by three disulphide bonds, one between the two α-chains (residue α-28) and two between the γ-chains (residues γ-8 & 9) (Hoeprich & Doolittle, 1983). The human fibrinogen molecule has 29 disulphide bonds of which 11 are found in the central domain (Hoeprich & Doolittle, 1983, Doolittle, 1984)

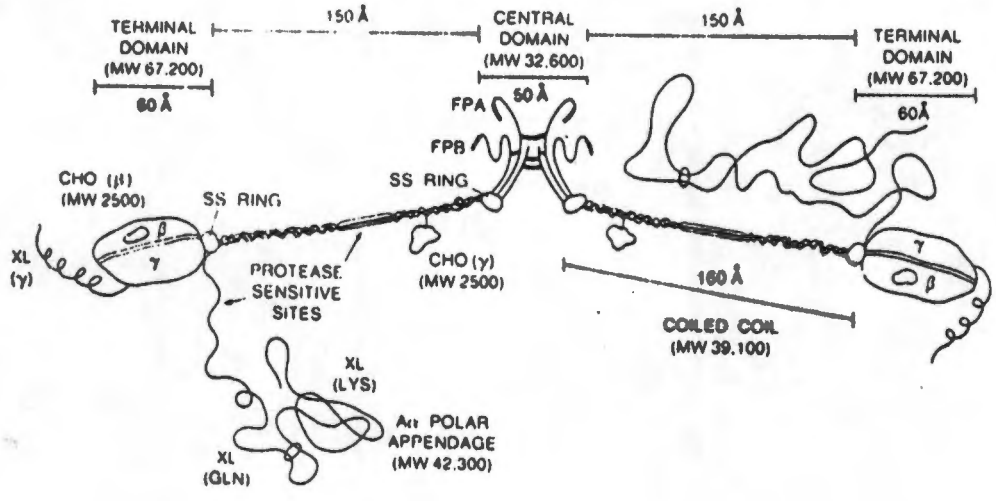

Figure 1: Schematic drawing of fibrinogen. The central region is the N-terminal disulphide knot (NDSK). This is joined to the two distal D-domains by connecting coiled coils. The fibrinopeptides FPA and FPB are shown. (Doolittle, 1984)

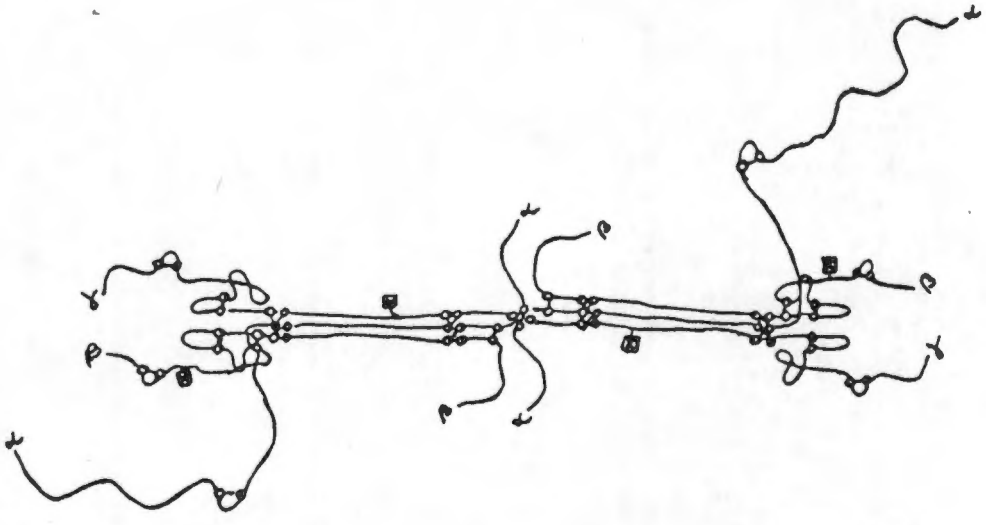

Figure 2: The schematic depiction of the 29 disulphide bonds in human fibrinogen of which 11 are found in the central domain. (Doolittle, 1984).

Fibrinogen is a glycoprotein with the carbohydrate moieties located on the Bβ- and γ-chains while the Aα-chains do not contain carbohydrate (Gaffney, 1972, Pepper et al, 1974). An examination of the synthesis of fibrinogen reveals that the α-chain receives its core carbohydrate early as a cotranslational event. The Bβ-chain is glycosylated later, possibly at the time of polypeptide termination or shortly before release from the ribosome into the cisternal space of the rough ER (Nickerson & Fuller, 1981). The sialic acid residues of the carbohydrate moiety have been shown to be low affinity sites whose occupancy by Ca^{2+} and physiological calcium concentration may facilitate fibrin polymerisation (Dang et al, 1989).

1.2.1 The amino acid sequence of fibrinogen

The quest for the complete amino acid sequence of fibrinogen dominated fibrinogen research in the 1970's (Okude & Iwanaga, 1971, Sharp et al, 1972, Takagi & Doolittle, 1975, Lottspiech & Henschen, 1977, Doolittle et al, 1977a,b,c, 1979a,b). The completed amino acid sequence as per Henschen (1983) is shown in figure 3.

1.2.2 The Gamma Chain

The γ-chains of human fibrinogen are 411 amino acids long and are primarily important in coagulation as being the location of polymerisation sites (Olexa & Budzynski, 1981) as well as the site for the Factor XIIIa induced crosslinking (Chen & Doolittle, 1970) and the Ca^{2+}

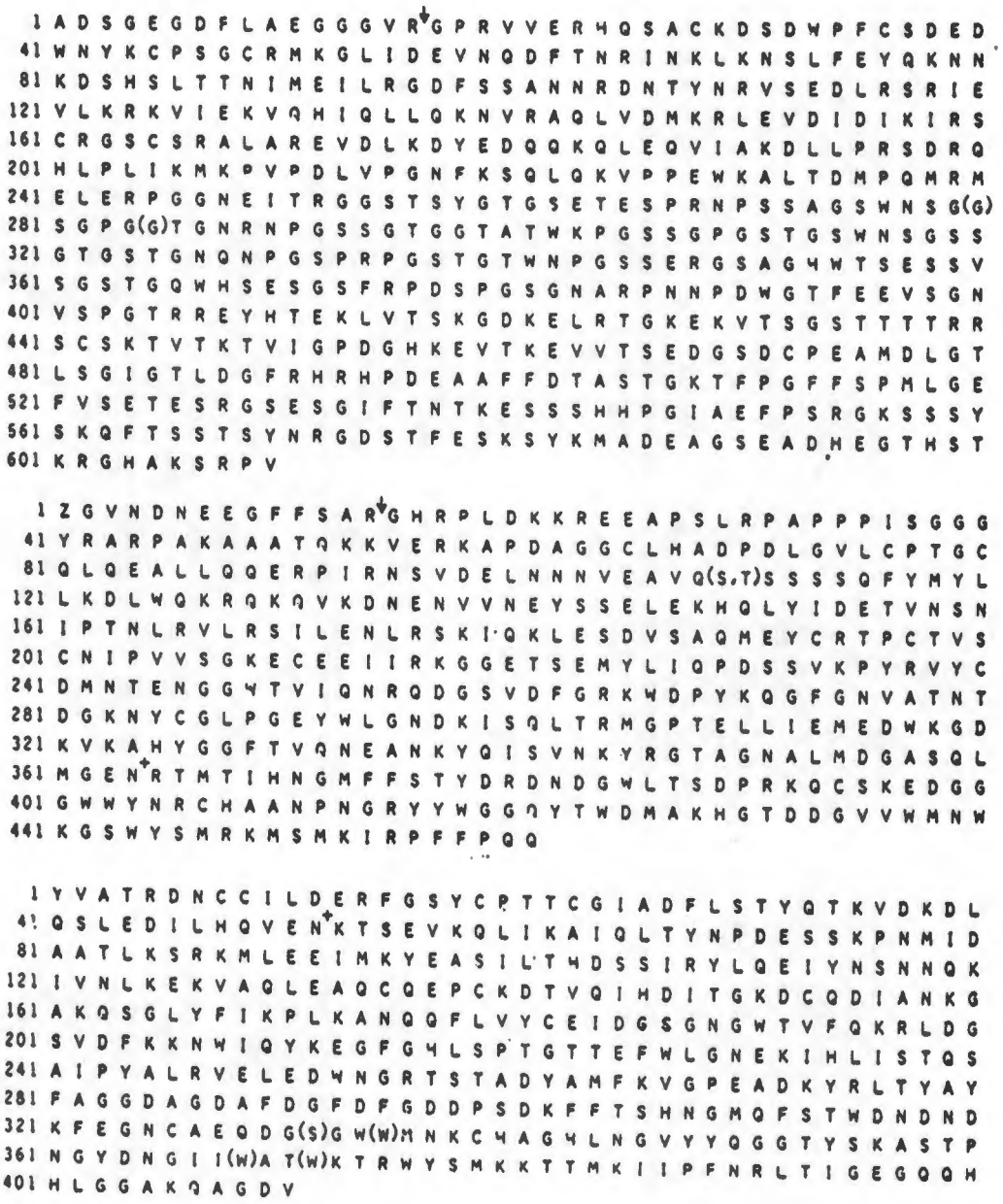

Figure 3: The complete amino acid sequences in human fibrinogen Aα-, Bβ- and γ-chains. The arrows indicate the sites of thrombin cleavage resulting in the removal of FPA and FPB, and + indicate the carbohydrate side chains. (Henschen et al, 1983).

binding sites (Varadi & Scheraga, 1986). The human fibrinogen γ-chain is heterogenous with respect to charge, sialic acid content and molecular weight (Wolfenstein-Todel & Mossesson 1980, 1981). Three forms of fibrinogen γ-chains have been purified from normal human plasma (Francis et al, 1984, 1988).

1.3. The polymerisation of Fibrinogen and Fibrino(geno)lysis

1.3.1 Polymerisation of Fibrinogen to Fibrin Gels

The formation of a blood clot begins with the triggering of the blood clotting cascade that is a step-wise sequential system of activation of proenzymes to their active enzyme forms that in turn activate the next proenzyme. The cascade may be triggered by extrinsic or intrinsic factors. Both pathways converge to activate prothrombin to thrombin which in turn converts fibrinogen to fibrin in the presence of Ca^{2+} ions.

Thrombin removes a pair of (hexadeca)peptides, fibrinopeptide A (FPA), from the amino terminus of the Aα-chain of fibrinogen (Hoeprich & Doolittle, 1983). This exposes an association site 'A' in the amino terminal region. This site binds specifically to the corresponding site always available in the carboxy terminal region of (the D-domain), the 'a' site (Kudryk et al, 1974). This association proceeds in an end to end fashion with half staggered overlaps resulting in the formation of linear protofibrils. This is the beginning of a loose clot. After formation of some protofibrils, fibrinopeptides (FPB) are removed from the amino terminals of the Bβ-chains. This reveals another site of association in the aminoterminal region called site 'B' (Blomback et al, 1978). The removal of FPB results in a tight aggregation of fibrinogen that progressively

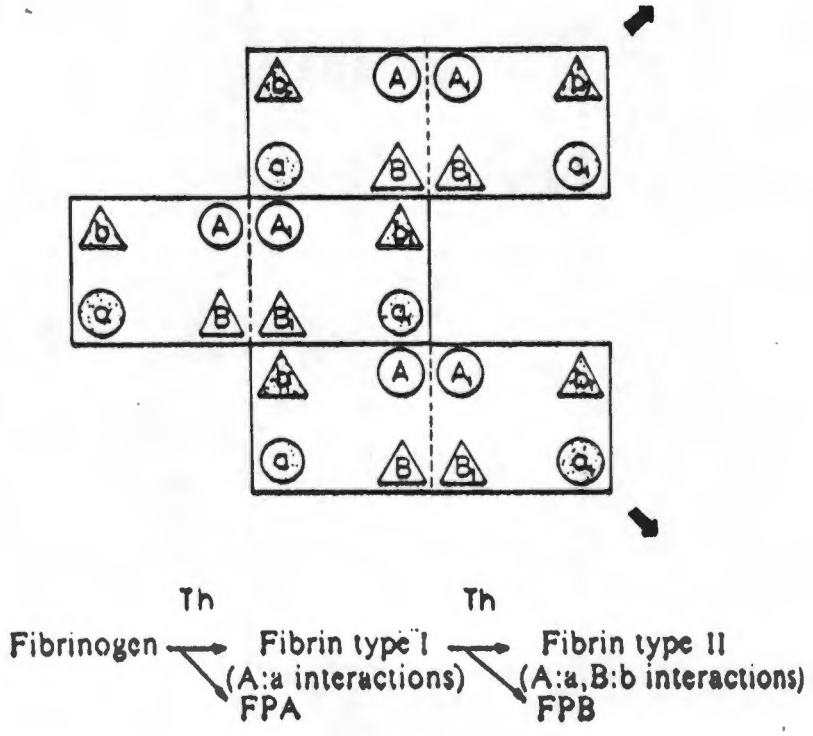

Figure 4: A schematic representation of the sequence of events in fibrin formation. The possible interactions at the polymerisation sites A:a and B:b are schematically shown. The dimeric nature of fibrinogen dictate that each of these sites are present in duplicate ie. AA_1 etc. The lower part of the figure summarises the events occuring during the formation of the two types of fibrin, I and II.
(Blomback et al, 1978).

blocks a concomitant release of FPA when treated with copperhead snake venom below 25^{o}C (Shainoff & Dardik, 1979).

The end to end association in the protofibrils aligns the carboxyterminal domains of the adjacent molecules and creates a new association site, site 'b' (Olexa et al, 1980, 1981). This alignment is stabilised by the formation of Factor XIII induced crosslinks (described later) (Lorand, 1980). Sites B and b then make specific and complementary lateral associations that allow the protofibrils to grow laterally. This completes the formation of a clot that is both mechanically rigid as well as resistant to lysis.

1.3.2 Location of the Polymerisation sites

Fibrinogen exists as a trinodular unit and therefore a half staggered orientation for polymerisation resulting from the interaction of the central E knot domain with the distal carboxy terminal domains would seem a logical one (Heene & Matthias, 1973, Olexa & Budzynski, 1980, Smith, 1980). The development of a model for the mechanism of fibrin polymerisation resulted from an examination of the binding between fibrinogen, fibrin and their degradation products (Kudryk et al, 1974, Blomback et al, 1978, Olexa et al, 1980, 1981, Horwitz et al, 1984).

Olexa (1980) reported evidence for four different polymerisation sites on human fibrinogen. Two of the sites 'A' and 'B' are located in the N-terminal domain and become exposed with thrombin cleavage of the fibrinopeptides FPA and FPB. The other two sites 'a' and 'b' are thrombin independent. The sites 'a' and 'b' are distinguishable as 'a' occurs in the

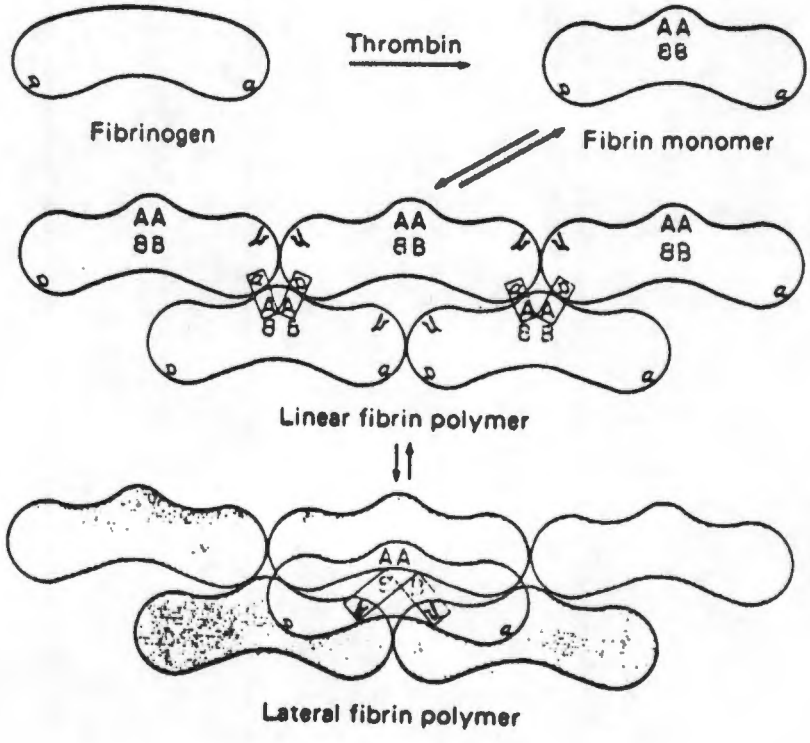

Figure 5: The model for fibrin polymerisation. The fibrinogen is depicted as a flexible banana model. The interaction of the polymerisation sites are shown. (Olexa & Budzynski, 1980).

carboxy-terminal region of fragment D while the 'b' site only becomes available in the C-terminal region of aligned fibrin-D-dimer. One polymerisation site was localised at the C-terminal domain of fibrinogen within the γ-chain between amino acids 303-411 (Olexa & Budzynski, 1981, Southan et al, 1985, Varadi & Scheragen, 1986). The location of the γ-chain crosslink acceptor site is on the γ-chain carboxy terminal end (Fretto et al, 1978, Holm et al, 1985).

Polymerisation inhibition studies with synthesized short peptides corresponding to the amino termini sequences of the α-and β-chains showed that peptides based on the sequence Gly-Pro-Arg from the α-chain were effective inhibitors of fibrin polymerisation (Doolittle & Laudano, 1980, Laudano et al, 1983, Doolittle, 1984, Furlan, 1982). Thus, a primary polymerisation site complementary to that located in the C-terminus of fragment D, site 'a' is present in the N-terminus of the fibrin α-chain. Another inference of the synthetic peptide study was that the polymerisation in those systems is driven by the G-H-R knobs combining with complementary 'holes' ordinarily occupied by G-P-R 'knobs' (Doolittle, 1984). The maintenance of native conformation is essential for the expression of polymerisation site 'b' with the portion of the fibrinogen molecule present in the high molecular weight fraction but not in the low molecular weight fraction. The Bβ-chain His-16 which lies only one residue away from the thrombin susceptible bond was shown to be essential for polymerisation site A leading to end-to-end association of fibrinogen upon the release of FPA (Shimizu et al, 1986). The most recent contribution to the polymerisation site saga is that the fibrin polymerisation site in the N-terminal domain of fibrin may be composed of sequence derived from both the α- and β-chains (Pandya

et al, 1991)

1.3.3 The Transglutaminases

The transglutaminases are the enzymes that catalyse the formation of ε(γ-glutamyl)-lysine bonds between the γ-carboxy group of a glutamine residue on one polypeptide chain and the ε-amino group of a lysine residue side chain on another with the loss of ammonia. This is the result of a Ca(II) dependent acyl transfer reaction (Lorand et al, 1980). This class of enzyme is widely distributed in the various tissues and body fluids. Each has distinctive physical properties and distribution in the body (Ichinose et al, 1990). The transglutaminase that is of particular importance to this study is the plasma enzyme that completes the formation of the fibrin clot by inducing ε(γ-glutamyl) lysine crosslinks between the antiparallel di-γ-chains (Chen & Doolittle, 1970) as well as the α-chains of fibrin of the long protofibrils to form a solidly meshed clot. This enzyme is Factor XIIIa of the coagulation cascade.

1.3.3.1 Human Factor XIII: Fibrin Stabilising Factor: Laki-Lorand Factor

Factor XIII is a glycoprotein that circulates in the blood as a proenzyme. During the final step of the blood coagulation cascade, the proenzyme is activated to Factor XIIIa by thrombin in the presence of calcium ions that then catalyses the polymerisation of fibrin monomers into a tightly crosslinked rigid clot which now has increased resistance to lysis (Lorand et al, 1980, Ichinose et al, 1986). Clots formed in the absence of Factor XIIIa, eg. in genetically determined deficiency, are dissociable in 4M urea (See Addendum IV). Factor XIII is a tetramer of two pairs of dimerised subunits a_2b_2

with a total molecular weight of 320 000 daltons. The two catalytic a subunits are 75 000 daltons each and the two non-catalytic b subunits are 80 000 daltons each (Schwartz et al, 1973).

The active enzyme (Factor XIIIa) is generated during the final stages of the blood coagulation cascade by the release of the activation peptide which is 4000 daltons from the amino terminus of each of the catalytic a subunits. Subsequent to this proteolytic event, a series of Ca^{2+} dependent reactions occur.

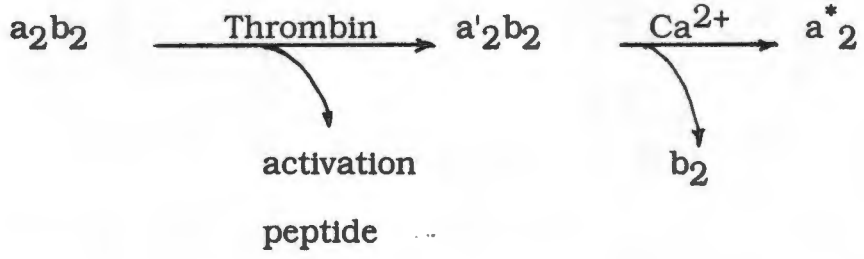

The tetramer dissociates into an active dimer (a'_2) and releases the two non-catalytic subunits. The a'_2 ensemble undergoes a conformational change by binding calcium ions thus unmasking the active-centre thiol group in the final active form (a^*_2) - i.e.(Factor XIIIa) (Lorand et al, 1981, Lewis et al, 1985, Ichinose, 1990).

Non-crosslinked polymeric fibrins I & II (polymerised des-A and des-A,B-fibrinogens were shown by Lewis et al (1985) to be powerful promoters of the thrombin catalysed release of the activation peptide from a_2b_2. This occurs through the formation of a complex between the non-crosslinked polymer with FXIII. The complex has a higher affinity for thrombin than does free Factor XIII. In addition the system has a negative feedback system of regulation as the enhancement of the active peptide release decreases dramatically as the product of activation, Factor XIIIa, catalyses the crosslinking of

the fibrin substrates (Lewis et al, 1985).

1.3.3.2 The Factor XIIIa Catalysed crosslinking of Fibrin

The thrombin activated Factor XIIIa catalyses the fusion of fibrin units producing γ-glutamyl-ε-lysine site chain bridges intermolecularly (Lorand et al 1981). This crosslinking occurs between the carboxy terminal regions of antiparallel γ-chains of fibrin (Chen & Doolittle, 1970) and the sites on the α-chain that are highly susceptible to proteases.

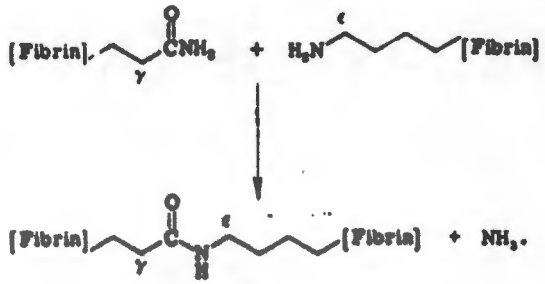

These two isopeptidic crosslinks result in the formation of a di-γ-chain linking adjacent D-domains. The assignment of the sites of crosslink remain as a matter of some controversy. While it has been demonstrated unequivocally that K-406 is the acyl acceptor, either of two Q residues are the putative acyl donor. These are the adjacent glutamines Q-398 or Q-399. The latter seems to be the dominant site accounting for more than 80% of the crosslinks (Purves et al, 1987)

1.3.3.3 The Factor XIII Gene

The Factor XIII b subunit encoding gene (F13B) was found to be on chromosome 1q31–32.1 (Webb et al, 1985) and the gene coding for the Factor XIII a subunit (F13A) was localised to chromosome 6p24–25 (Board et al, 1988). The F13A gene contains 15 exons with a total of 3905 bases (Cundmann et al, 1986). The exon 15 is the largest and codes for the carboxy terminus of the protein and the 3' non-coding region of the gene. The entire activation peptide (amino acids 1-37) is encoded by exon 2. The active site Cys-314 region is encoded by exon 7. The thrombin cleavage site (between K-513 and S-514) that leads to inactivation is encoded for on exon 12. The two putative calcium-binding sites are encoded by exon 6 and 11 respectively. It would appear that the introns separate the gene into the functional and structural domains (Ichinose & Davie, 1988).

The b subunit amino acid sequence has been determined by cDNA cloning and amino acid sequencing. Each of the non-catalytic subunits consists of 641 amino acids (Ichinose et al, 1986). The b subunit contains 10 tandem repeats of 60 amino acids known as GP-1 structures, short consensus repeats (SCR), or sushi domains (Bottenus, 1990). The sushi structures have characteristic disulphide bonds between the first and third and second and fourth cysteines (Ichinose et al, 1990).

The F13B gene is 28 kilobases in length consisting of 12 exons. The exons range from 64 to 222 bases in length while the introns range in size from 87 to 9970 bases. Each sushi domain was found to be encoded for by a single exon. The internal homologies of the sushi domains at the DNA level range from 36% to 43% (Bottenus et al,

1990). Many of the genes coding for multiple sushi domains on other protein eg. those in the complement receptor types 1 and 2, Factor H, decay accelerating factor (DAF) and the α subunit of C4 binding protein are also located at chromosome 1q32 (Webb et al, 1989).

1.3.3.4 Other Transglutaminases

There are four other transglutaminases present in the human body. They are a) the tissue transglutaminase found in the cell cytosol of all tissues and organs; b) epidermal transglutaminase; c) hair follicle transglutaminase; and d) prostrate transglutaminase (Chang & Chang, 1986, Davies et al, 1985, Fesus et al, 1987).

1.3.4 Calcium and Fibrin(ogen)

Calcium has been shown to play an important role in all stages of the clotting process. This interaction begins with the activation of thrombin – a calcium dependent reaction. The divalent cation has been shown to greatly accelerate the polymerisation of fibrin and decrease clotting time significantly (Boyer et al, 1972, Endres & Scheraga, 1972, Kanaide et al, 1982, Alkjaersig & Fletcher, 1983, Furlam et al, 1982). Alkjaersig & Fletcher (1973) report that in the presence of Ca^{2+}, during polymerisation, additional binding sites appear to play a role, since dimer formation was now superceded by the formation of higher oligomers. Laudano and Doolittle (1983) on an examination of the effect of Ca^{2+} on the binding of various peptides to fibrinogen found the influence of the divalent cation to be predominantly on the G-H-R-P (β-chain type) binding site. Calcium was found to increase site accessibility.

Calcium is also required for the thrombin dependent activation of coagulation Factor XIII (Greenberg, 1985, Lewis et al, 1978). Fibrinogen has three high affinity calcium specific binding sites (Marguerie et al, 1977). Two of the 3 sites on human fibrinogen are located in the D-domains (Lindsey et al, 1978b). The two sites are equivalent with identical binding constants (log k = 5.045) (Lindsey et al, 1978b). Recent data indicates that the D-domain calcium binding site is located on the γ-chain segment of γ-303-355/356 (Dang et al, 1985, Varadi and Scheraga, 1986). The presence of calcium ions increase the surface area of fibrinogen, due mainly to the C-terminal regions of Aα-chains moving from an inward orientation to a more solvent exposed position. This conformational change leads to the molecule being more prone to form intermolecular associations due to the exposure of those sequences important for interaction. These effects are mediated through binding to low-affinity calcium sites on the molecule (Apap-Bologna et al, 1989).

1.3.5 Fibrino(geno)lysis

Intravascular fibrin clots that are due either to a response to vascular injury or thrombosis needs to be removed to restore free flow of blood through the vessels. This is achieved through the fibrinolytic pathway. The solid fibrin deposits are degraded to soluble complexes by the serine protease plasmin that is activated from the zymogen plasminogen through the action of plasminogen activators. These serine proteases catalyses the hydrolysis of the Arg-561-Val-562 bond in plasminogen (Fears, 1989). Due to the restricted substrate specificity of plasmin, mechanisms to localise

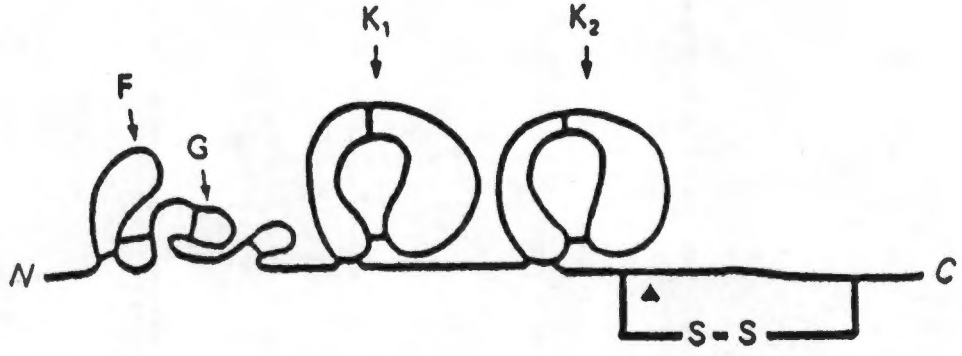

Figure 6: A schematic representation of tissue plasminogen activator (t-PA). The figure emphasises A-chain domains:fibronectin-like finger (F), epidermal growth factor-like sequence (G), Kringles 1 and 2 (K_1,K_2). The plasmin-cleavage site is indicated by ▲ (Fears, 1989).

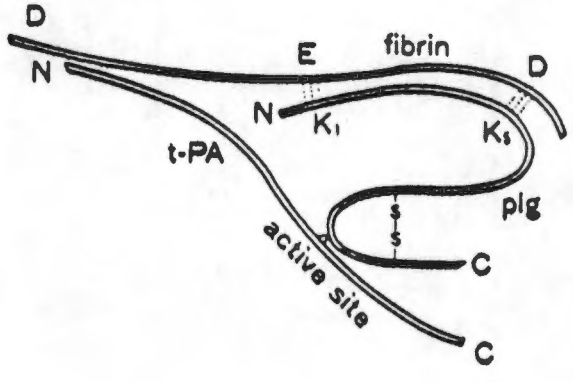

Figure 7: A schematic portrayal of a trimolecular complex formed between t-PA, plasminogen and fibrin. The Kringle K_1 of plasminogen interacts with the E-domain of fibrin and K_5 with the D-domain. The plasminogen in turn, interacts with the active site of the t-PA. (Takada et al, 1990).

the generation of plasmin and confine its action to the site of the clot are required (Norrman et al, 1985). There are two recognised mechanisms:

a) Tissue plasminogen activator (tPA) is efficient only in the presence of fibrin (Fears, 1989, Norrman et al, 1985, Takada et al, 1990, Varadi & Pathy, 1983, Higgins & Vehar, 1987). In the absence of fibrin the tPA activation of plasminogen decreases 1000-fold (Ranby, 1982),

b) the plasmin generated but not engaged in fibrin degradation is rapidly inhibited by the α_2-plasmin inhibitor (Wiman & Collen, 1978, Sakata & Aoki, 1982).

Fibrin acts as both substrate and cofactor contributing to the increased plasmin production by forming a ternary complex with plasminogen and the tissue type plasminogen activator (Fears, 1989, Higgins & Vehar, 1987). The plasminogen binding sites thought to be in the D-fragment are controlled by the carboxy terminal of the γ-chain (Varadi & Patthy, 1983, Lucas et al, 1983a,b) while the kringle 2 domain of tPA is implicated in the binding of the activator to fibrin (Larsan et al, 1988, Wojta et al, 1989). Fibrin also interacts with a second endogenous activator, the single chain urokinase-type plasminogen activator (Fears, 1989, Takada et al, 1990, Lucas et al, 1983).

1.3.6 Plasmin digestion of fibrinogen

The subunit chains of fibrinogen differ in their susceptibility to plasmin digestion. The order of susceptibility is $\alpha > \beta > \gamma$ (Pizzo et al, 1972, Gaffney & Dobos, 1971). Plasmin digestion leads to the formation of

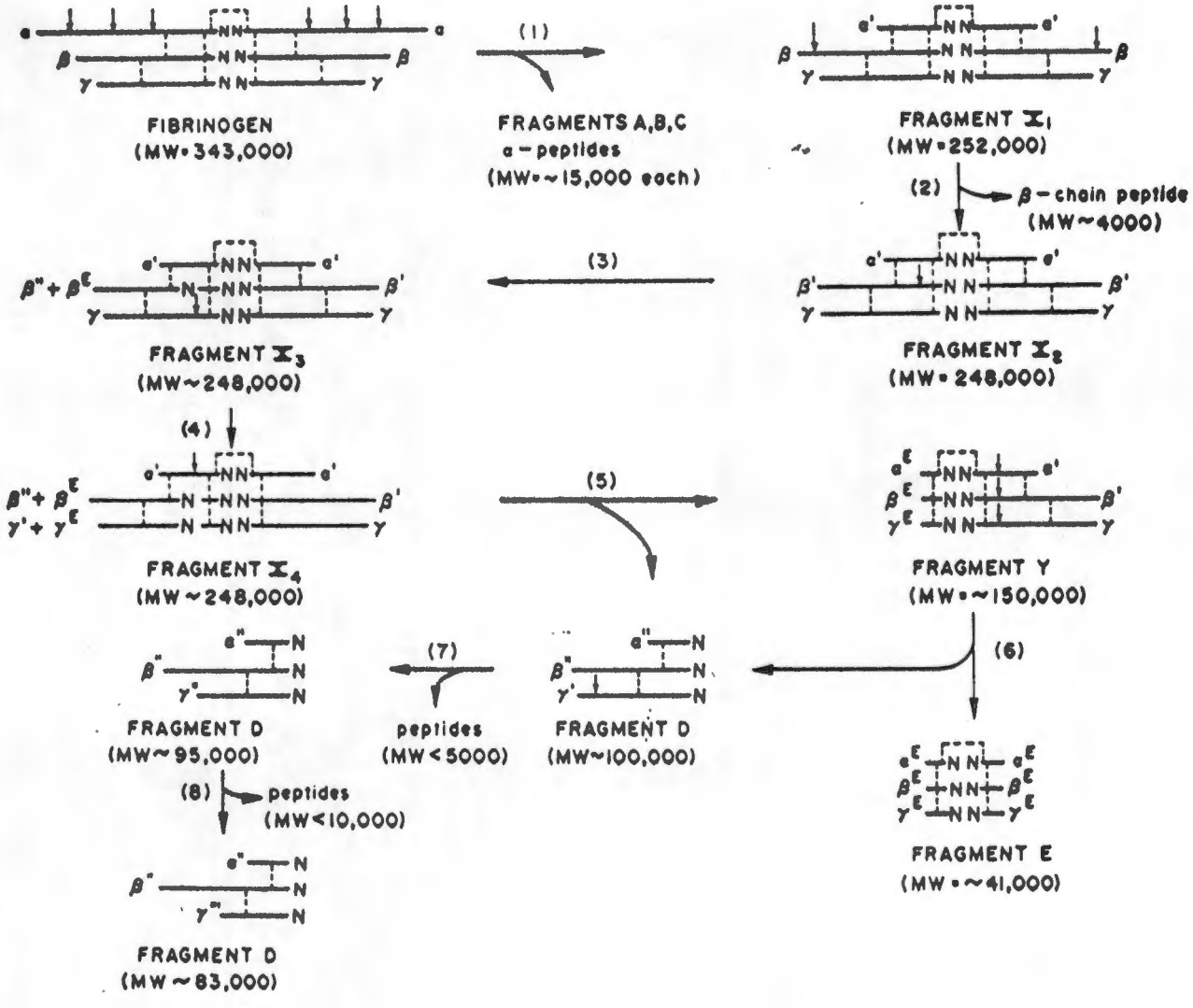

Figure 8: The effect of plasmin on fibrinogen. A schematic representation of the sequential reactions that occur during the plasmin digestion of human fibrinogen. The final product of the digestion are fragment E (M_r 41 000) and fragment D (M_r 83 000). (Pizzo et al 1972).

fragments X and Y together with the associated low molecular weight products. These fragments are further digested to finally yield fragment D (Fig.8). Further digestion occurs in the absence of calcium ions but this is not physiologically relevant (Purves et al, 1980). Digestion begins with hydrolysis at the carboxyterminal of the Aα-chain concomitant with the appearance of fragment X releasing fragments A, B & C. This is followed by an initial release of a small portion of the β-chain at the amino terminus (Mossesson et al, 1972, Pizzo et al, 1972, Budzynski et al, 1974). Each cleavage exposed further plasmin susceptible sites in a cooperative manner. N-terminal digestion on all three chains releases the D-fragment to yield fragment Y and the release of the second D-fragment yields fragment E. Thus the final products of plasmin digestion of fibrinogen are the fragments D and E and low molecular weight peptides from each chain (Pizzo et al, 1972, Mossesson et al, 1972, Lucas et al, 1983).

1.3.7 The Plasmin degradation of crosslinked fibrin

The plasmin digestion of a fibrin gel presents a more complex pattern due to the complicated polymerised structure reinforced with Factor XIIIa induced crosslinks between the γ-chains (Lorand et al, 1980). Francis and Marder (1982) developed a model for the complete plasmic digestion of crosslinked fibrin. The degradation has been divided into four distinctive phases:

Phase 1 involves an initial limited proteolysis without interfering with the covalent attachment of the D and E domains to the other parts of the matrix. This phase is characterised by the extensive cleavage of the α polymer chains.

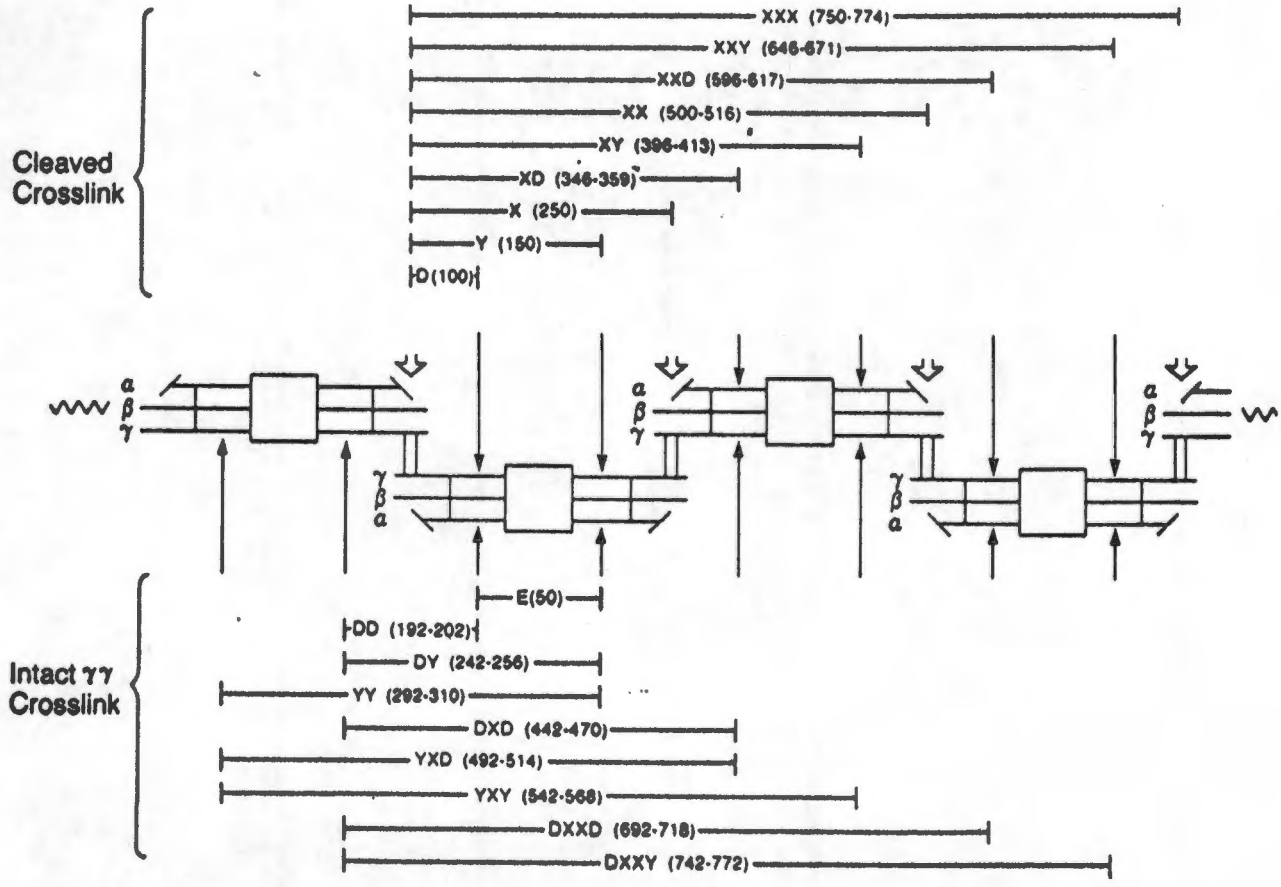

Figure 9: The effect of plasmin on fibrin. A schematic diagram of a four-unit fibrin polymer joined by Factor XIIIa catalysed crosslinks, indicating the principal cleavage sites for plasmin and the fragments resulting their from. The final products of plasmin digestion are fibrin are the E fragment and the D-dimer fragment. (Francis & Marder, 1982).

Phase 2 denotes the degradation of fibrin to the extent of all degradation products are still attached to the matrix but now via non-covalent linkages.

Phase 3 involves the release of the soluble complex into solution.

Phase 4 describes the degradation of soluble complexes subsequent to release from the matrix.

Figure 9 illustrates the progressive plasmic degradation of crosslinked fibrin indicating both the points of cleavage and the composition of the resulting degradation products. The soluble crosslinked degradation products are DD/E, DY/YD, YY/DXD and XXD/DXY. Upon release into solution these fragments are further digested by plasmin to release as final plasmic products fragments E and D-dimer (Frances & Marder, 1982, 1983).

1.3.8 Calcium and Fibrinolysis

In the presence of calcium (II) the final product of fibrinogenolysis is the fragment D(cate), M_r 93 000, which is protected from further plasminolysis by calcium. The absence of Ca^{2+} results in the further plasmin digestion of fragment D to a smaller D-fragment (M_r 80 000) by breakdown of the γ-chain (Purves et al, 1978, Haverkate and Timan, 1977). The smaller D-fragment displays more crosslinking intermolecularly with chemical crosslinking agents suggesting the loss of the γ-chain remnant results in a more open conformation, in the case of D(cate), however, the cleavage of more plasmin susceptible bonds is protected against by the presence of calcium ions (Britton et al, 1982).

The final product of fibrinolysis, fragment D-dimer, is plasmin resistant by virtue of calcium ions (Haverkate & Timan, 1977, Purves & Lindsey, 1978a,b, Lindsey et al, 1978, Purves et al, 1980). The chelation of calcium ions unmasks plasmin susceptible sites (Purves et al, 1978). The plasmin digestion of fibrin in the absence of calcium results in the formation of a non-covalently linked D-dimer fragment (NCDD), the crosslink fragment is attached to the two D-domains electrostatically through non-covalent associations (Lindsey et al 1978, Purves et al, 1980). While tightly bound to the parent molecules at higher temperatures, the crosslink peptide could be lost below 15^{o}C (Purves et al, 1980).

1.4 Fibrinogen & Fibrin Interactions

The two important macromolecular interactions of fibrinogen and fibrin discussed thus far are the binding of thrombin to fibrinogen (Jakubowski & Owen, 1989) initiating clot formation and interaction with plasminogen initiating the fibrinolytic pathways (Bok & Mangel, 1985). Additionally, there are three major and several minor fibrinogen interactions of physiological relevance.

An important macromolecular interaction of fibrinogen is that with fibronectin. Fibronectin is a 'molecular glue' (McDonagh, 1981) found in an extrinsic membrane form in connective tissues and basement membranes and in a soluble liver-produced form in plasma produced by a different transcript of the gene (Mosher, 1980, Pearlstein et al, 1980, Purves et al, 1984). Fibronectin interacts, in addition to fibrinogen, with collagen, sulfated proteoglycans, gangliosides & bacterial cell wall

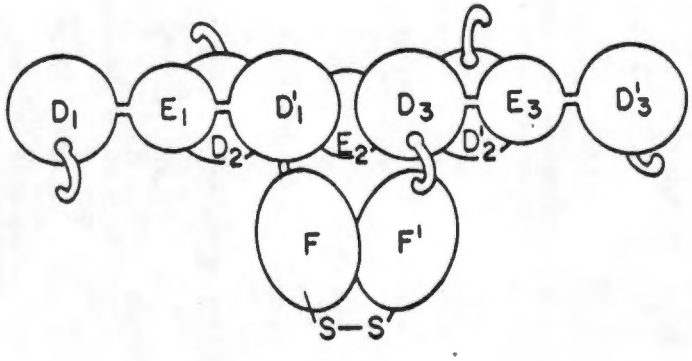

Figure 10: The possible interaction of fibronectin and fibrin. The polymerisation of fibrin may bring the carboxyl portions of the a-chains together and allow the dimeric fibrinectin molecule (F) to bind at two sites rather than one. The disulphide linkage between F and F^1 are indicated. (Mosher, 1980).

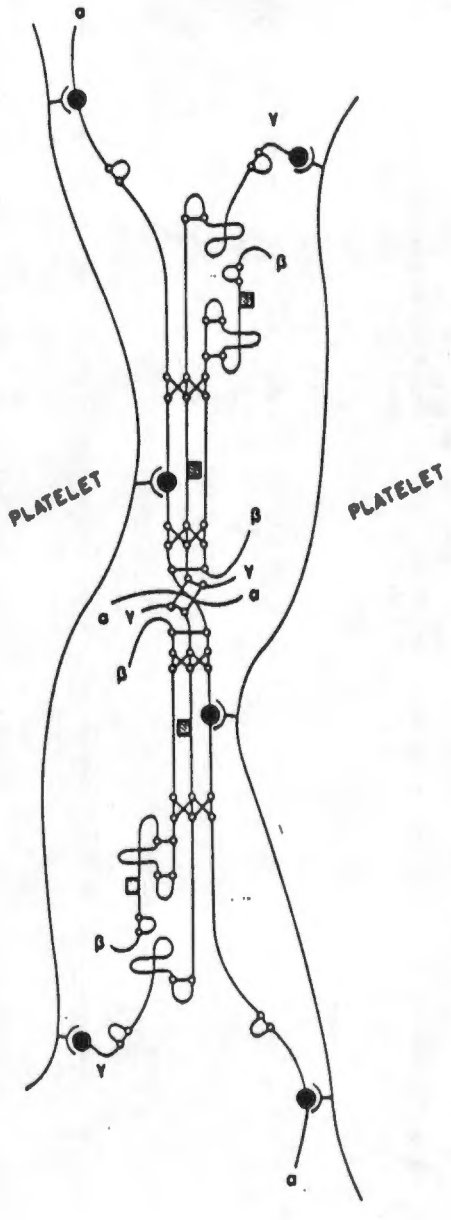

Figure 11: The proposed model of interaction between human fibrinogen and human platelets. The hatched boxes represents carbohydrates on the β- and γ-chains of fibrinogen. The platelet receptor recognition domains are marked as black dots encompassing sequences 95-98 and 572-575 on the a-chain and sequence 400-411 on the γ-chain. One molecule of fibrinogen can be engaged in cis and trans interaction with platelet receptors. (Hawiger et al, 1989).

components implying functions as an adhesive and opsonic glycoprotein (Mosher, 1980). The role of plasma fibronectin as an opsonin, however, is not clear at all (Purves et al, 1984).

In the presence of thrombin activated Factor XIIIa, fibronectin is incorporated 1mol/340 KDa unit weight of fibrin. This leads to an increase in the gel turbidity and the permeability coefficient suggesting that the width of the strands of the gel increases as a result of fibronectin incorporation (Okada et al, 1985). The secondary and tertiary structure of fibronectin is essential to binding (Isaacs et al, 1989). Binding to Factor XIII occurs in the absence of Ca^{2+}, suggesting that a domain on the transglutaminase other than the catalytic site is needed to complex with fibronectin (Turner & Lorand, 1989).

Fibrinogen binds to activated platelets and may have a fundamental role in the process underlying platelet aggregation. This binding occurs according to the law of mass action possibly dependent on allosteric modulation of the platelet receptor on binding a fibrinogen molecule (De Cristofaro, 1988). Platelet receptor sites of interaction have been localised on fibrinogen γ-chains (Kloczewiak et al 1982a, 1984, 1989) and α-chain (Hawiger et al, 1982, 1989). The γ-chain receptor recognition site is located between γ-400 and γ-411 (Kloczewiak, 1984) and the α-chain site is in the amino terminal region (Hawiger et al, 1989) (Fig.11). The binding is Ca^{2+} dependent (Phillips & Baugham, 1983).

Human fibrinogen interacts with the cell wall component of certain staphylococci inducing clumping. An average of 2130 fibrinogen molecules bind per bacterial cell with $K_D = 9.9 \times 10^{-9}$

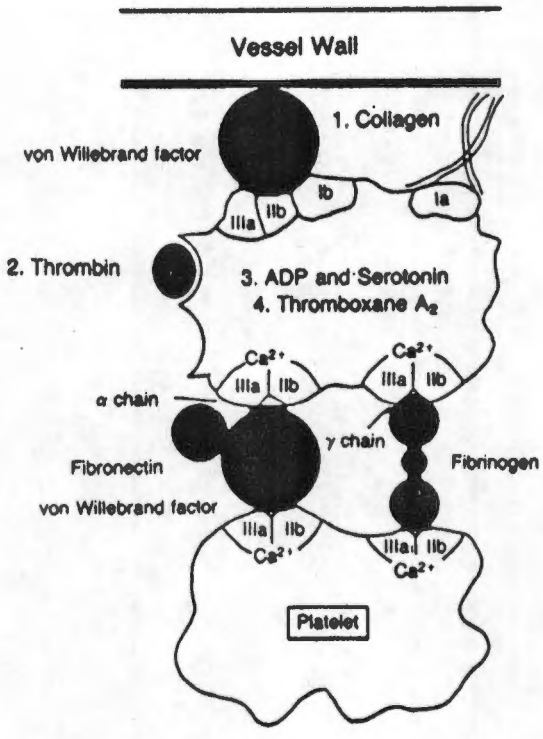

Figure 12: The Interactions of fibrinogen in response to vessel wall lesion. Interactions among platelet receptors, thrombin, fibrinectin, von Willebrand factor, glycoproteins and fibrinogen. The γ-chain of fibrinogen interacts with glycoproteins IIIa/IIb, the receptors on the platelet. (Fuster et al, 1992).

(Hawiger et al, 1982). The staphylococcal receptor binding site in fibrinogen has been located on the γ-chain between residues 397-411 (Strong et al, 1982). The valency of fibrinogen in regard to its receptor binding domain and the availability of this domain is essential for the staphylococcal clumping reaction.

Fibrinogen has also been shown to induce the aggegation of erythrocytes (Maeda et al 1987) and binds a multi-kringle containing lipoprotein(a), a plasma component whose concentration is related to the development of atherosclerosis (Fuster et al, 1992a,b). This binding is catalysed by plasmin (Harpel et al 1989).

1.5 Assaying the degradation products of Fibrinogen and Fibrin

The identification and measure of fibrinogenolytic degradation products (FgDP) and fibrinolytic degradation products (FbDP) in plasma remains an essential means of gauging physiological condition. A number of pathologic conditions are characterised by increased levels of FgDP and FbDP, thus the clinical utility of assaying the degradation products is well established. Earlier methods included gel filtration and SDS polyacrylamide electrophoresis analysis (Alkjaersig et al, 1977). The obvious limitation of these techniques was that reasonably high concentrations were required for any valid assay. What was required was a technique that could detect much smaller amounts and differentiate fibrinogen and fibrin proteolysis products in plasma specifically.

The rapid advances in the development of immunochemical detection techniques has held much promise for the development of

degradation product assays sensitive to fibrinogen antigens at low concentrations in plasma. These assay systems include radioimmunoassays and enzyme linked immunosorption assays (ELISA) (Whitaker et al, 1985). Research emphasis in recent years has been focussed on removing the obvious limitation of using polyclonal antibodies to fibrinogen and/or fibrinogen derivatives D and E by developing specific monoclonal antibodies (Elms et al, 1986, Grumberg et al, 1987, Schielan et al, 1991). The monoclonal antibody DD-3B6/22 that is specific for the crosslinked fibrin derivatives (fibrin D-dimer/fibrin D-dimer-E fragment) used in a later agglutination procedure has led to the development of the solid phase 'Dimertest' for fibrinolytic products in serum or plasma (Elms et al 1986, Greenberg et al, 1987). The monoclonal Ab FDP-14 binds FgDP and FbDP but not parent fibrinogen. It has its epitope in the E-domain of the fibrinogen molecule on the Bβ-chain amino acids 54-118 (Kopper et al, 1987, 1988). Monoclonal antibodies have been raised using epitopes on the α-chain (Mao et al 1990) and the γ-chain (Schielan, 1991).

While the immunologic approach is the most viable due to the high levels of sensitivity attainable, a severe limitation of the technique is the lack of absolute specificity of the antibodies especially as fibrinogen is present in large amounts relative to low concentrations of FbDP and FgDP with short half lives. An accurate measure of fibrinogen and fibrin degradation products in vivo requires assays that will distinguish with reasonable sensitivity between Y-D, $(Y\text{-}D)_{XL}$ (D-Y), Y, X, D, D-dimer and E

The need for an accurate assay for the specific analysis of fibrinolytic degradation products cannot be emphasised sufficiently. In a recent review of coronary heart disease (1992) Fuster and colleagues implicate defective fibrinolysis as a thrombogenic risk factor in patients with coronary disease.

1.6 Snake Venom Enzymes and Fibrinogen

Snake venoms are injected directly into the body through grooves on the fangs and the venom travels quickly into the bloodstream to be transported to their points of physiological action. It is not surprising, therefore, that a large number of snake venoms express their physiological toxicity in the blood, having a notable effect on coagulation.

Snake venoms are a prolific source of enzyme, many have proved to be useful tools in coagulation studies, especially in the determination of fibrinogen and fibrin structure and sites of polymerisation. At least 26 enzyme types have been described, ten of which are common to all snake venoms; and the other sixteen are scattered throughout the five families of poisonous snakes (Russel, 1980).

The snake venom enzymes affecting coagulation may be broadly divided into those with procoagulant activity (Fortova et al, 1990, Kirby et al, 1979, Niewiarowski et al, 1979) and those with anticoagulant activity (Pandya Budzynski, 1984, Pandya et al, 1983). The former may be subdivided into

1) those enzymes that activate prothrombin to thrombin eg. enzymes in

venom of Echis carinatus (Morita & Bon, 1987a, b) and venom of Oxyuranus s. scutellatus (Walker et al, 1980); and

2) the thrombin-like fibrinogenolytic enzymes eg. enzymes from the venoms of Bothrops jararaca (Maruyama et al, 1990), Crotalus atrox (Nikai et al, 1983), ancrod of Agkistrodon rhodostoma and batroxubins from Bothrops moojeni and B.marajoenis (Muzbek & Hanck, 1979) as well as other Bothrops species (Nahas et al, 1979), and Cerastes vipera (Farid & Tu, 1989).

There is a third class of snake venom enzymes of particular importance as tools for structural determinations, the fibrinogeno and fibrinolytic enzymes (Bajwa et al, 1980, 1981). These may belong to the procoagulant or anticoagulant categories. The fibrinogenases may be further categorised according to which of the chains are digested, thus the α- and β-fibrinogenases (EC. 3.4.21.5) (Ouyang et al, 1979, Ouyang & Huang, 1979, Moran & Geren, 1981, Teng et al, 1985). Finally, there are those venoms containing both procoagulant and anticoagulant factors eg. C.cerastes and C.vipera (Labib et al, 1981), B.gabonica and Agkistrodon c. piscivorus (Bajwa et al, 1982), and Agkistrodon C. contortrix (Dyr et al 1983). The snake venom proteases may be divided into the serine proteases (Kruzel & Kress, 1985) or the zinc metalloproteinases (Evans, 1981, Bjarnason & Fox, 1983, Fox et al, 1986). The zinc(s) in the proteases may play a catalytic or structural role or in the case of some venoms eg. Crotalus atrox, both (Bjarnason & Tu, 1978). There are also venom proteases that display a calcium ion dependence for activity eg. haemorrhagic principles from Crotalus h. horridus (Civello et al, 1983) and Agkistrodon contortrix (Dyr et al, 1989).

1.6.1 Puff Adder (Bitis arietans) Venom Proteases

The venom of the Puff adder (Bitis arietans) exhibits a high haemorrhagic activity when tested in mice or rabbits (Homma & Tu, 1971). Various researchers have attempted to isolate and purify the individual haemorrhagic principles (Morris et al, 1980, Morris & Lawrence, 1980, van der Walt, 1972, Purves et al, 1986). Mebs & Panholzer (1982) separated crude puffadder venom into 5 fractions, three displaying haemorrhagic activity. Lawrence and Morris (1981) isolated a potent, basic metalloproteinase fraction from puffadder venom, M_r 24 000, that could destroy all detectable trypsin and chymotrypsin inhibitory activity when incubated with human plasma. The protease hydrolyses casein and effects the activation of plasma prekallikrein and inactive renin (Lawrence & Morris, 1981, Morris & Lawrence, 1980).

Purves et al (1986) isolated a haemorrhagic principle from puffadder venom that displays fibrinolytic properties to be referred to as 'PAV protease'. The M_r 25 000 enzyme, with properties similar to van der Walt's protease A (1971), displays the ability to cleave fibrin-D-dimer into apparently symmetrical monomers (Purves et al, 1986, 1987, 1989). Fibrin-D-dimer is the terminal plasmic digestion product of crosslinked fibrin in the presence of calcium. The PAV protease monomerisation of fibrin-D-dimer begins with a rapid cleavage of the di-γ-chain followed by an independent progressive reduction of the β-chain (Purves et al, 1986, 1987). Sequence studies show that the PAV protease displays a unique site specificity on the di-γ-chain, cleavage occurring between the Factor XIIIa (EC 2.3.2.13) catalysed crosslinks (Purves et al, 1987).

The activity is inhibited by EDTA but unaffected by the inhibitors hexane-diamine and PMSF (Purves et al, 1986). The protease hydrolyses casein but displays no EDTA-sensitive activity against chromozyms PL, PK, TRY and TH and demonstrates no esterolytic activity against tosyl-arginine-methyl-ester (Purves et al, 1986).

2. METHODS

2.1. Preparation and purification of fluorescent-f-D-dimer, f-D-momomer and non-fluorescent fibrin-D-dimer

Preparation

Fluorescent-D-dimer (f-DD) and fluorescent-D-monomer (f-D) was prepared as described previously (Purves et al, 1978a,b, 1986). Human fibrinogen (Sigma) was made up to 1mg/ml in 100mM Tris, pH 7.4, 150mM NaCl; and clotted at 37°C in the presence of 2.45 mM dansylcadaverine (Sigma) with 100U of Thrombin (Parke-Davis) in 5mM $CaCl_2$ (final). Dansylcadaverine, a fluorescent lysine analogue, was dissolved in 6M HCl and titrated to pH 7.00 with 6M NaOH before addition to the fibrinogen solution. The fibrinogen preparation was sufficiently contaminated with Factor XIII to obviate the necessity of adding the transglutaminase.

The resulting clot was spun down and washed repeatedly with and eventually homogenised in 100mM Tris, pH 7.4, 150mM NaCl, 10mM $CaCl_2$. The suspension was digested by 0.05mg/ml plasmin at 37°C. Plasmin was the product of the activation of 10mg plasminogen (Sigma) by 500 Ploug units of Urokinase (Leo) in 2ml 100mM Tris, pH 7.4, 150mM NaCl.

Purification

The digest was filtered and dialysed against 5mM Tris, pH 8.6, 1mM $CaCl_2$. The dialysate was chromatographed on a (25 x 1cm) DE-52 (Whatman) ion exchange column, eluting with 5mM Tris, pH 8.6 with a 0-300mM NaCl gradient to separate the D and E fragments. The

fractionation was analysed by SDS-polyacrylamide gel electrophoresis (Laemmli, 1970) on polyacrylamide gels with 6-15% density gradients. F-D-dimer and f-D-monomer containing fractions were pooled and concentrated with immersible CX-10 ultrafiltration units (Millipore).

The f-D-dimer was separated from f-D-monomer by molecular sieving. The concentrate was loaded in no more than 2ml onto a (100 x 2.5cm) Ultrogel AcA 34 agarose molecular sieving column. Fractions were eluted with 100mM Tris, pH 7.5 containing 150mM NaCl, 1mM $CaCl_2$ and 4M urea. An important restriction of the procedure was the low flow rates which were usually below 22.5 ml/hour. Increased flow rates resulted in the build up of excess pressure in the column. After SDS-PAGE analysis of the fractionation, the relevant fractions were pooled, dialysed to remove urea, and concentrated.

Non-fluorescent fibrin-D-dimer was prepared in the same manner but omitting the addition of dansylcadaverine. In the absence of the fluorescent lysine analogue, fibrin-D-dimer and the E fragment were the sole degradation products of plasmin digest of the clot, thus the DE-52 ion exchange chromotography proved to be an adequate purification technique eliminating the need for further molecular sieving or gel filtration of the fractions in the preparation of non-fluorescent fibrin-D-dimer.

2.2 Preparation of Puffadder Venom Protease

Fresh puffadder venom was obtained from J. Visser, Hout Bay, Cape Town. The crude venom was taken up in 0.1 M Tris, pH 7.4 containing 0.15 M NaCl and 1 mM $CaCl_2$ and filtered. The filtrate was subject to fast protein liquid chromatography utilising QMA

medium (Millipore) eluting with the same buffer. The fractionation was analysed on 6-15% SDS-polyacrylamide gels. The fractions were also analysed for f-D-dimer cleavage activity. This was determined by reacting each fraction with f-D-dimer in 0.1 M Tris, pH 7.4 containing 150 mM NaCl, 1 mM $CaCl_2$ and 1 mM zinc acetate and the cleavage products were monitored on 6-15% polyacrylamide gels. The active fractions were pooled and concentrated using CX-10 ultrafiltration units. These fractions were subject to molecular sieving on a Sephacryl S300 (Pharmacia) (100 x 2.5 cm) column. The fractions were analysed by SDS-PAGE as well as for cleavage activity.

2.3 Modification of fibrin-D-dimer with Diethylpyrocarbonate

Diethylpyrocarbonate (ethoxyformic anhydride) is a specific modification agent for histidine and tyrosine residues. Diethylpyrocarbonate (BDH), 6.78 M in ethanol, was added directly in 0.5µl aliquots to a 2.5 ml of 0.15mM fibrin-D-dimer solution in 0.1M Tris, pH 7.37 with continuous stirring to a final concentration of 5.42mM DEPC, at room temperature (Rogers et al, 1977). The modified protein DEPC-fibrin-D-dimer was then separated from excess reagent on a PD-10 Sephadex G-25M column (Pharmacia).

PD-10 G-25M columns are effective for desalting and removing low molecular weight molecules while large molecular weight molecules such as proteins pass through the gel filter unretarded. The columns were equilibrated with 25ml of 0.1M Tris, pH 7.37. The sample was loaded in 2.5ml and this eluant was discarded. The DEPC-fibrin-D-dimer was then eluted with 3.5ml 0.1M Tris, pH 7.37.

Regeneration of histidines

The diethypyrocarbonate modification of the histidine and tyrosine residues in fibrin-D-dimer protein fragment was reverted with hydroxylamine. To 2.0ml of the DEPC-fibrin-D-dimer solution in 0.1M Tris, pH 7.37; 0.5ml NH_2OH from a 360mM stock (25g/l) was added with stirring for 20 minutes at room temperature. The final hydroxylamine concentration was 59.5mM. All excess reagent was removed by gel filtration through PD-10 Sephadex G-25M columns (Melchior & Fahrner, 1970).

2.4 Assay Techniques

2.4.1 Polyacrylamide Gel Electrophoresis

Polyacrylamide gel electrophoresis of proteins and peptide fragments were performed as per method of Läemmli (1970) in the presence of 0.1% sodium dodecylsulphate. The SDS-polyacrylamide gels were set up isocratically or with density gradients. The electrophoresis was performed in a Hoefer model SE600 electrophoresis apparatus drawing power from a Hoefer PS1200DC power pack. A typical PAGE was run for $1^3/_4$ hours at 60mA at room temperature. All samples were treated with SDS before loading. In the case of analysis of reduced protein fragments, the disulphide bonds were reduced by incubation with β-mercaptoethanol. Gels were run in Tris/glycine/SDS (TGS) buffer at pH 8.6. The tank buffer was prepared by dissolving 14.4g glycine, 3g Tris and 1g sodium dodecylsulphate in H_2O made up to 1 litre.

The gels were stained in Commassie blue stain and destained in ethanol: acetic acid: water in 3:1:10 ratio. Commassie blue stain was prepared by dissolving 2.5g Commassie brilliant blue R-250 (Sigma), 250g trichloroacetic acid (Sigma) in 750ml methanol and 1550 ml

water. When greater sensitivity was required, a silver staining technique was used as described previously (De Moreno et al, 1985). Densitometric gel scans were performed on a Helena Cliniscan II Gel Scanner.

2.4.2 Protein Determinations

Protein concentrations were determined utilising the Biorad protein assay. The assay is based on the observation that the maximal absorbance for Commassie Brilliant blue G-250 in an acidic medium shifts from 465 to 595 nm upon conjugation of the dye with protein. Using the molar extinction coefficient of the dye-protein complex and the Beers-Lambert law, it is possible to determine the protein concentration spectrophotometrically (Spector, 1978). A calibration curve of OD_{595} vs concentration constructed from protein standards of known concentration and the protein concentrations of the unknown samples are calculated from the calibration curve.

The assay: To 100µl standard or unknown sample in a test tube, was added 5ml protein concentration dye reagent (Biorad). After standing for 5 min, absorbance was measured at 595nm.

2.4.3 Chromozyme PL assay for plasmin activity

Plasmin, activated from plasminogen by urokinase, was tested for activity using the substrate chromozym PL (Boeringer Mannheim). Chromozym PL, M_r 634.7, is tosylglycl-prolyl-lysine-4-nitroanilide acetate. The assay buffer comprised 10mM Hepes, 10mM Tris/HCl, pH 7.8, 100mM NaCl and 1% polyethylene glycol 6000.

The substrate was prepared by dissolving 20mg chromozym PL in 1ml water at pH 4.0 with HCl.

The assay was conducted as follows: To 1ml buffer in a cuvette was added 100µl substrate solution and 10µl plasmin/glycerol solution at 2.5 mg/ml. The assay was monitored spectrophotometrically at 405nm.

2.4.4 Assaying the fibrinolytic activity of Puffadder venom protease

The assay buffer used was 0.1M Tris, pH 7.4, 0.15M NaCl, 1mM $CaCl_2$ and 1mM $ZnCl_2$. The assay was conducted as follows: 20µl of f-D-dimer (17µg/µl)was added to 25µl buffer and 5µl PAV protease (28 µg/ml).

The reaction mixture was incubated for 90 minutes at 37°C. The reaction was terminated by adding an equal volume of SDS sample digest buffer containing EDTA. Samples were analysed on 6-15% SDS-polyacrylamide gels.

For the studies of pH dependence, zinc concentration dependence and effect of enzyme concentration, the respective parameters were varied while the other parameters were kept constant.

2.4.5 Differential Zinc Binding Study

F-D-dimer and PAV protease samples were incubated independently in 0.1M Tris, pH 8.0, 1mM Zn^{2+} buffer with 150mM NaCl for 90min at 25°C. Identical controls were set up in zinc-free 0.1M Tris, pH 8.0 containing 150mM NaCl. Extrinsic/unbound zinc was removed by a spin column procedure (Penefsky, 1977).

Spin column desalting: Spin columns were set up in 2ml syringes plugged with glass wool and polypropylene discs. The syringes were filled with swelled G25 sephadex (Pharmacia). The columns were packed by centrifugation at 1200 rpm for 2min. The eluant was

discarded. The samples were loaded onto the column in 100 µl volumes and spun at 2000 rpm for 5 min. The eluants were collected in Eppendorf micro test tubes positioned in the centrifuge tubes below the spin columns.

The zinc incubated substrate and enzyme eluates were mixed with zinc-free enzyme and substrate respectively and assayed for PAV protease f-D-dimer digestion activity in 0.1M Tris, pH 8.0 with 150mM NaCl and 1mM $CaCl_2$ in a time course study at 37°C. Aliquots of the reaction mixture were drawn at set time intervals and the reaction was stopped by the addition of an equivalent volume of SDS sample digest buffer containing 2mM EDTA and boiling. The protein products were analysed by PAGE 6-10% SDS-polyacrylamide gels (Laemmli, 1970). The gels were densitometrically scanned on a Helena Cliniscan II Gel Scanner.

2.4.6 Absorption Spectroscopy

Absorption Spectra were obtained on a Varian DMS 100 Spectrophotometer fitted with a thermostated cell holder. The temperature was controlled by an external waterbath (Haake). All absorption spectroscopic studies were performed at 25°C in 1cm quartz cuvettes (Helma).

2.4.6.1 Stoichiometric Determinations

The wavelength of maximum absorption and molar extinction coefficient of dansylcadaverine were determined from the absorption spectrum of a stock solution of the fluorescent lysine analogue and application of the Beer's-Lambert law. The stoichiometry of the fluorescent dansyl groups per molecule f-D-dimer was calculated

from the difference spectra of dansylcadaverine conjugated f-D-dimer against the non-fluorescent protein (fibrin-D-dimer) over the range 220nm to 600nm.

2.4.6.2 Cobalt-D-dimer Spectra

Fibrin-D-dimer was diluted to 1.425 x 10^{-4}M in 0.1M Tris, pH 7.4 degassed with helium. The spectrophotometer was baseline corrected for the buffer and the protein spectra in the visible wavelength range. Cobalt difference spectra were observed over the range 350nm to 800nm by titrating with $CoCl_2$ in 3mM increments.

Similar spectral studies were conducted with diethylpyrocarbonate modified fibrin-D-dimer and with hydroxylamine-reverted DEPC-fibrin-D-dimer.

2.4.7 Fluorescence Spectroscopy

Fluorimetric monitoring of the PAV protease cleavage of f-D-dimer and the extrinsic fluorescence measurements were performed on a Hitachi F-3000 Fluorescence Spectrophotometer fitted with a thermostated cell holder using 1 cm quartz cells (Helma). The cell temperature was regulated by an external waterbath.

2.4.7.1 PAV Digestion of f-D-dimer

The wavelengths of maximum excitation and emission for dansyl fluorescence were determined by performing excitation and emission scans independently. These were resolved at excitation: 340nm, emission: 520nm. All subsequent dansyl fluorescence measurements were performed using these wavelength parameters. The rate of cleavage of f-D-dimer by PAV protease was monitored as

the rate of decay of the absolute fluorescence of the dansyl fluorophore in the fluorescent conjugated substrate. The assay was performed as follows: To cuvette was added 100µl of a 8.25 x 10^{-5}M f-D-dimer solution and 900µl of assay buffer: 0.1M Tris, pH 8.0, 150mM NaCl, 1mM Ca^{2+}.

To examine the effect of zinc(II), the reaction was conducted in the presence of 1mM zinc acetate. The reaction mixtures in the cuvette were stirred and incubated at 37°C and monitored fluorimetrically - excitation: 340nm, emission: 520nm - in a time scan mode.

2.4.7.2 Zinc Titration of Fibrin-D-dimer

Fibrin-D-dimer (1.78 x 10^{-7}M) in 0.1M Tris, pH 8.0 containing 150mM NaCl was titrated with Zn^{2+} at 25°C. The zinc stock solution used was concentrated (100mM zinc acetate) to reduce the dilution effects. The binding of zinc to the dimer molecules was monitored by determining the change in the protein intrinsic fluorescence that is dominated by tryptophan (experimental sensitivity $\varepsilon\Phi F = 11 \times 10^{-2}$). The experimental sensitivity of a fluorophore is a product of the molar extinction coefficient and the fluorescence quantum yield (OF) (Cantor & Schimmel, 1980). Tryptophan fluorescence was determined with excitation wavelength 280nm; emission 340nm (ref). Zn^{2+} titration of DEPC modified fibrin-D-dimer was performed under the same conditions.

2.4.8 Fluorescence Anisotropy

Fluorescence polarisation measurements were performed on an Aminco SPF-500 Ratio Spectrofluorimeter fitted with a thermostated cell holder. The temperature was controlled by an external circulating

waterbath (Haake) fitted with a heater and compressor unit. The sample temperature was measured with a precalibrated digital thermometer with a probe inserted in a spare cuvette filled with 20% sucrose in the sample chamber. The sample chamber was flushed with dry nitrogen to prevent condensation. Fluorescence polarisation intensity measurements were taken over the temperature range 4^{o}C to 40^{o}C.

Fluorescence anisotropy (r) was calculated using equation 1 (Cantor & Schimmel, 1980).

$$r = \frac{I_{II} - gI_I}{I_{II} + 2gI_I}$$

where I_{II} is the fluorescence intensity (in arbitory units when the excitation and emission polarised are in parallel and I_I is the fluorescence intensity with the polarisors perpendicular. The instrumental correction factor (g) consisted of the ratio of vertically to horizontally polarised emission with the excitation polariser in the horizontal plane (Brand & Witholt, 1967).

2.5. EDTA Inhibition of PAV Protease Digestion of f-D-dimer

Samples (5ml) of PAV protease in 0.1M Tris, pH 7.4, 150mM NaCl were incubated with varying concentrations of EDTA - E1 : 0mM, E2 : 2mM, E3 : 4mM, E4 : 10mM and E5 : 50mM EDTA for 10 min at 35°C in a total volume of 25µl each. The EDTA incubated PAV protease samples and controls (0.5 µl enzyme/25 µl reaction solution) were individually mixed with 10µl f-D-dimer and 12.5µl, 0.1M Tris, pH 7.4, 150mM NaCl buffer. The mixtures were incubated at 37°C for 20 min and reactions were stopped by boiling with an equal volume of SDS sample digest buffer. The samples were analysed on 6-15% SDS polyacrylamide gels for D-dimer cleavage activity.

Zinc and EDTA incubated PAV protease

The effect of Zn^{2+} on the EDTA inhibition of PAV protease activity was investigated as follows. Zn^{2+} from a 100mM Zinc acetate stock solution was added to samples from E2 to E5 in amounts to render the added EDTA and Zn^{2+} equimolar;eg. to E3 that was incubated in 4mM EDTA, Zn^{2+} was added to a final concentration of 4mM. Samples E6 - E9 now contained equimolar amounts of EDTA and Zn^{2+} ranging from 2mM to 50mM. The enzyme samples E6 - E9 were mixed with f-D-dimer and tested for f-D-dimer cleavage activity as described above.

2.6 Computer modelling was done using the 'Desk Top Molecular Modeller' modeling programme available from Oxford University Press. The coordinates of the atoms in the crosslink peptide were estimated from a model built utilising a modelling kit and the structure was optimised using DTMM.

The computer programme ESTA (Equilibrium Simulation for Titration Analysis) was used in determining the concentration of the free zinc(II) species in solution when analysing the binding of zinc(II) to f-D-dimer as monitored by changes in the intrinsic fluorescence of the protein fragment. The free zinc(II) was determined by setting up the appropriate model of all the species in the reaction solution and their respective formation constants (see results) and the programme calculated the equilibrium distribution of the chemical species in solution.

3. RESULTS

3.1 Purification of f-D-dimer, f-D-monomer and fibrin-D-dimer.

The plasmin digest of the fibrin clot contained three major protein components : the fluorescent f-D-dimer, f-D-monomer and non-fluorescent E fragments. The digest was dialysed against 5 mM Tris, pH 8.6, 1 mM $CaCl_2$. The dialysate was fractionated on a DE-52 ion exchange column (Fig.13) using a 0-300 mM NaCl gradient. The f-D-dimer and f-D-monomer fragments eluted between 143mM and 196mM NaCl. The E fragment eluted between 196mM and 250mM NaCl. The f-D-dimer and f-D-monomer containing fractions were pooled, concentrated and loaded in 1.5 ml volumes onto a (100 x 2.5 cm) AcA 34 (Ultrogel) molecular sieve column. The molecular sieving resulted in the complete separation of the monomer and dimer as evidenced in the SDS-PAGE analysis (Fig.14).

3.2 Purification of the PAV Protease

The clear yellow filtrate of Puffadder venom in 0.1 M Tris, pH 7.4, 0.15 M NaCl, 1 mM $CaCl_2$ was fractionated on a Mono Q column (Millipore). The fractionation was analysed on 6-20% SDS-polyacrylamide gels (Fig.15b). Analysis of the f-D-dimer cleavage activity of the fractions (Fig.15c) associates the activity with an approximately 25000 dalton fragment. The highly active fractions were pooled, concentrated and gel filtered on a Sephacryl S300 column. No further fractionation was observed, however, this partially purified preparation proved adequate for the subsequent digestion experiments and no other contaminating activities were observed.

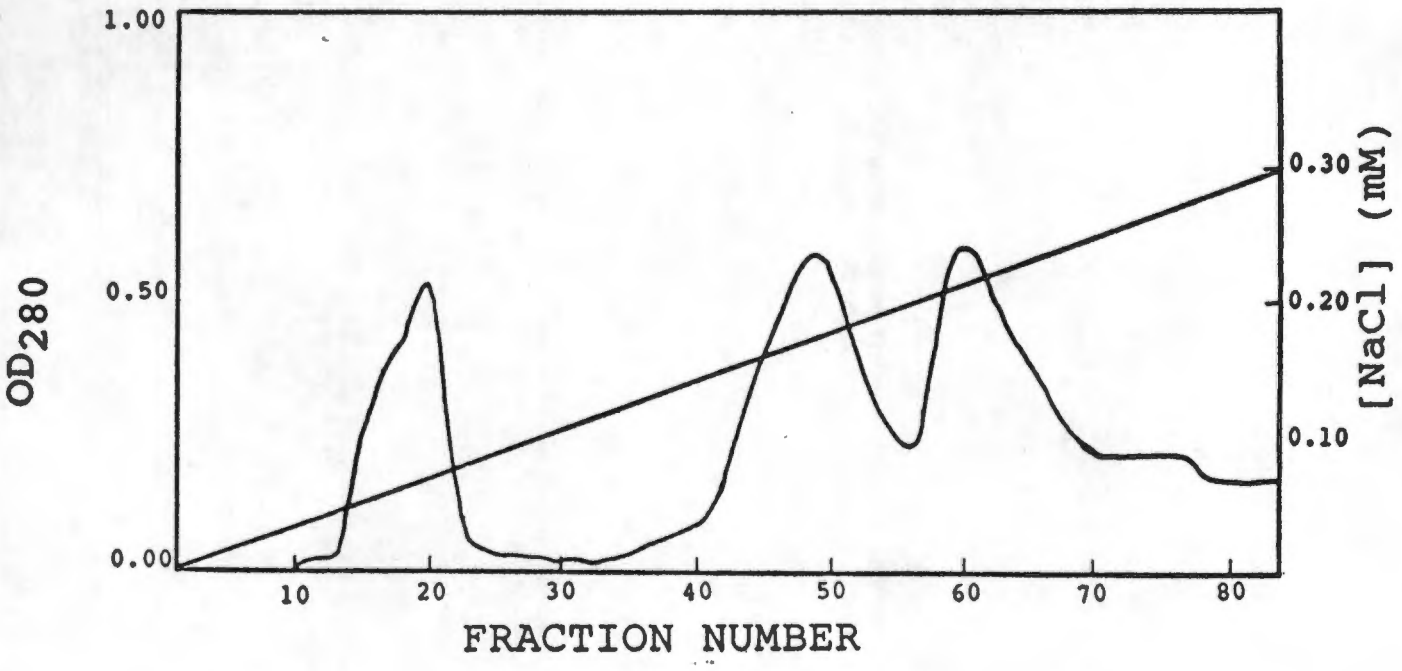

Figure 13: The anion exchange fractionation of a plasmic digest of fibrin. The fibrin degradation products were eluted with a 0-300 mM NaCl gradient from a DE-52 (Whatman) (25 x 1cm) column. The flow rate was 90 ml/hr.

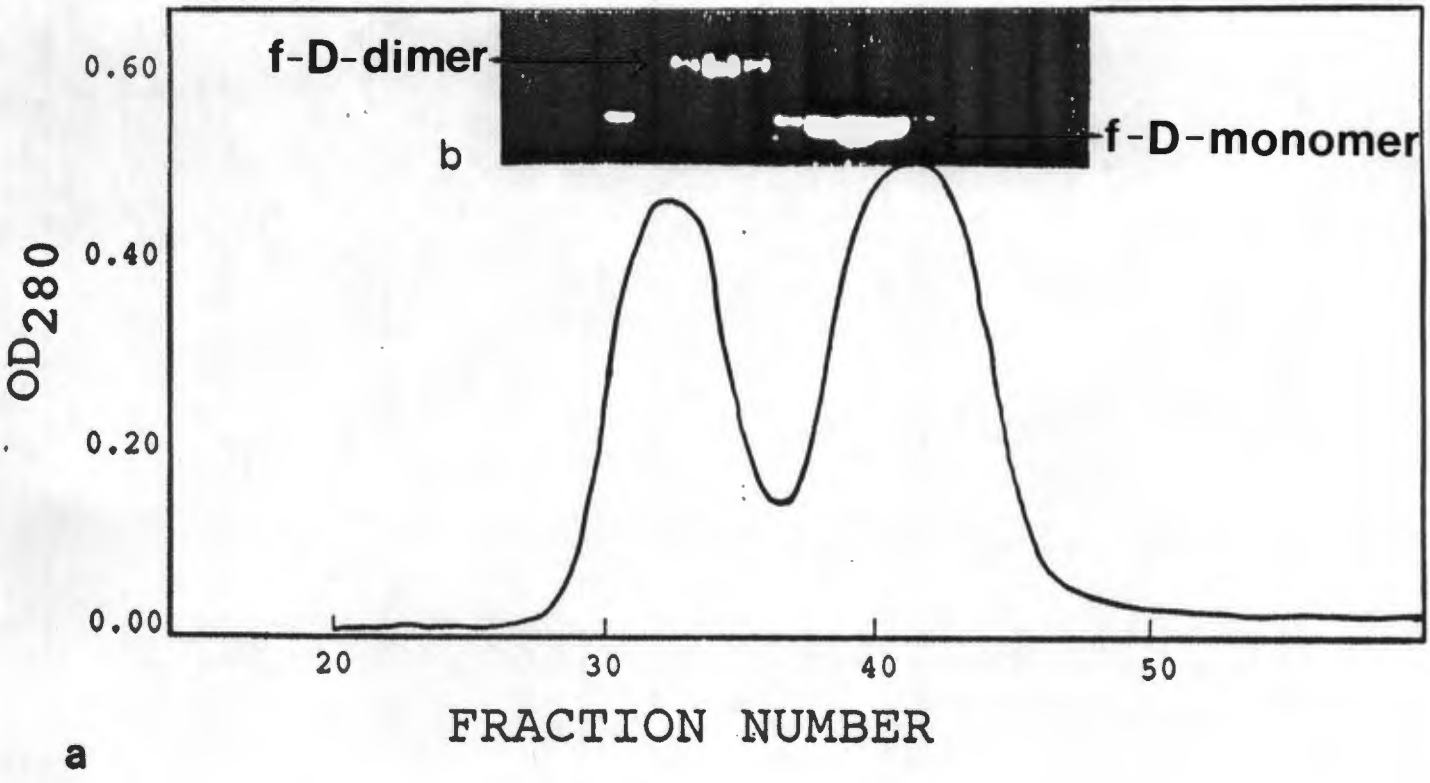

Figure 14: The molecular sieving of the f-D-dimer and f-D-monomer containing fractions from the anion exchange fractionation.

a) The fractionation was conducted on a (100 x 2.5cm) AcA34 (Ultrogel) column eluting with 0.1 M Tris pH 7.5, 150 mM NaCl, 1mM $CaCl_2$ and 4 M urea.

b) The fractionation was analysed on a 6-15% SDS-PAGE. The fluorescent bands were visualised under UV-light (above).

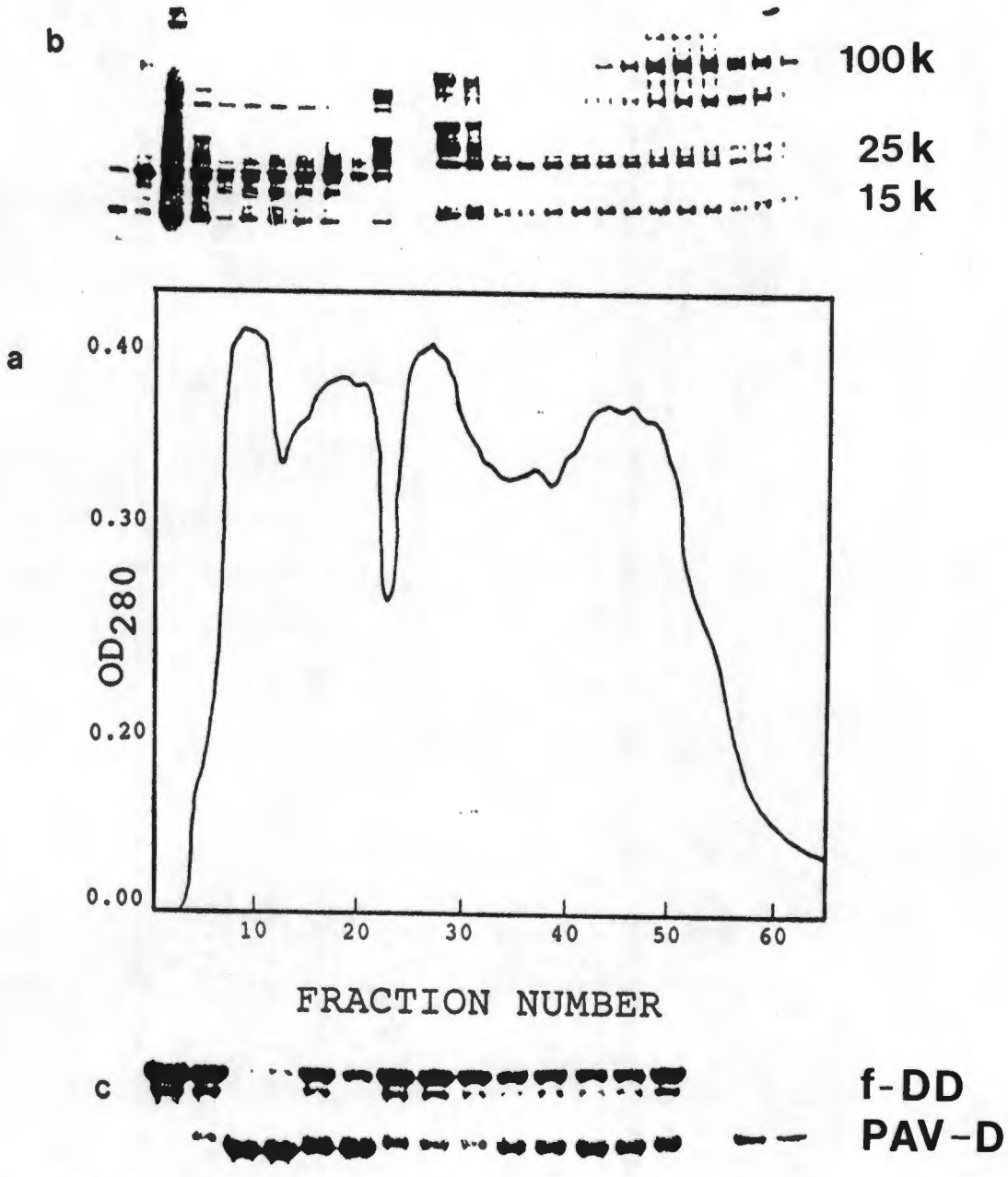

Figure 15: Crude puffadder venom was subjected to ion exchange chromatography on a QMA (medium) monoQ (Millipore) column by FPLC. The elution buffer used was 0.1M Tris pH 7.4, 150mM NaCl and 1mM $CaCl_2$.

b) The fractions were analysed by 6-15% SDS-PAGE.

c) The fractions were analysed for f-D-dimer cleavage activity (see text). The reaction mixtures were analysed by 6-15% SDS-PAGE

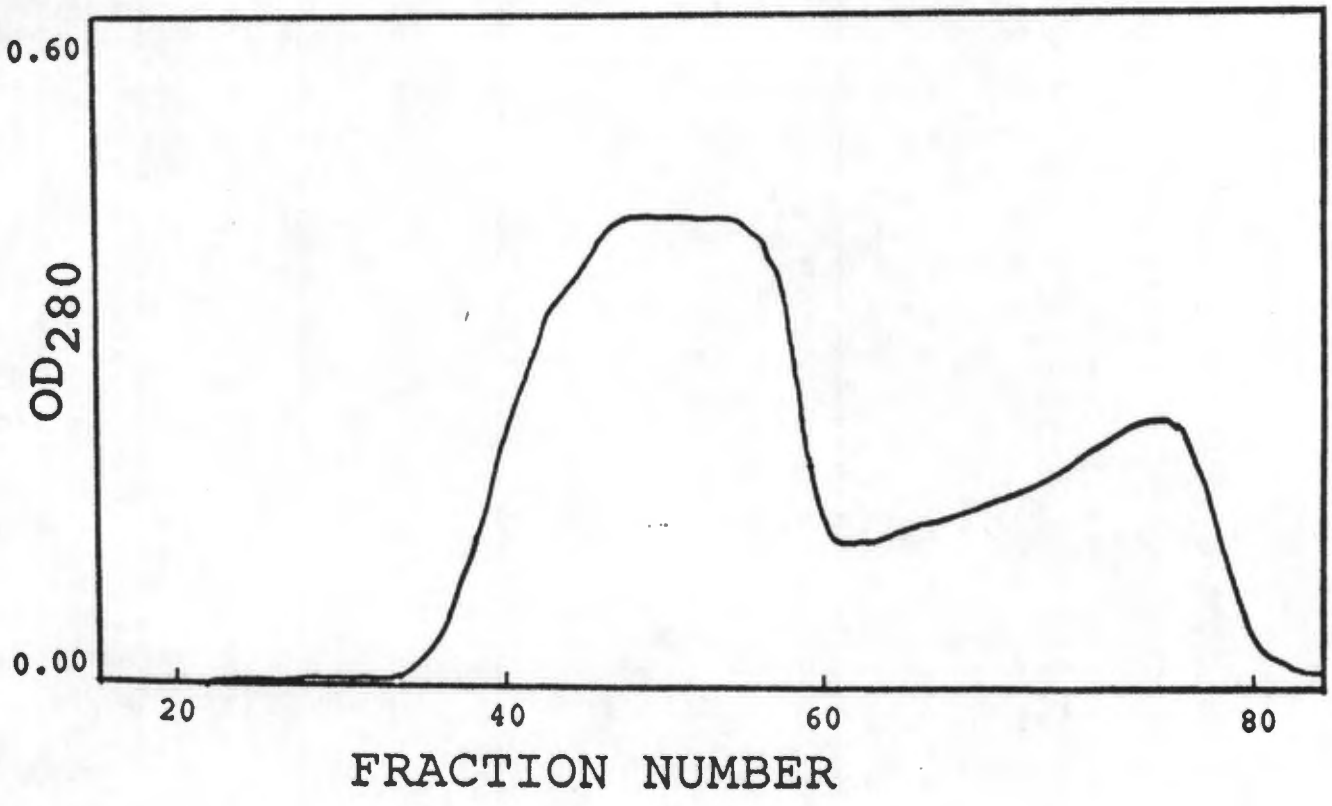

Figure 16: The gel filtration of the active PAV protease fractions from the QMA ion exchange chromatography.

3.3 Fluorescent-D-dimer and Fluorescent-D-monomer Dansylcadaverine Stoichiometry

The absorption spectrum of a standard solution of dansylcadaverine (1.52×10^{-4}M) in 0.1M Tris, pH 8.0, 150mM NaCl, 1mM $CaCl_2$, yielded an absorbance maximum at 326nm. The Beer-Lambert law $A = \varepsilon cl$ was used to determine the molar extinction coefficient maximum of the dansyl group : $\varepsilon = 3.56 \times 10^3\ M^{-1}\ cm^{-1}$.

Analysis of the difference spectra of f-D-dimer against non-fluorescent fibrin-D-dimer (Fig.18b) calculated a ratio of dansylcadaverine: f-D-dimer = 1.218×10^{-5}M: 7.25×10^{-6}M. This reduces to a stoichiometry of 1.77:1.

The dansylcadaverine: f-D-monomer stoichiometry was calculated as 1.09:1 in a similar manner.

Determination of the fluorescence/concentration ratios.
For this investigation, three random f-D-dimer samples and three f-D-monomer samples were chosen from the molecular sieved fractions from Ultrogel AcA34 fractionation. The sample purity was checked by SDS-PAGE. The protein concentration of each sample was accurately determined using the BioRad method and the absolute fluorescence - excitation: 340nm, emission: 520nm - was determined.

From the data, the absolute fluorescence/protein ratio was determined. The ratio of the absolute fluorescence per protein molecule of f-D-dimer to f-D-monomer was calculated as 2.05:1.

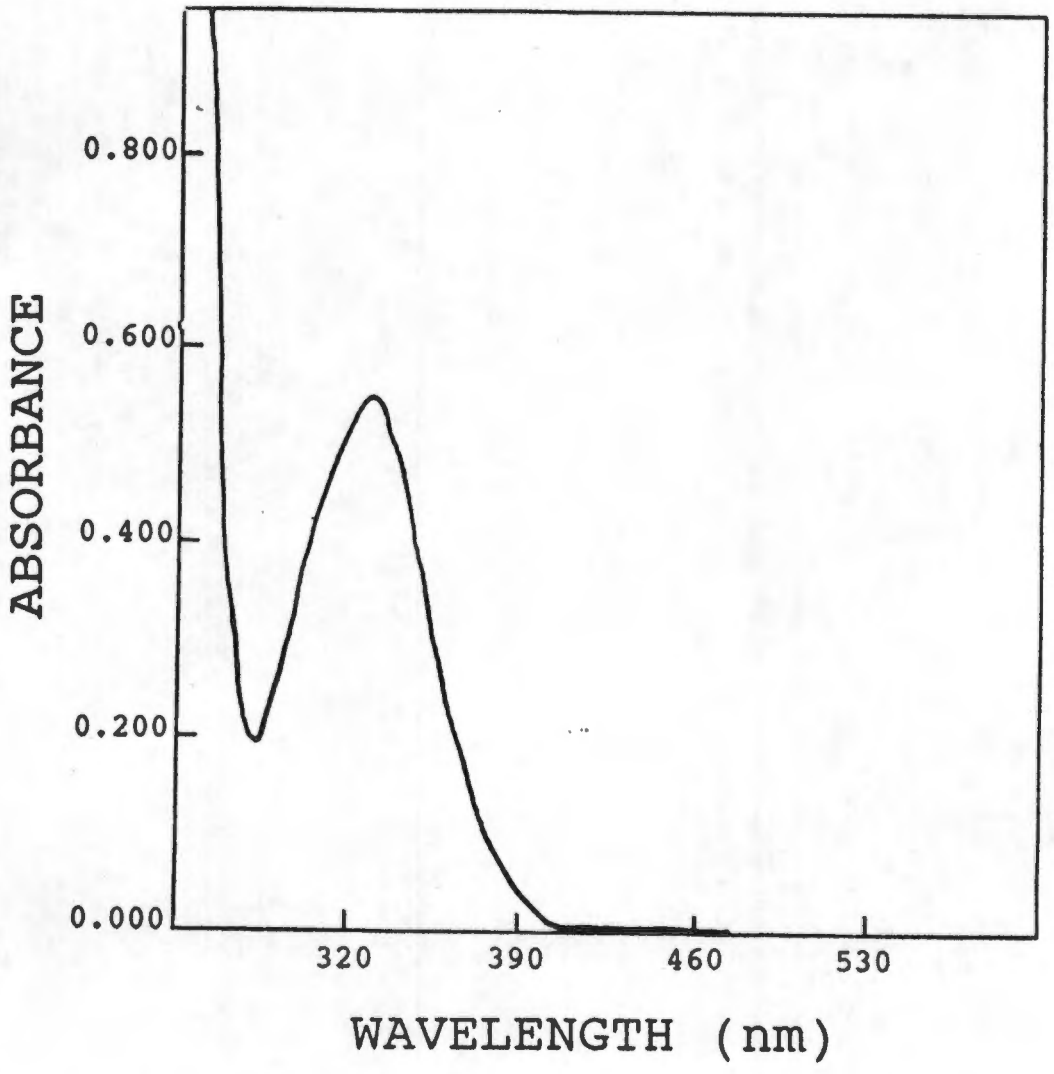

Figure 17: The Absorption profile of dansylcadaverine in 0.1 M Tris pH 8.0, 150mM NaCl, 1mM $CaCl_2$. Peak maximum was observed at 326 nm.

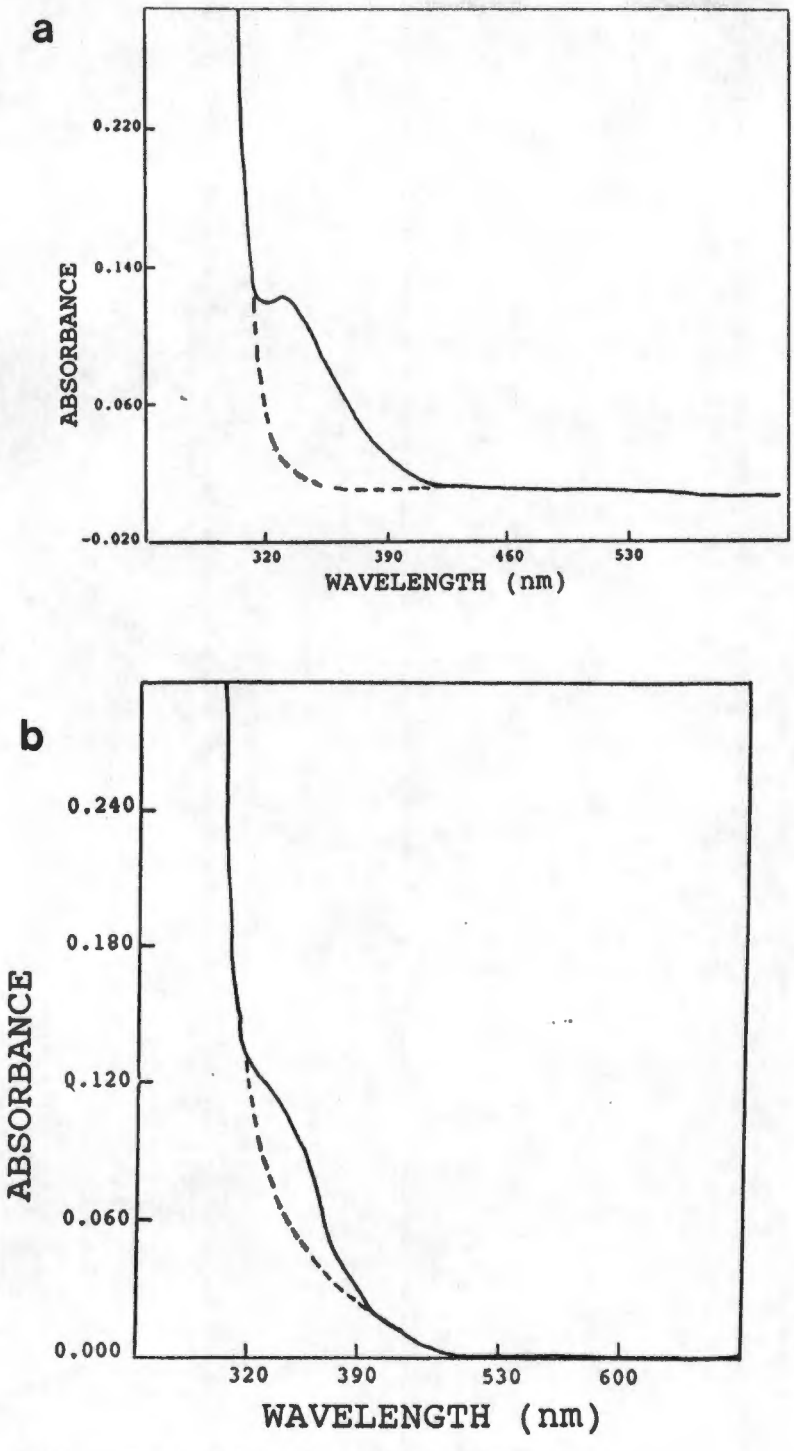

Figure 18: The UV absorption profile of

a) f-D-monomer in 0.1M Tris 8.0, 150mM NaCl, 1mM $CaCl_2$. The dashed line represents the absorption profile of non-fluorescent fibrin-D-monomer.

b) F-D-dimer in the buffer above. The absorption profile of non-fluorescent fibrin-D-dimer (---) was subtracted from the f-D-dimer spectrum to calculate the dansylcadaverine: f-D-dimer stoichiometry (see text).

3.4 The Phenomenon of PAV Protease f-D-dimer cleavage

3.4.1 The PAV protease cleavage of f-D-dimer

The digestion of f-D-dimer with PAV protease in 0.1 M Tris, pH 7.4, 0.15 M NaCl, 1mM $CaCl_2$ and 1 mM zinc acetate results in the cleavage of the di-γ-chain and digestion of the β-chain. Time course studies analysed on SDS-PAGE indicate that the monomerisation of the dimer by cleavage of the di-γ-chain to produce PAV-D-monomer, a peptide fragment of lower molecular weight than the plasmin-derived monomer is the first event, followed by the subsequent hydrolysis of the β-chain.

The pH dependence of the digestion was tested over a wide pH range (Fig.19). The enzyme is active over the range pH 6.4 - pH 9.75 but maximal in the pH range 7.0 - 8.0.

3.4.2 Extrinsic Fluorescence of f-D-dimer during PAV Digestion

The decrease of absolute fluorescence of f-D-dimer is an indication of the cleavage of the substrate (Purves et al, 1986). The fluorescence decay data (Fig. 21) was fitted by a least squares method using the Levenberg-Marquardt algorithm (Marquardt, 1963). The f-D-dimer cleavage data, both in the presence and absence of zinc was fitted best by a biexponential (equation 2), implying a biphasic reaction. The fit lead to the deduction that a rapid phase occurs first followed by a slower second phase.

$$y = F_{\infty} + \Delta F_{fast}\, e^{-k_{fast}.t} + \Delta F_{fast}\, e^{-k_{slow}.t}$$

where F = fluorescence (Ex 340nm, Em 520nm) at saturation.

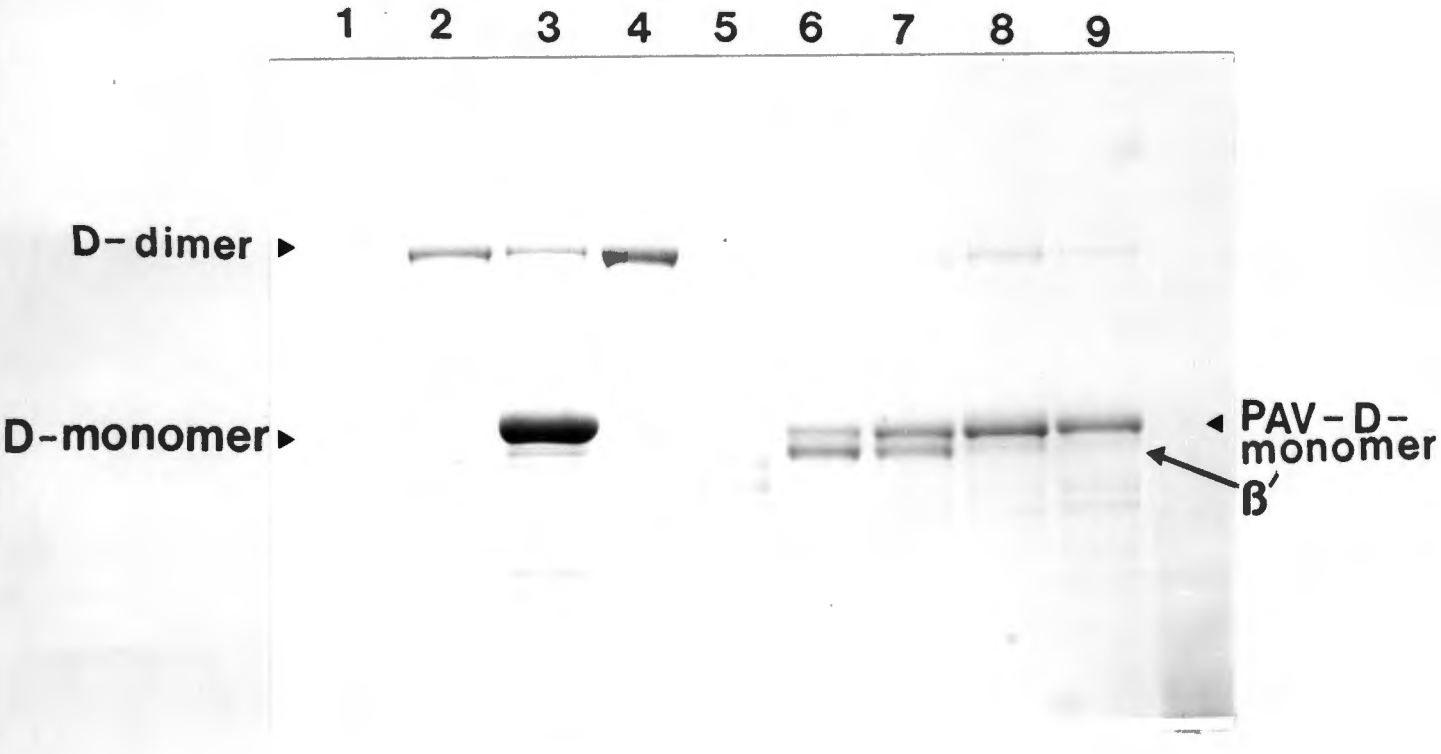

Figure 19: The pH-dependence of the PAV protease digestion of f-D-dimer. Lanes 2 and 3 are the f-D-dimer and f-D-monomer. The activity was tested at pH 1.75
(Lane 4), pH 3.35 (Lane 5), pH 6.40 (Lane 6), pH 7.53 (Lane 7), pH 8.36 (Lane 8) and pH 9.75 (Lane 9).

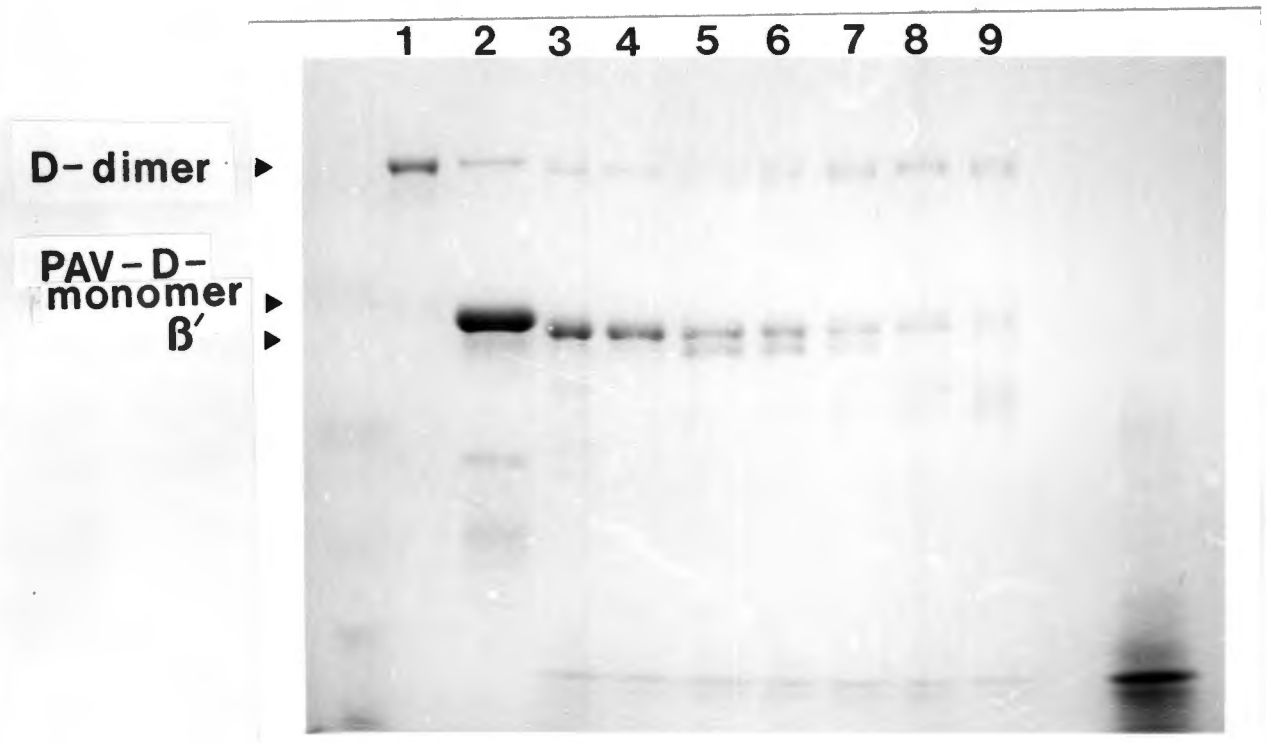

Figure 20: Effect of zinc(II) ions on the PAV protease digestion of f-D-dimer. The digestion was conducted in 0.1M Tris, pH 7.4, 150mM NaCl, 1mM $CaCl_2$ and, 0mM zinc(II) (Lane 4), 0.5mM zinc(II) (Lane 5), 1mM zinc(II) (Lane 6), 2mM zinc(II) (Lane 7), 5mM zinc(II) (Lane 8) and 10mM zinc(II) (Lane 9). The cleavage of the di-γ-chain occurred at all concentrations of zinc(II) with optimum activity in the range 0.5 - 1.0mM. The digestion of the β-chain occurred over the range 0.5mM - 2mM.

ΔF_{fast} = change in fluorescence for the fast phase of the reaction.

ΔF_{slow} = change in fluorescence for the slow phase

k_{fast} and k_{slow} are the reaction rate constants for the fast and slow phases respectively.

The rate constants of the PAV protease digestion of f-D-dimer in 0.1M Tris, pH 8.0, 150mM NaCl, 1mM $CaCl_2$ were

$k_{fast} = 0.220 \pm 0.040\ min^{-1}$

$k_{slow} = 0.044 \pm 0.017\ min^{-1}$

The rate constants of the PAV protease digestion of f-D-dimer in 0.1M Tris, pH 8.0, 150mM NaCl, 1mM $CaCl_2$, 1mM Zn^{2+} were

$k_{fast} = 0.910 \pm 0.010\ min^{-1}$.

$k_{slow} = 0.100 \pm 0.070\ min^{-1}$

The flourescence data of f-D-monomer PAV protease digestion in 0.1M Tris, pH 8.0, 150mM NaCl, 1mM $CaCl_2$ was fitted to a monoexponential curve:

$$F(t) = F_{oo} + (F_o - F_{oo})\, e^{-kt}$$

where F_o = Fluorescence at t = 0

indicating a monotonic decay. The rate constant was calculated at $k = 0.433 \pm 0.017\ min^{-1}$.

The results indicate that for the PAV protease digestion of f-D-dimer, a 4.136 fold protentiation of activity in the presence of Zn^{2+} ions was noted.

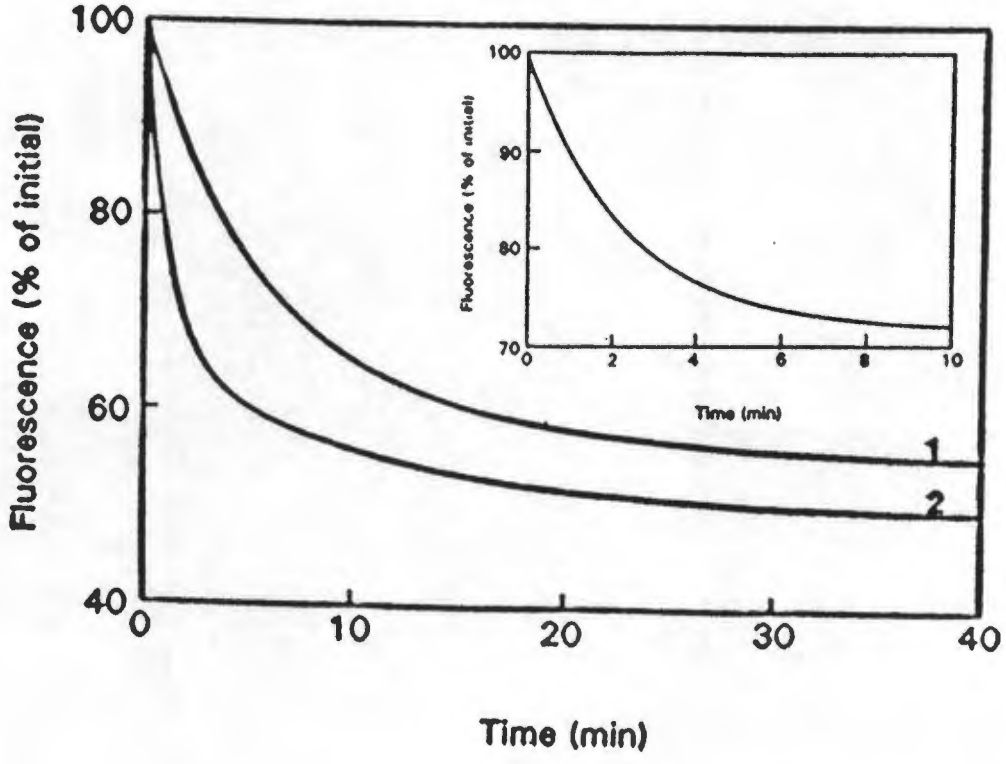

Figure 21: Effect of zinc ions on the PAV protease digestion of f-D-dimer. The progress of the reaction was monitored by measuring the decay of fluorescence of the conjugated dansyl moiety - excitation 340 nm; emission 520 nm - expressed as a percentage of initial fluorescence. The digestion conducted (1) in the absence of zinc ions and (2) in the presence of 1 mM Zn^{2+} (zinc acetate). Points on the curve were digitised at regular intervals utilising a graphics tablet (Summa Sketch II) and analysed by least squares. The protease cleavage of f-D-dimer was potentiated 4.136-fold in the presence of zinc ions.(k_{fast} = 0.91 $\pm$ 0.01; k_{slow} = 0.01 $\pm$ 0.07)
Inset: The PAV protease digestion of f-D-monomer. Monotonic decay was observed indicating a monophasic reaction. The rate constant was calculated at k = 0.043 $\pm$ 0.02.

3.4.3 EDTA inhibition of PAV protease f-D-dimer cleavage activity

PAV protease has been shown to be unaffected by protease inhibitors such as phenylmethylsulphonyl fluoride and hexanediamine (Purves 1986). The EDTA inhibition of PAV protease cleavage of f-D-dimer was evaluated by a measure of f-D-dimer substrate remaining uncleaved after 20 minutes reaction (Fig.22a).

The control enzyme sample untreated with EDTA or zinc, cleaved 51% of the f-D-dimer substrate after 20 min; the E2 sample (in 2mM EDTA) cleaved 8.82%, E3 (4mM EDTA) 5.03%, E4 (10mM EDTA) 1.87% and E5 (50mM EDTA) displayed 100% inhibition of activity.

The Zinc treated EDTA incubates of the enzyme displayed a regeneration of activity to varying degrees. The activity of the enzyme sample incubated in 50mM EDTA could not be regenerated with zinc.

PAV protease is a zinc metalloproteinase and EDTA (ethylenediamine tetra-acetic acid) is a metal ion chelator. The PAV protease cleavage of f-D-dimer proceeds even in the absence of extrinsic zinc, therefore EDTA inhibition of activity must result from a chelation of zinc or other metal cations bound to the enzyme. This chelation alters the enzyme structure sufficiently to affect inhibition. The inhibition was approximately 82% at 2mM EDTA and 100% at 50mM EDTA. The activity was regenerated in some incubates by adding zinc to the EDTA incubated enzyme in equimolar quantities. The zinc treated samples of enzyme incubated with 2mM (E6) and 4mM (E7) EDTA were regenerated to 100% activity and there was sufficient Zn^{2+} in excess to potentiate the activity even further. The 10mM (E8) EDTA incubate was regenerated to 46% activity and the 50mM (E9)

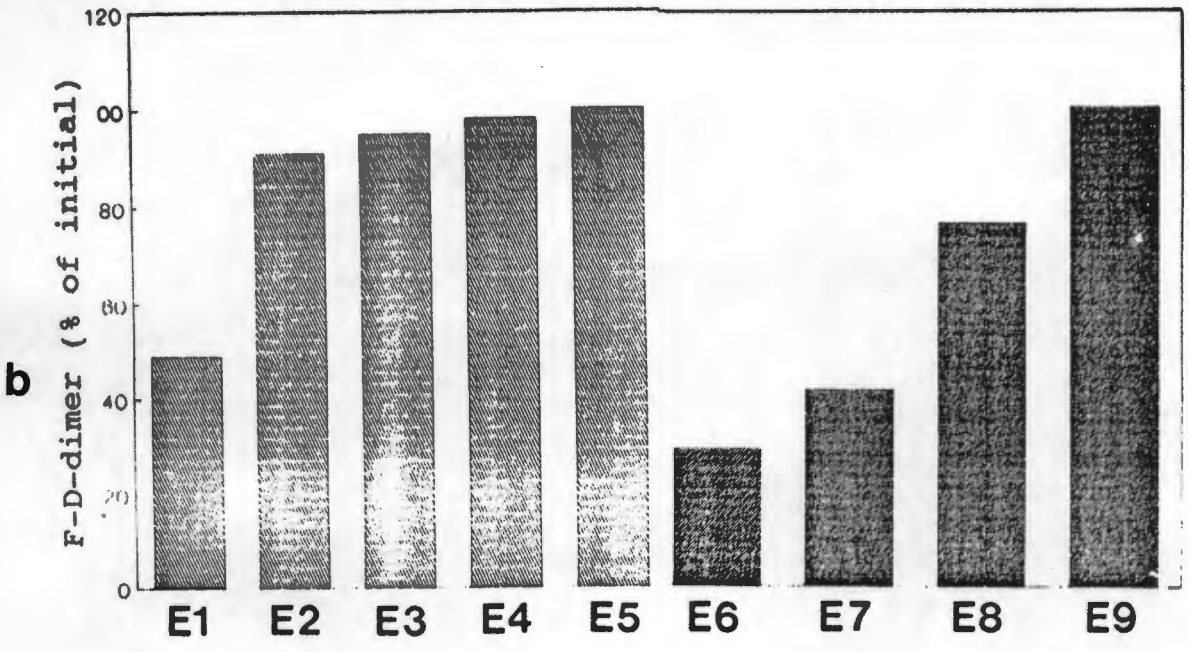

Figure 22: The EDTA inhibition of PAV protease digestion of f-D-dimer and regeneration of activity by the addition of zinc(II).
The EDTA incubates and the zinc treated EDTA incubates of PAV protease were tested for f-D-dimer digestion activity (see text).

a) The reactions were analysed by SDS-PAGE; f-D-dimer was incubated with E1 (Lane 4), E2 (Lane 5), E3 (Lane 6), E4 (Lane 7), E5 (Lane 8), E6 (Lane 9), E7 (Lane 10), E8 (Lane 11), E9 (Lane 12).

b) The densitometric analysis of the EDTA treated PAV protease samples and the zinc treated EDTA incubated PAV protease samples..

EDTA incubate not at all. This leads to the speculation that the zinc atoms bound to the enzyme protein are divided into structural and catalytic types. The inhibition resulting from the chelation of catalytic zincs at lower EDTA concentrations was easily reversed with zinc addition, but at higher EDTA concentrations, structural zincs were chelated out of the enzyme inducing irreversible structural changes and thus, activity could not be regenerated.

3.5 Zinc and the D-dimer fragment

3.5.1 Differential Zinc Binding Study

The differential zinc binding study provided a means of determining whether the zinc potentiation of fibrin-D-dimer digestion by the snake venom enzyme was due to a zinc-substrate interaction, a zinc-enzyme interaction or both.

The gel scan data for both the zinc incubated substrate and native substrate were fitted best by least squares to bi-exponential equations corroborating the fluorescence data (Fig. 23). The snake venom digestion of the zinc bound f-D-dimer species yielded a rapid phase rate constant
$k_{fast} = 0.55 \pm 0.04\ min^{-1}$ and the native f-D-dimer species
$k_{fast} = 0.20 \pm 0.06\ min^{-1}$. This represents a zinc potentiation of 2.75 fold. The zinc incubated PAV protease yielded negligible potentiation of activity when compared with the native enzyme.

3.5.2 Intrinsic Fluorescence changes in f-D-dimer due to Zinc binding

The intrinsic fluorescence of proteins is due primarily to tryptophan residues [experimental sensitivity ($E\Phi_F = 11 \times 10^{-2}$)] with additive

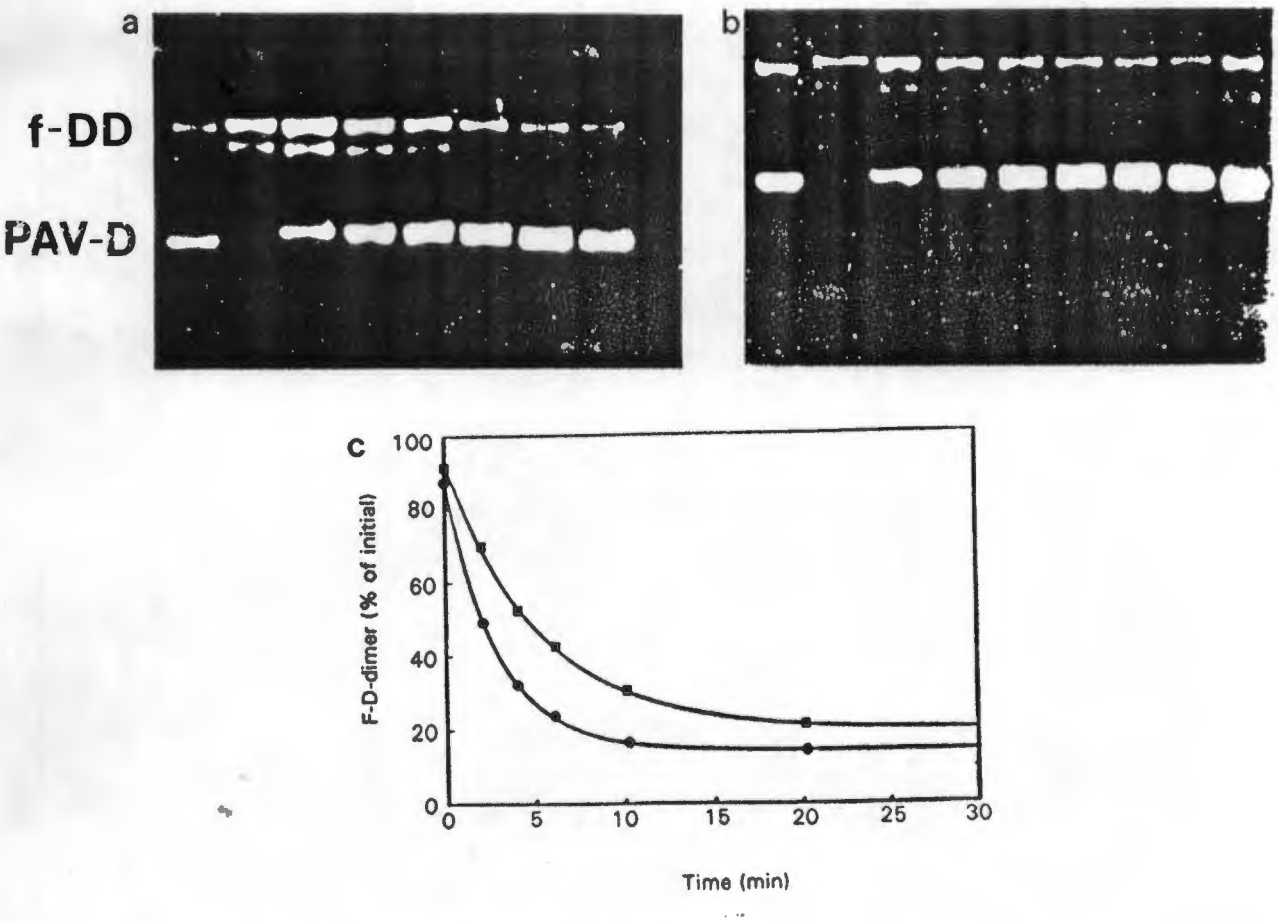

Figure 23: The differential zinc study.

a) 6-10% SDS-PAGE of a time course reaction of the PAV protease digestion of native f-D-dimer (i).

b) 6-10% SDS-PAGE of the time course reaction of the PAV protease digestion of f-D-dimer incubated with 1mM zinc. Zinc acetate (ii).

c) The densitometric quantitation of f-D-dimer substrate during the PAV digestion in zinc free buffer.

i) f-D-dimer incubated in 0.1M Tris, pH 7.4, 150mM NaCl, 1mM $CaCl_2$ (■).

ii) f-D-dimer incubated in 1 mM zinc acetate, 0.1 M Tris, pH 7.4, 150mM naCl, 1mM $CaCl_2$ (●).

Free zinc was removed by a G25 spin column procedure before the f-D-dimer was added to the PAV.

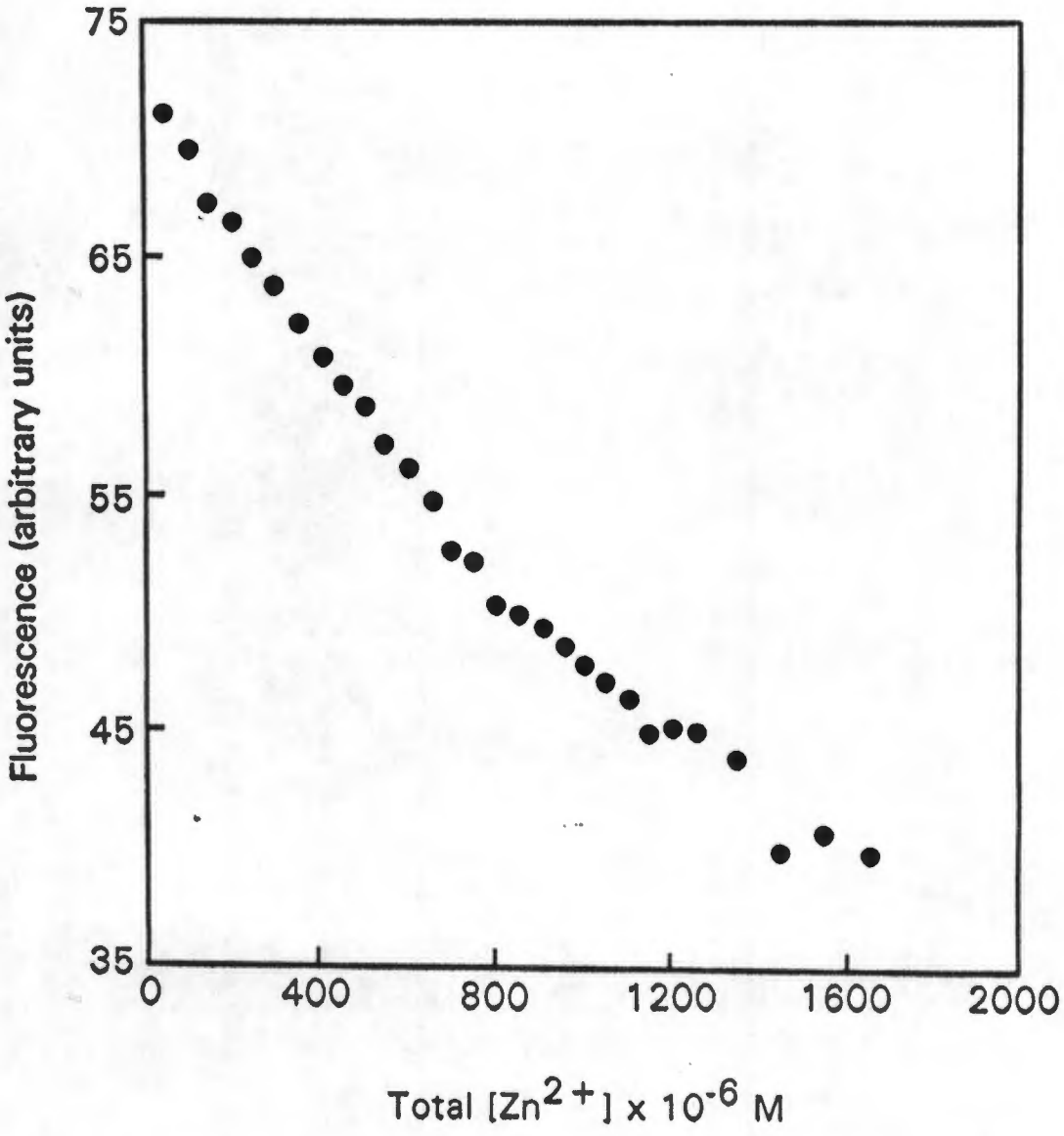

Figure 24: Intrinsic fluorescence changes during titration of f-D-dimer samples (1.78×10^{-7} M) in 0.1 M Tris, pH 8.0 were titrated with increments of zinc(II) ions. The change in tryptophan fluorescence was used to monitor the binding (see text). Intrinsic fluorescence was determined - excitation, 280 nm; emission 340 nm.

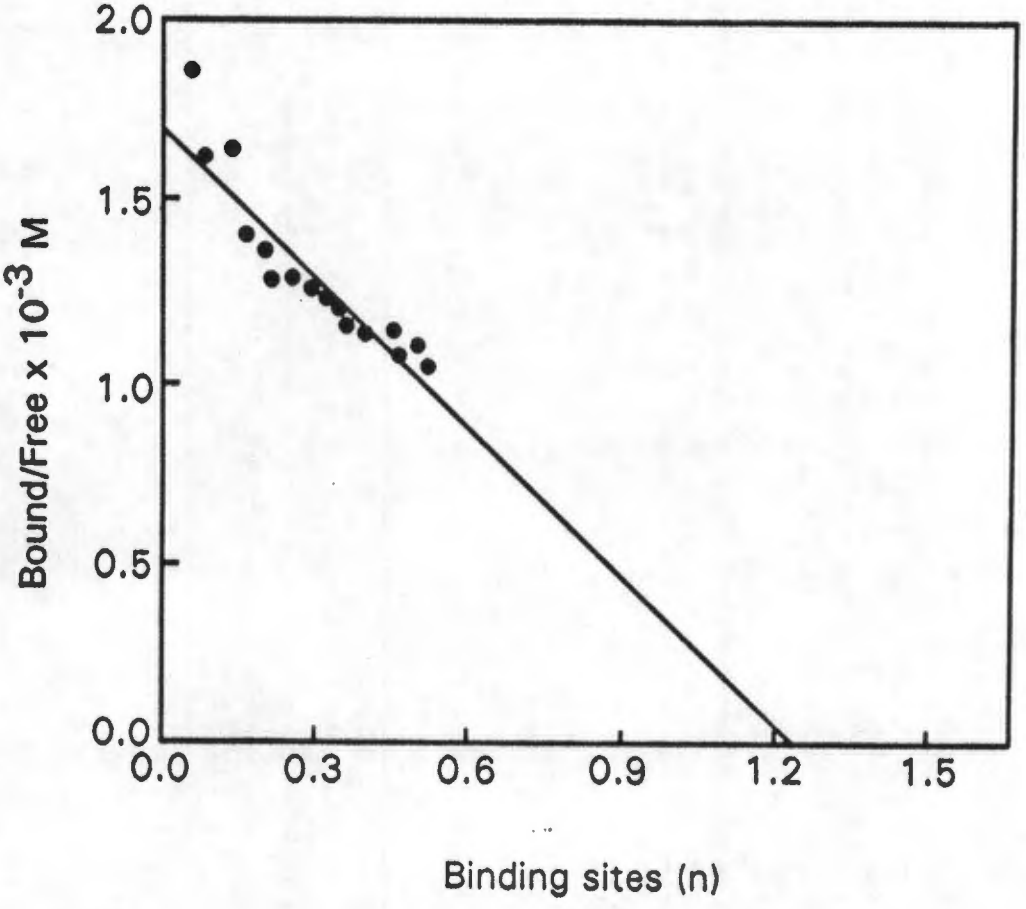

Figure 25: Scatchard plot analysis of zinc binding to f-D-dimer. The data was fitted using least squares. The plot yielded a slope ($-k_D$) of $-7594 \pm 9.96\ M^{-1}$ and Y intercept of

$$1.706 \times 10^{-3} \pm 0.06 \times 10^{-3}.$$

The X intercept yields binding sites

n = 1.26. Data points at high $[Zn^{2+}]$ could not be reliably obtained due to the formation of significant concentrations of insoluble zincate complexes.

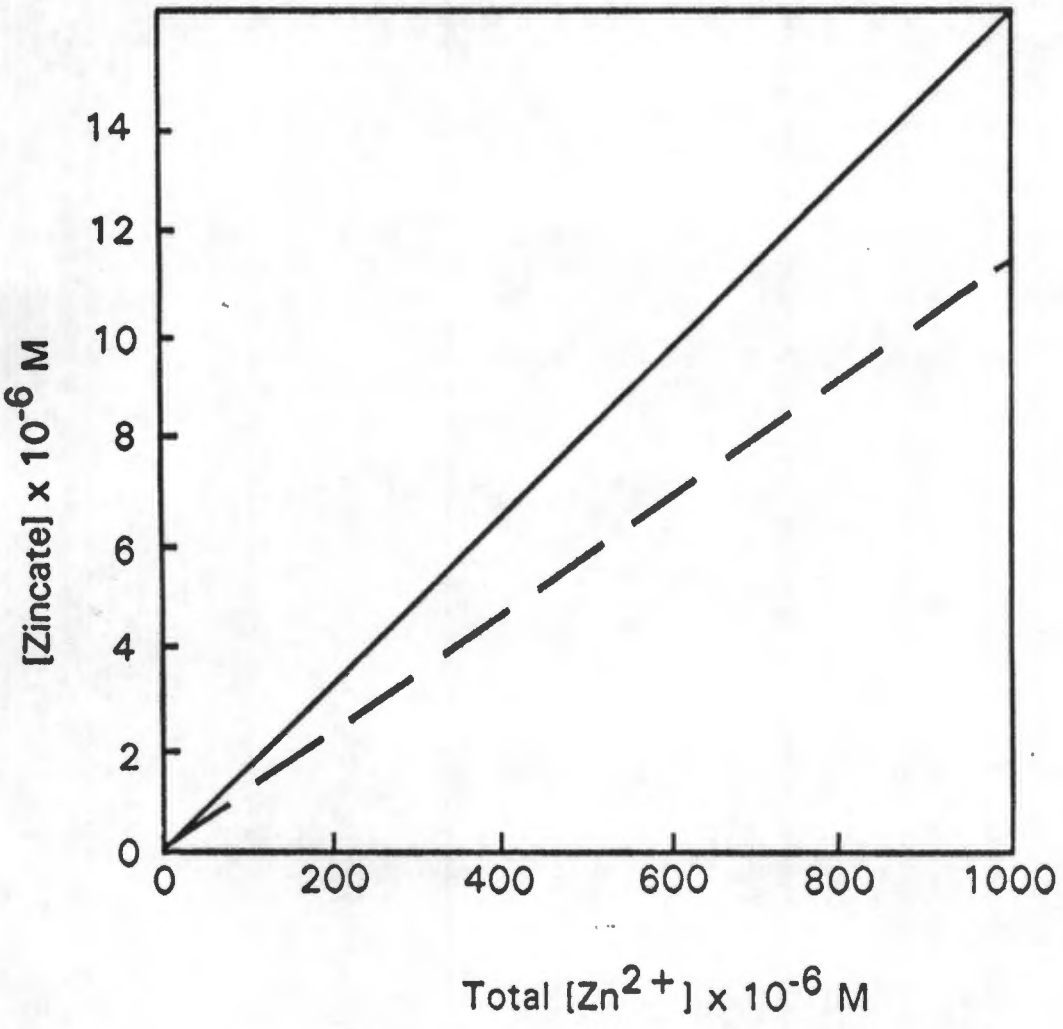

Figure 26: The corresponding increase in the zincate concentrations with progressive increments of Zn^{2+} (---) represents the $[Zn(OH)^{+}]$ and (——) the $[Zn(OH)_2]$.

contributions from tyrosines when present in large numbers ($E\Phi_F = 2 \times 10^{-2}$) (Cantor & Schimmel, 1980). The intrinsic fluorescence of a protein is sensitive to conformational change and, in the absence of protein-protein associations and gross denaturation, changes in tryptophan fluorescence can be attributed to structural perturbations brought about by ligand binding (Lakowicz, 1984).

The fibrin-D-dimer zinc titration data is represented graphically in Fig.24. The concentrations of the free zinc species and the Zn^{2+} complexes in reaction solution were determined using the computer programme ESTA (Equilibrium Simulation for Titration Analysis) (May & Murray, 1988). This programme calculates the distribution of significant species in solution from known equilibrium constants for each of the complexes.

The following model was set up for the system of Zn^{2+} in 0.1M Tris, pH 8.0.

					βH
H^+	+	OH^-	$\rightleftharpoons$	H_2O	-13.950
H^+	+	Tris	$\rightleftharpoons$	H Tris$^+$	8.073
Zn^{2+}	+	Tris	$\rightleftharpoons$	Zn(Tris)$^{2+}$	2.270
Zn^{2+}	+	OH^-	$\rightleftharpoons$	$Zn(OH)^+$	-8.950
Zn^{2+}	+	$2OH^-$	$\rightleftharpoons$	$Zn(OH)_2$	-16.800
Zn^{2+}	+	$3OH^-$	$\rightleftharpoons$	$Zn(OH)_3^-$	-28.250
Zn^{2+}	+	$4OH^-$	$\rightleftharpoons$	$Zn(OH)_4^{2-}$	-41.250
$2Zn^{2+}$	+	OH^-	$\rightleftharpoons$	Zn_2OH^{3+}	-8.950

where βH = log k with respect to H^+

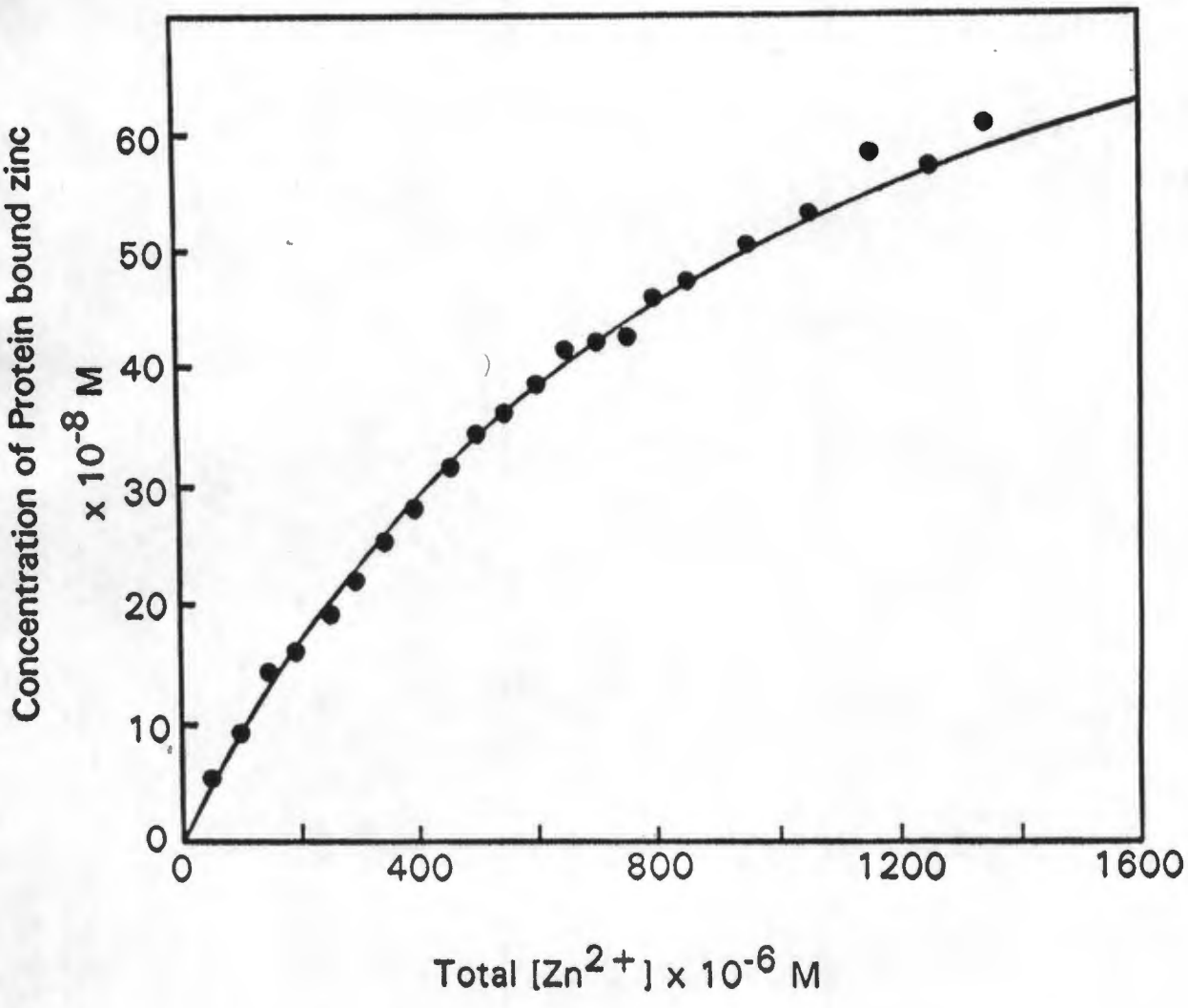

Figure 27: The calculated and measured concentrations of protein bound zinc species (zinc-f-D-dimer) produced with increasing increments of zinc.

(●) Indicates the concentration of the zinc-f-D-dimer species measured from experimental data. The solid line represents the species concentration as predicted by the programme ESTA. The close correlation is indicative of the suitability of the programme for the analysis of such titrations.

The program calculates the concentrations of each individual species of complex at each titration point from the total Zn^{2+} Tris, free H^+ concentrations and the βH values of the significant complexes. All the equilibrium constants were obtained from Martell & Smith (1974). The constants were expressed in βOH, from which βH was calculated using log k_w = 13.95.

Assuming a stoichiometry of 1 zinc atom per D-dimer molecule, a binding constant of log k = 4.01 $\pm$ 0.04 was calculated.

ESTA also calculated the concentrations of the zincate species (Fig.26).

Scatchard Plot Analysis of Titration Data

A Scatchard plot is a plot of ν/L vs ν. The plot is linear with Y intercept n/k_d , X intercept = n and slope = $-1/k_d$, and therefore the binding constant k = negative slope of the line.

When the titration data was analysed with Scatchard plots (Fig.25), a binding constant of log k = 3.88 $\pm$ 0.01 was found and binding sites n = 1.26.

It is important to note that a fundamental limitation to the zinc titration experiments was the high concentration of precipitable zinc hydroxides generated (Fig.26) making it difficult to obtained reasonable data at high concentrations of zinc(II).

Table Zinc titration of D-dimer by Intrinsic Fluorescence

Total [Zn] $X10^{-6}$	[Bound Zn] $X10^{-8}M$	L $X10^{-5}M$	$\frac{[\text{Bound Prot}]}{[\text{Free Prot}]}$	[Free Zn] $X10^{-5}M$	Log k
50	0.949	4.99	0.0563	0.510	4.04
100	1.660	9.99	0.1028	1.020	4.00
150	2.550	14.99	0.1672	1.531	4.04
200	2.848	19.99	0.1904	2.043	3.97
250	3.441	24.99	0.2396	2.555	3.97
300	3.896	29.99	0.2802	3.067	3.96
350	4.549	34.99	0.3433	3.580	3.98
400	5.083	39.99	0.3997	4.093	3.99
450	5.617	44.99	0.4610	4.606	4.00
500	6.131	49.99	0.5254	5.120	4.01
550	6.527	54.99	0.5825	5.634	4.01
600	6.922	59.99	0.6363	6.140	4.01
650	7.417	64.99	0.7143	6.664	4.03
700	8.386	69.99	0.8907	7.179	4.09
750	8.425	74.99	0.8987	7.695	4.06

3.5.2.1 Diethylpyrocarbonate Modification of fibrin-D-dimer

Diethylpyrocarbonate is a specific modification agent for histidine and tyrosine residues (Rogers et al, 1977; Melchoir & Fahrney, 1970) (see Addendum II). The acid anhydride modifies unsaturated nitrogens which would normally be available to ligand metal cations. The diethylpyrocarbonate modification of fibrin-D-dimer was tested by monitoring the OD_{242} of the reaction solution. When the DEPC modified fibrin-D-dimer was titrated with zinc, no changes in the tryptophan fluorescence were observed (Fig.28). The lack of structural perturbations indicated that the modified protein was not binding zinc. This implicated the histidine residues as ligands for coordinating the zinc atoms.

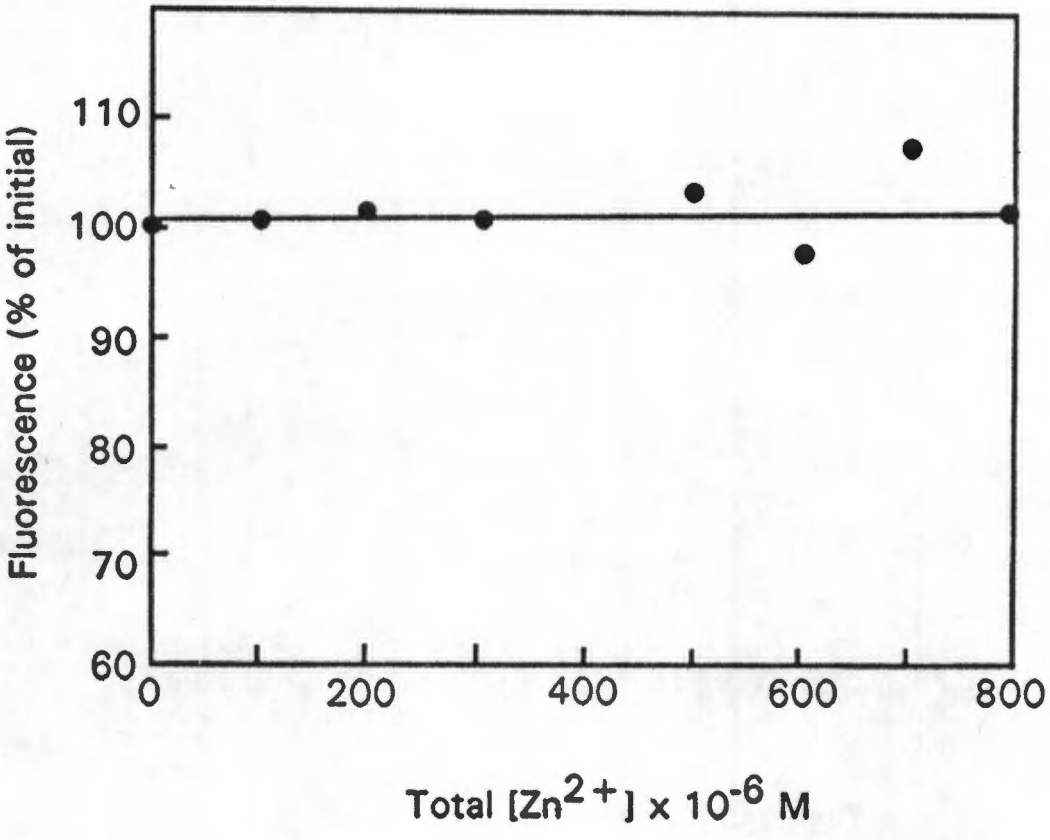

Figure 28: Zinc titration of diethylpyrocarbonate modified fibrin-D-dimer. No significant change in intrinsic fluorescence was observed with increasing increments of zinc(II) when the histidine residues of f-D-dimer were modified with the acid anhydride.

3.5.3 Fluorescence Anisotropy

The fluorescence polarisation characterisation of the two species: f-D-dimer and zinc-f-D-dimer was examined by fitting the fluorescence polarisation data into the Perrin equation.

$$\frac{1}{r} = \frac{1}{r_0} + \frac{\tau_f k}{r_0 V_h} \frac{T}{\eta} \qquad (3)$$

where $1/r_0$ is the reciprocal of the extrapolated anisotropy at the Y intercept.

k is the Boltzman constant, $k = 1.38 \times 10^{-23}$ JK^{-1}

τ_f is the fluorescence lifetime of the excited fluorophore;

$\tau_{(Dansyl)} = 13 \times 10^{-9}$s (Cantor & Schimmel, 1980a)

η is the viscosity of the solution, in this instance 20% sucrose obtained for each temperature from Weast (1987)

V_h is the molecular volume (spherical hydrated volume).

Plots of $1/r$ vs T/η produced straight lines (Fig.29) with y intercept $1/r_0$ and slope $\tau_f k / r_0 V_h$

The fluorescence anisotropy data of f-D-dimer in the absence and in the presence of zinc when analysed by Perrin plots had the same Y intercept at 2.674 ± 0.065. The slopes of the Perrin plots were $1.205 \times 10^{-2} \pm 3.6 \times 10^{-4}$ cPK^{-1} (centipoise per Kelvin) for f-D-dimer in 0.1M Tris, pH 8.0 with 150mM NaCl, 1mM $CaCl_2$ and 20% sucrose; and $1.025 \times 10^{-2} \pm 6.31 \times 10^{-3}$ cPK^{-1} for f-D-dimer in the same buffer but in the presence of 1mM Zn^{2+}.

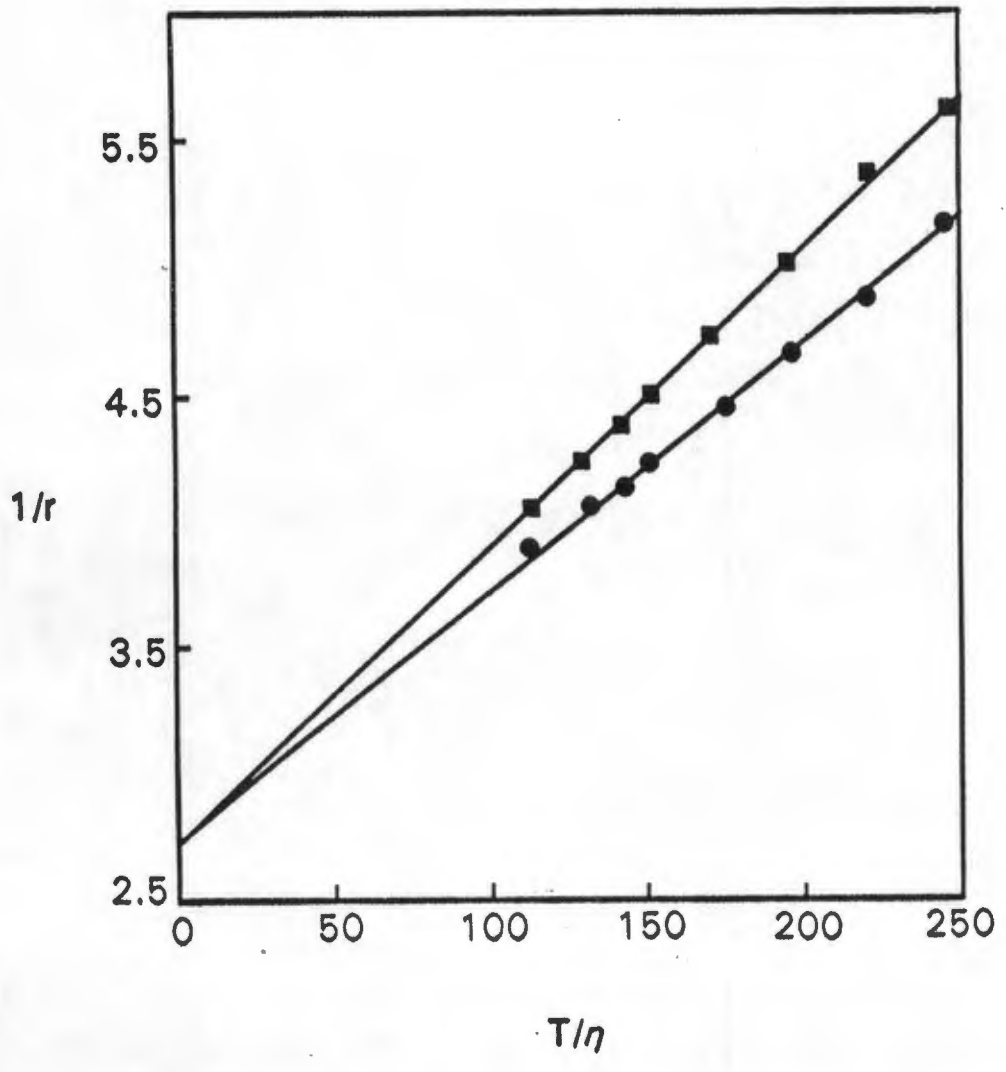

Figure 29: Perrin plots of f-D-dimer in the absence (■) and presence (●) of 1 mM Zn^{2+}. Fluorescence polarisation measurements were taken in 5°C and 50°C. The horizontal axis is T/η where T is the temperature in Kelvin, and η the viscosity in poise of 20% sucrose at the given temperature. The ordinate represents the reciprocal of the anisotropy measured - excitation, 340nm; emission, 520nm. Both zinc conjugated f-D-dimer and native f-D-dimer have the same ordinal intercept. The slope of the zinc f-D-dimer species was calculated at 1.205×10^{-2} cPK^{-1} and that of the native zinc free species 1.025×10^{-2} cPK^{-1}.

The spherical hydrated volume (V_h) of f-D-dimer in 1mM Zn^{2+} was calculated at V_h (Zn-f-DD) = $4.68 \times 10^{-20} cm^3$ and for zinc-free f-D-dimer: V_h (f-DD) = $3.98 \times 10^{-20} cm^3$. The results indicated a 17.58% larger (spherical model) volume for f-D-dimer in the presence of zinc.

Since volume of sphere = $4/3\Pi r^3$; the spherical volume of the Zn-f-D-dimer species corresponds to radius of 2.235×10^{-7}cm and the
f-D-dimer species 2.118×10^{-7}cm. The zinc induced a radius increase of 5.52% in the spherical volume of the f-D-dimer species. These results indicate a zinc induced conformational change in f-D-dimer.

3.5.4 Cobalt Absorption Spectroscopy

Zinc(II) is a spectroscopically silent d^{10} system. Substitution of zinc(II) with chromophoric paramagnetic Co(II), a d^7 system, results in a cobalt conjugate that is spectrally sensitive to changes in the metal environment (Martin et al, 1989, Bertini & Luchinat, 1984, Lever, 1984). The cobalt visible spectrum is also characteristic of the coordination number of the metal ion as well as the geometric shape of the inner coordination sphere (Lever, 1984).

3.5.4.1 Absorption Spectra of Cobalt-fibrin-D-dimer

The spectrum of 100mM $[Co(H_2O)]^{2+}$ complex was observed against a water reference. The defining parameters were λ_{max} = 511nm and molar extinction coefficient $\varepsilon = 4.69\ M^{-1}cm^{-1}$.

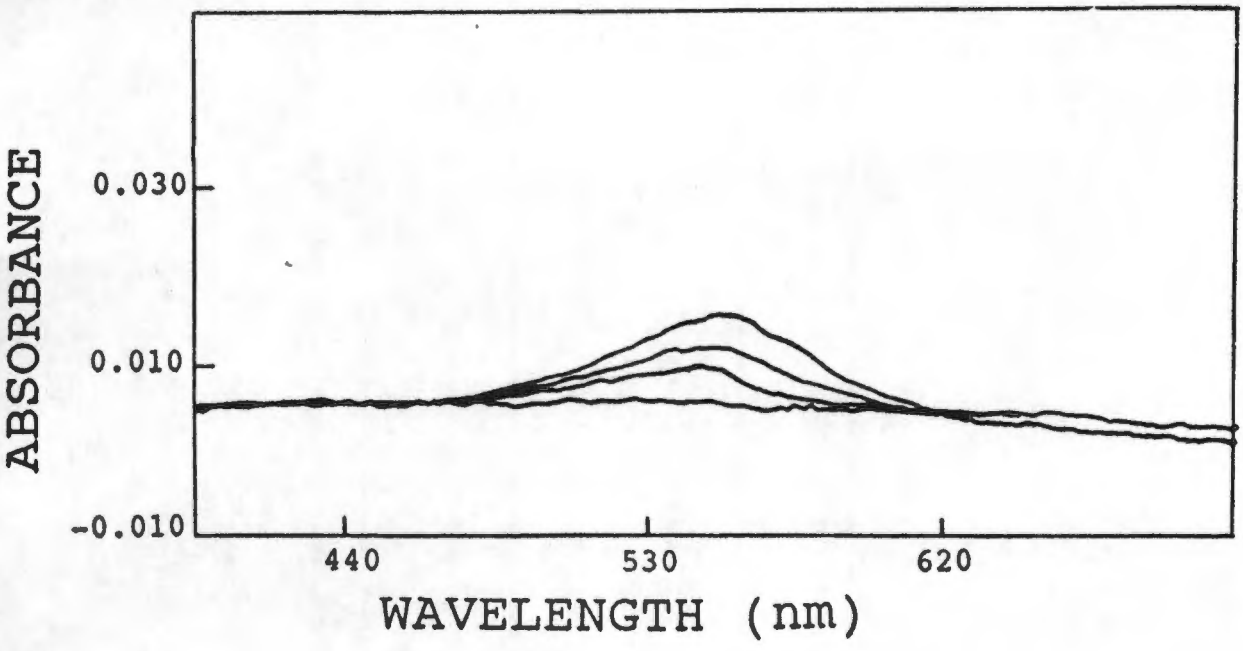

Figure 30: The cobalt titration of fibrin-D-dimer as monitored by absorption spectroscopy over the wavelength range 350nm to 800nm. The figure represents the difference absorption spectra obtained when fibrin-D-dimer was titrated with a) 0 mM, b) 3.8 mM, c) 7.4 mM and d) 10.2 mM $CoCl_2$ (see text).

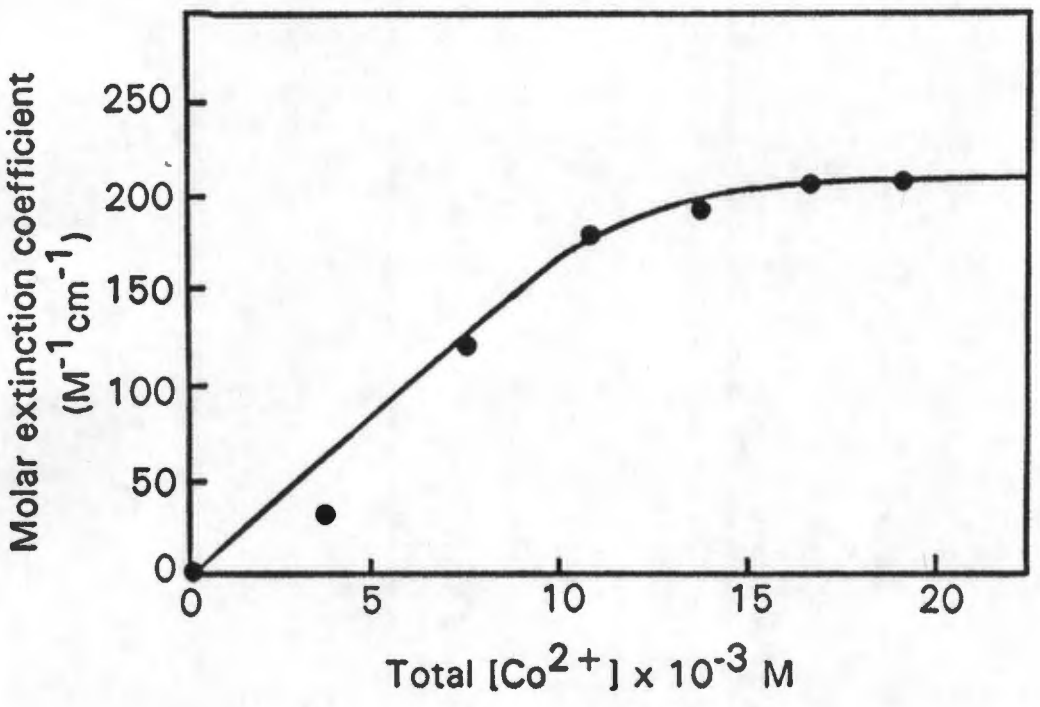

Figure 31. The binding of cobalt to fibrin-D-dimer. The difference spectrum of protein solutions with and without added cobalt was obtained. A single absorption band was observed with peak maximum at 545 nm ($\bar{\nu}$ = 18 348 cm^{-1}) for the cobalt-fibrin-D-dimer complex in 0.1 M Tris, pH 7.4. The molar extinction coefficient maximum for the complex was calculated at 210.52 M^{-1} cm^{-1}.

When a 1.425 x 10^{-4}M solution of fibrin-D-dimer (non-fluorescent) was titrated with cobalt after baseline correcting for buffer and protein spectra, the difference spectrum observed over the range 350 nm - 800 nm was characterised by a single broad peak with λ_{max} = 545nm ie ($\bar{\nu}$ = 18 348 cm^{-1}) (Fig.30). The protein solution was titrated to saturation with Co(II) (Fig.31). The maximum molar extinction coefficient was calculated at 210.52 M^{-1} cm^{-1}.

Generally a Cobalt(II) complex with molar extinction coefficient in the range 10^2 _ 10^3 M^{-1} cm^{-1} is characteristic of cobalt in a tetrahedral environment, thus the results would indicate that the Co(II) in fibrin-D-dimer is a tetrahedral coordination capsule. The wave number $\bar{\nu}$ = 18 348.6 cm^{-1} corresponds to a $^4T_1(P)$ $^{-4}A_2$ transition in a tetrahedral environment (Lever, 1984).

3.5.4.2 Absorption Spectra of Cobalt-DEPC-fibrin-D-dimer and Hydroxylamine Regenerated fibrin-D-dimer

Diethylpyrocarbonate modified fibrin-D-dimer was titrated with Co^{2+} under the same conditions as the native fibrin-D-dimer. No difference spectrum was observed in the visible wavelength range. The ethoxyformic anhydride specifically modifies histidine residues. The absence of a difference spectrum indicates that Co(II) is not bound to the fibrin-D-dimer due to the unavailability of the imidazole rings of histidine for metal ion coordination.

Hydroxylamine (NH_2OH) regenerates diethylpyrocarbonate modified

histidine residues (Melchior & Fahrney, 1970). When hydroxylamine treated DEPC modified fibrin-D-dimer was titrated with cobalt(II), characteristic (absorption) difference spectra were again observed. The maximum molar extinction coefficient ε_{max} was calculated at 168.65 M^{-1} cm^{-1}. The regeneration of the histidine residues results in the recovery of the absorption spectrum, implying that cobalt is again bound to the protein. This proves unambiguously that the cobalt is bound to histidine residues on fibrin-D-dimer.

It was crucial to remove all excess acid anhydride prior to treatment with hydroxylamine to prevent the formation of contaminating oxazoles and pyrazoles. The lower ε_{max} of the hydroxylamine-treated-DEPC-fibrin-D-dimer is due to the fact that not all the histidine residues are regenerated.

3.6 Effect of Other Metal Cations

In addition to zinc(II), the effect of Cd(II), Cu(II), Co(II) and Mg(II) on the PAV protease digestion of f-D-dimer was examined. The SDS-PAGE analysis of the reaction indicates that the digestion of the D-dimer fragment occurs in the presence of all the tested divalent cations. In all five cases, the major product of the digestion was the D-PAV-monomer fragment (Fig.32).

Only in the presence of zinc was digestion of the β-chain observed which leads to the deduction that the hydrolysis of the β-chain requires Zinc as a co-factor. In the presence of 1mM Cd, in addition to the D-PAV-monomer fragment, the other major product was a protein fragment with the same Rf value as plasmin derived D-monomer. In the presence of Cu the rate of the reaction was

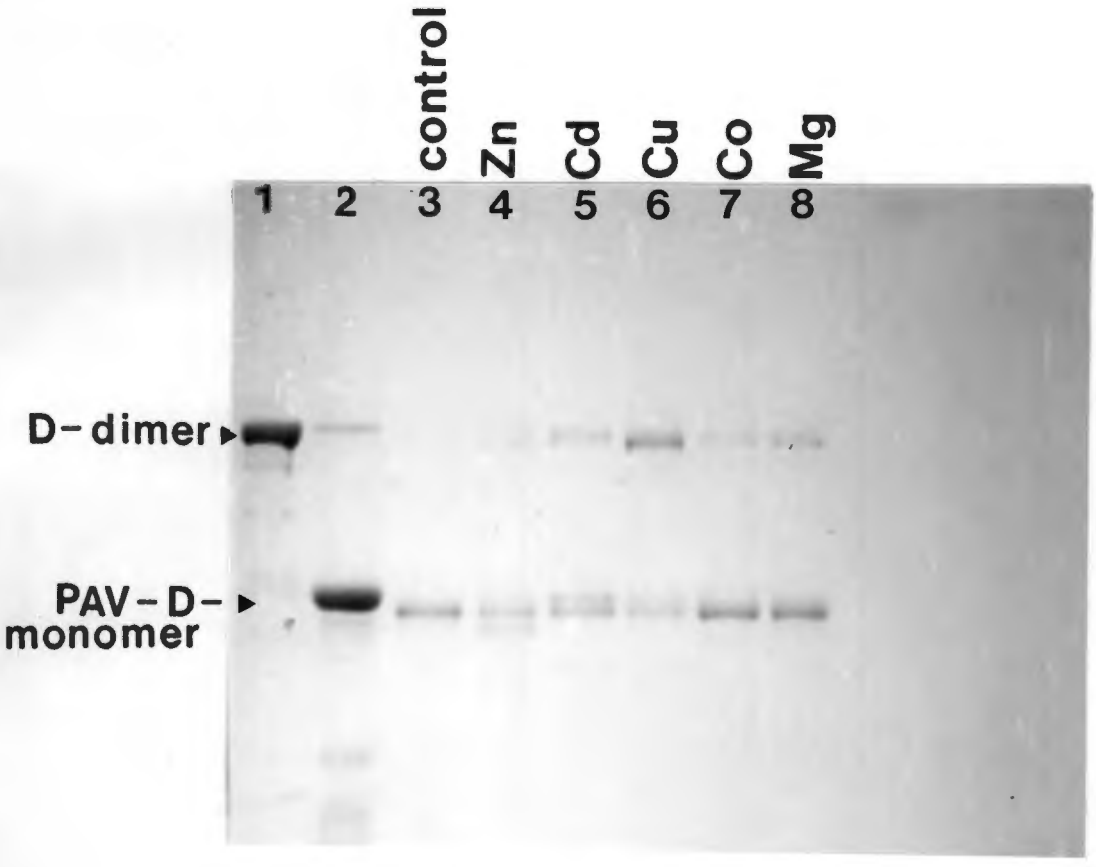

Figure 32: The effect of divalent metal cations on the PAV protease digestion of f-D-dimer. Lanes 1 and 2 represent f-D-dimer and f-D-monomer respectively. All reactions were performed in 0.1 M Tris, pH 7.4, 150 mM NaCl, 1 mM $CaCl_2$. Reactions were performed in the presence of zinc(II) (Lane 4), cadmium(II) (Lane 5), copper(II) (Lane 6), cobalt(II) (Lane 7) and magnesium(II) (Lane 8).

significantly decreased when compared with the control.

In addition to zinc, the binding of cadmium (Cd) and aluminium (Al) to fibrin-D-dimer was examined by measuring the changes in intrinsic fluorescence of the protein upon titration with the cation (Fig.24). The decrease in tryptophan fluorescence with increasing titres of Cd and Al indicates that both these metal cations bind to the macromolecule. Due to the high concentrations of metal hydroxides, no acceptable data could be obtained at higher metal ion concentrations. The binding constants of the liganding of Cd and Al to fibrin-D-dimer could not be calculated to a satisfactory accuracy due to the lack of sufficient titration data points.

4. DISCUSSION

Puffadder venom protease exhibits a unique ability to cleave the fibrin-D-dimer fragment into apparently symmetrical monomers. This occurs with a site specific cleavage of the D-dimer di-γ-chain and subsequent slower digestion of the β-chain (Purves et al, 1986). The γ-chain cleavage site was located by sequencing studies as being within the di-γ crosslinked region at the bond between γ-chain residues G404 and A-405 on each
γ-chain and accompanied by the heterogenous loss of ^{401}HLGG^{404} with both Factor XIIIa-induced crosslinks still intact.

where (I) indicates crosslinks

(Purves et al., 1987)

The enzyme is active over a wide pH range. In the presence of zinc, the di-γ-chain cleavage activity is observed over the range pH 6.40 - pH 9.75. The β-chain digestion activity is zinc dependent and has a smaller pH range; 6.40 - 8.5. This is accounted for by the fact that at higher pH values, the predominant complexes of zinc would be the zincates $Zn(OH)_2$ and $Zn(OH)^+$ and even $Zn(OH)_4^{2-}$ leaving only small concentrations of free Zn^{2+} in solution to act as a cofactor for β-chain digestion. The PAV protease digestion of f-D-dimer is potentiated by the presence of zinc(II) ions. Analysis of the digestion with fluorescence measurements using a fluorescent conjugated substrate calculates the potentiation as 4.136 fold. The zinc induced enhancement of the the reaction rate could be due to

an interaction of zinc(II) with either the enzyme or substrate or both. These possibilities were investigated in a differential zinc binding study, the results of which indicated a negligible potentiation through the enzyme, but a significant potentiation through the protein substrate.

These findings were further reinforced when changes in the intrinsic tryptophan fluorescence (Ex 280nm, Em 340 nm) were observed when the protein was titrated with zinc(II). Sodium dodecylsulphate polyacrylamide gel electrophoretic analysis showed a total absence of gross protein denaturation or protein-protein associations, therefore the changes in intrinsic fluorescence on zinc titration could only be attributed to structural perturbations brought about by ligand binding to the macromolecule. When the titration data was analysed with the assistance of the computer programme ESTA with the primary assumption of a Zn: fibrin-D-dimer stoichiometry of 1:1, a binding constant for the binding of zinc to fibrin-D-dimer was calculated at $\log k = 4.01 \pm 0.01$. Scatchard analysis of the data confirms the zinc: fibrin-D-dimer molar ratio of 1:1, binding sites n = 1.26, and calculates binding constant of $\log k = 3.88 \pm 0.01$

The fluorescence anisotropy measurements of fluorescent-D-dimer in the presence and in the absence of zinc(II) ions, when analysed by Perrin plots, reveals an 18% increase in the calculated volume (spherical hydrated model) of f-D-dimer in the presence of zinc. According to the model developed by Perrin and others, each fluorophore may be visualized as a set of absorption and emission dipoles.

These dipoles are characterized by definite spatial relationships to each other and to the axes of the molecule. The rotational relaxation times of the fluorescence anisotropy are directly related to molecular shape and size (Brand & Witholt, 1967). The native f-D-dimer and the Zn-f-D-dimer species have the same r_o value, ie. the anisotropy at $T/\eta = 0$ which would indicate that the zinc induced conformational change is localised and that the basic structure of macromolecule remains unchanged. The fluorescence anisotropy measurements confirm that zinc binds to f-D-dimer in a manner that induces a region specific or localised conformational change in the protein.

The coordination state and configuration of the coordination capsule of the bound metal ion was determined by studying a cobalt-fibrin-D-dimer complex. Cobalt(II) ($[Ar]3d^7$) is frequently substituted for the spectroscopically silent zinc(II) to characterise complexes as the optical absorption spectrum is sensitive to the nature of the coordination state (Frankel et al, 1987). The cobalt-fibrin-D-dimer complex absorption profile in the visible spectral range; 350nm - 800 nm, has a single broad absorption peak with peak maximum at $\nu = 18348\ cm^{-1}$ and maximum molar extinction coefficient of $\varepsilon_{max} = 210.52\ M^{-1}cm^{-1}$. This is characteristic of high spin cobalt(II) complexes when the cobalt is bound in a tetrahedral coordination capsule ($\varepsilon = 10^2 - 10^3\ M^{-1}cm^{-1}$) with d-d transitions that are spin allowed and Laporte forbidden (Lever, 1984).

Diethylpyrocarbonate specifically modifies histidine and tyrosine residues (Rogers et al, 1977, Melchior & Fahrney, 1970). The acid anhydride modifies unsaturated nitrogens on histidine that would

normally be available to ligand metal cations. No zinc binding was apparent when DEPC-fibrin-D-dimer was titrated with zinc and monitored by tryptophan fluorescence changes. The DEPC-modified protein fragment also failed to complex Co(II) as evidenced by the absence of an absorption peak in the difference visible spectrum on titration with cobalt, therefore the DEPC modification of fibrin-D-dimer rendered the protein fragment incapable of binding metals and this therefore implicates the histidine residues as necessary donor ligands for metal binding.

The DEPC modification is reverted by hydroxylamine (NH_2OH), regenerating the histidine residues (Melchior & Fahrney, 1970). The hydroxylamine-treated-DEPC-fibrin-D-dimer yielded a characteristic absorption band in the visible region with molar extinction coefficient of 168.65 $M^{-1}cm^{-1}$ when titrated with cobalt(II). The regeneration of the histidine residues therefore restored metal binding properties to the protein and the complex generated is characterised as tetrahedral similar to the native Co-fibrin-D-dimer complex. This confirms unequivocally that zinc binds to f-D-dimer with the liganding histidine residues in a tetrahedral geometry.

A Model for the Zinc induced Neoepitope

The evidence presented indicates that histidine residues in fibrin-D-dimer bind one zinc per molecule in a tetrahedral configuration in a manner that potentiates the site specific cleavage of the molecule in the crosslink region by a snake venom protease. Zinc potentiates the cleavage of the di-γ-chain between G-404 and A405 on both chains and titration with zinc also increases the extrinsic fluorescence of the

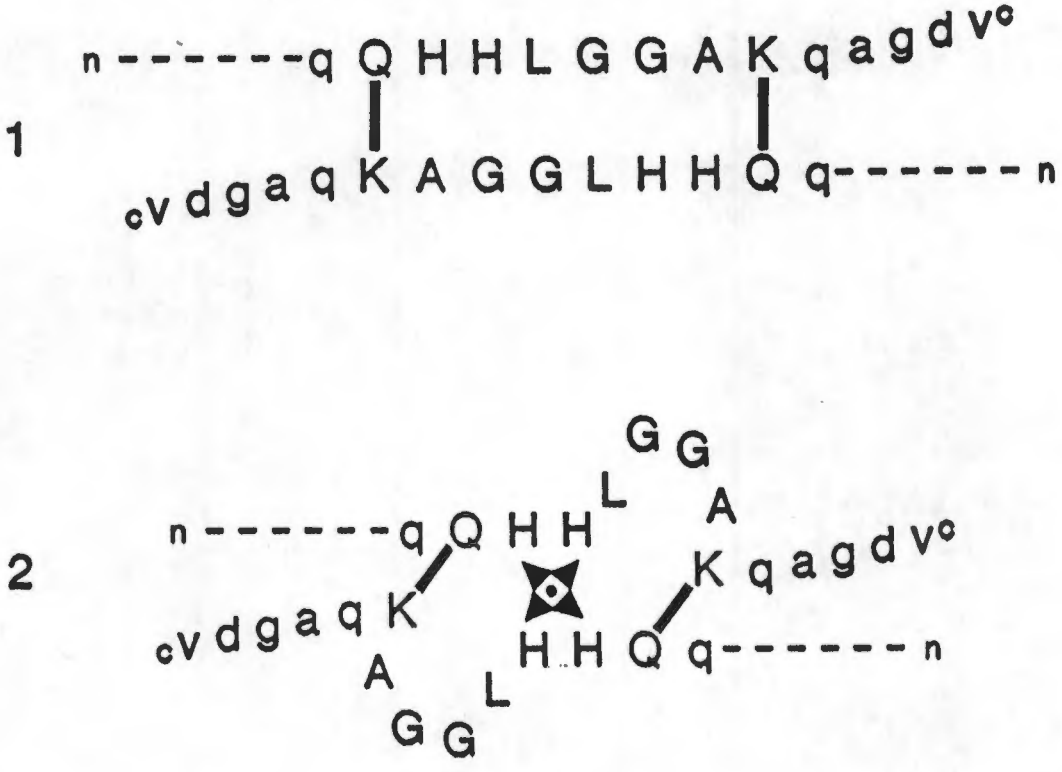

Figure 34: Proposed model for the zinc induced neo-epitope of fibrin-D-dimer. The figure represents the crosslink region of fibrin-D-dimer before (1) and after (2) the binding of zinc. The solid bars represent the transglutaminase induced isopeptide crosslinks between Q^{399} and K^{406}, n represents the continuation of the peptide to the N-terminus, c is the carboxy terminus of the chain and ★ represents the zinc(II) ion.

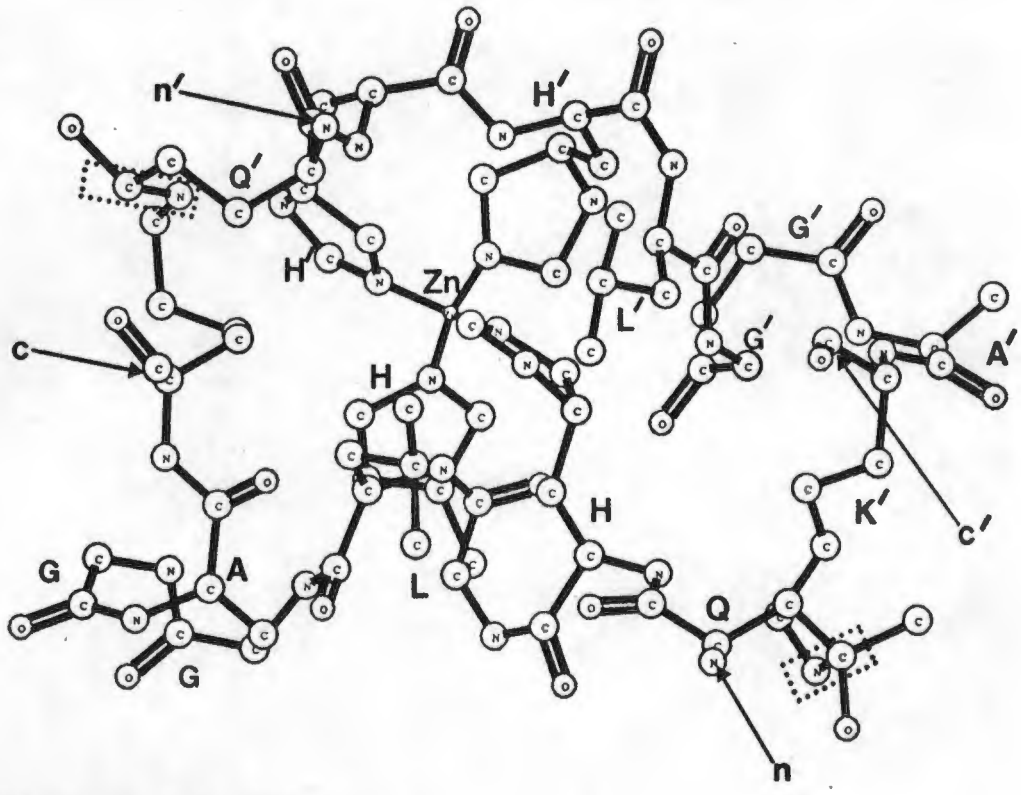

Crosslink with Zinc

Computer model of the crosslink peptide of fibrin-D-dimer with Zinc (supra). The zinc atom is liganded to 4 histidine residues (see text). The Factor XIII induced crosslinks are boxed. The residues of the two γ chains are labelled X and X' respectively. It is apparent from this model that the GGA peptides are forced to the periphery of the molecule and are thus easily accessible for PAV protease cleavage.

macromolecule (possibly by inducing a localised change in the dielectric constant or relative permittivity in the immediate environment of the fluorophore).

The proposed model for this zinc-induced new conformation would be as follows: zinc is bound within the crosslink region of the di-γ-chain of the protein molecule coordinated to two pairs of adjacent histidine residues H-401 and H-402 on each of the antiparallel crosslinked protein γ-chains. The zinc atom is liganded to the histidines via the ε nitrogen of the histidine imidazole rings creating a strained tetrahedral geometry about the zinc ion (Fig.34).

The imidazole ring is abnormally basic for a compound with a sp^2 hybridized nitrogens (pK_a = 7.0, Kb = 1.6 x 10^{-7}). This is due to the symmetry of the conjugated acid and the consequent resonance stabilisation. The mesomeric effect in particular affords histidine an enhanced proton acceptor status with excellent liganding properties for zinc under physiological conditions (Streitweiser & Heathcock, 1981).

The liganding histidines are adjacent and therefore lack spacer sequences so that the coordination with the metal cation induces localised strain in the peptide chain. Relief of strain requires a rearrangement of the di-γ-chain crosslink region to allow the zinc coordination capsule to achieve a tetrahedral geometry. The geometry would not be a perfect classical tetrahedron but distorted tetrahedron succumbing to physical constraints and the limitations of the Jahn-Teller effect.

The proposed structure (Fig.34) is further stabilised by the hydrophobic interactions between the imidazole rings and neighbouring leucine isobutyl side chains. The nett result of this conformational change of the di-γ crosslink peptide is the exposure of the distorted G-404 - A405 peptide bond on the outer periphery of the molecule. An unusual site specificity (between two glycines and an alanine residue) is thereby created by virtue of this conformation despite the lack of significant side chain residues.

The biphasic nature of the protease digestion of the f-D-dimer may now be explained. The initial cleavage on one of the γ-chains occurs rapidly accompanied by a proportional change in the hydrophobic environment of the dansylcadaverine fluorophore and the subsequent increased solvent fluorophore collisions. This accounts for the initial sharp decrease in absolute fluorescence. This first cut also results in great reduction of conformational strain on the molecule. The consequent relaxation of the molecule renders the cleavage site on the second γ-chain less accessible and therefore less susceptible to cleavage.

This accounts for the 9-fold slower reaction rate for the second phase of the digestion (k_{fast} = 0.91 min^{-1} vs k_{slow} = 0.01 min^{-1}).

Physiological Significance.

The plasma zinc concentration in normal individuals is in the range of 10.7 - 16.9 μM (Failla, 1982). Thirty five percent is tightly bound to α-2-macroglobulin (Parisi, 1970) and a large percentage of the remainder is in zinc enzymes and zinc proteins resulting in a very low free Zn^{2+} concentration in plasma. Given that albumin binds zinc fairly strongly, pk = 6.98, n = 1, it would be fair to assume that

albumin is probably responsible for binding a major fraction of free zinc in human plasma (Marx, 1988). The binding constant we calculated for zinc binding to fibrin D-dimer is of the order of pk = 3.88, therefore, offers weak competition to albumin for zinc(II) ions. This could mean that the physiological significance in vivo is minimal. However, if one speculates that in the case of a puffadder bite, the venom injection contains a rich load of divalent cations, this may increase the free zinc ion concentration locally to sufficiently high levels to render the postulated zinc potentiated substrate effect physiologically significant. In addition there may well be a collaborative mechanism in plasma with high concentration divalent cations eg. calcium(II) and zinc released from platelets..

The in vitro significance of zinc binding to fibrin-D-dimer is less speculative. It can be concluded from the zinc induced intrinsic fluorescence changes and the volume changes that zinc(II) ions induce a considerable conformational change in the fibrin-D-dimer structure. Scatchard plots put the zinc:fibrin-D-dimer stoichiometry at 1:1 and infers a pk of 3.88. We conclude that a novel fibrin-specific epitope could be manifest in the presence of zinc ions and could provide a means to determine fibrin degradation products more specifically.

ADDENDUM I: Derivation of the Scatchard Equation

Consider the case of a macromolecule M, which contains n binding sites for ligand L. Each site has the same microscopic ligand dissociation constant k_d. The binding sites are assumed to be independent, ie. the microscopic dissociation constant k for a particular site is the same regardless of the occupancy of the other sites. The equilibrium characterising the ligand binding interaction would read as follows:

$$M_0 + L \rightleftharpoons M_1$$
$$M_1 + L \rightleftharpoons M_2$$
$$\vdots \quad \vdots \quad \vdots$$
$$M_{n-1} + L \rightleftharpoons Mn$$

The yield of moles of ligand bound for molecule of macromolecule, designated $\bar{\nu}$, would be given by

$$\bar{\nu} = \sum_{i=0}^{n} i\,(M_i) \Big/ \sum_{i=0}^{n} (M_i)$$

If we consider the equilibrium of the site i only, and let Θi be the fractional saturation of the site i, then

Θi = (Bound site i)/[(Free site i) + (Bound site i)]

We multiply the numerator and denominator by $\dfrac{(\text{Free site}_i)}{(\text{Free site}\,i)}$

then,

$$\Theta_i = \frac{(\text{Free site}_i)\left\{(\text{Bound site}\,i)/(\text{Free site}\,i)\right\}}{(\text{Free site}\,i)\left\{1 + (\text{Bound site}\,i)/(\text{Free site}\,i)\right\}}$$

Now $\dfrac{(\text{bound site } i)}{(\text{Free site } i)} = L/(k_d)_i$

Therefore $\theta_i = \dfrac{L/(k_d)_i}{1 + L/(k_d)_i}$

Thus for n sites, $\nu = \sum_i^n \theta_i$

$$\Rightarrow \nu = \frac{n L/(k_d)_i}{1 + L/(k_d)_i}$$

thus $\nu + \nu L/(k_d)_i = n L/(k_d)_i$

$$\Rightarrow \nu/L = n/(k_d)_i - \frac{\nu}{(k_d)_i}$$

Thus generally for each site,

$$\boxed{\frac{\nu}{L} = \frac{n}{k_d} - \frac{\nu}{k_d}}$$

ADDENDUM II: Proposed mechanism for the diethylpyrocarbonate modification of histidines and regeneration by hydroxylamine.

Mechanisms of DEPC modification of Histidines

The phenomenon of diethylpyrocarbonate modification of histidine residues has been reported (Rogers et al, 1977, Melchior & Fahrney, 1970), however, the mechanism of the modification has not. Diethypyrocarbonate or ethoxyformic anhydride is a classical ester acid anhydride with the following structure:

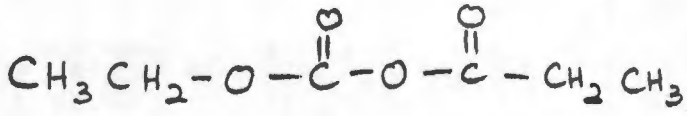

The reaction of ethoxy formic anhydride would follow one of two directions.

A.

1. The ethoxyformic anhydride at acid pH values dissociates resulting in the formation of a carbocation.

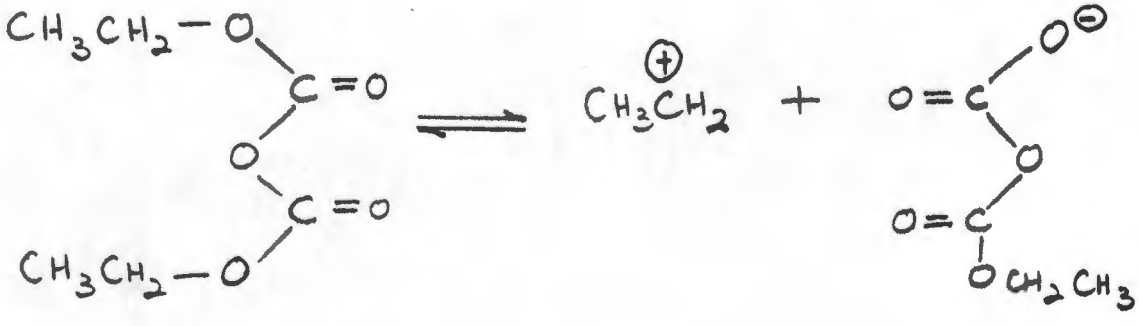

2. The histidine ring rearranges the localisation of electrons with the E nitrogen donating its lone pair of electrons resulting in the formation of a

nucleophile.

3. The nucleophile attacks the electrophile in the classical manner.

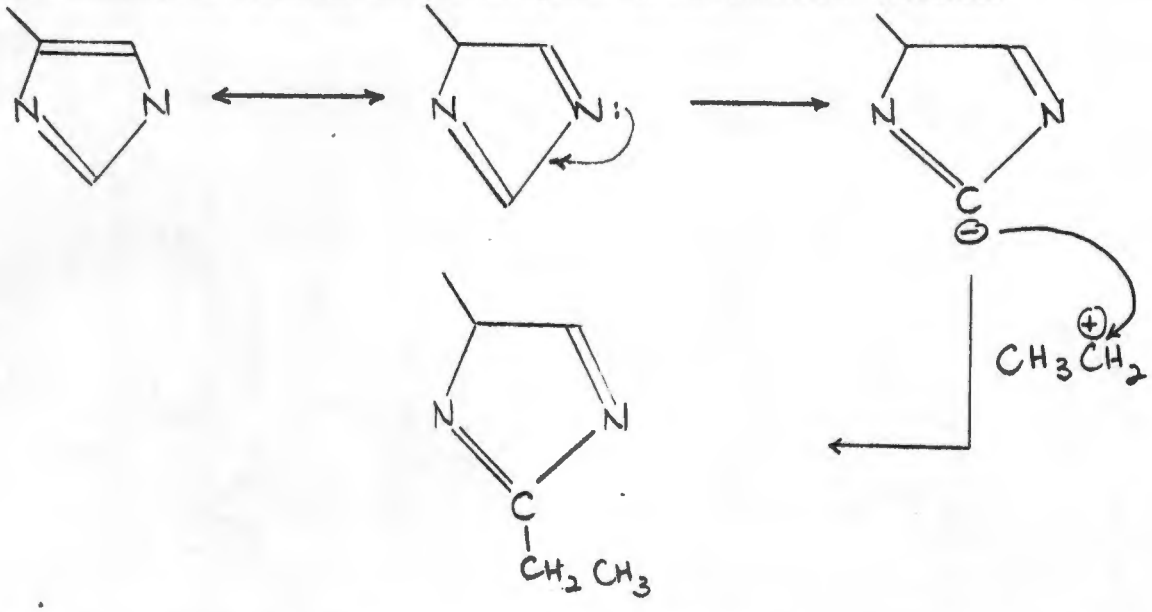

This results in the irreversible alkylation of the histidine ring. The inability to ligand metals via the E nitrogen would be as a result of steric hinderance. While the mechanism is plausible, it seems the less likely possibility as the nucleophile could be easily negated at low pH values by spontaneous protonation. This mechanism for modification also does not allow for hydroxylamine regeneration, being irreversible, and the alkylated histidine could not be the major product of modification.

B. The mechanism that with result in the dominant product of the recemate is more likely to be as follows:

A fundamental limitation of this mechanism is that the pH of the reaction be as close to pH 7.00 as possible. These histidines have to be deprotonated, therefore, pH > pKa (His) (pKa _ 6); and to prevent the hydroxide ion from becoming the deminant nucleophile, higher pH values would not be recommended.

1. The deprotonated histidine serves as nucleophile utilising the lane pair of electrons on the epsilon nitrogen.

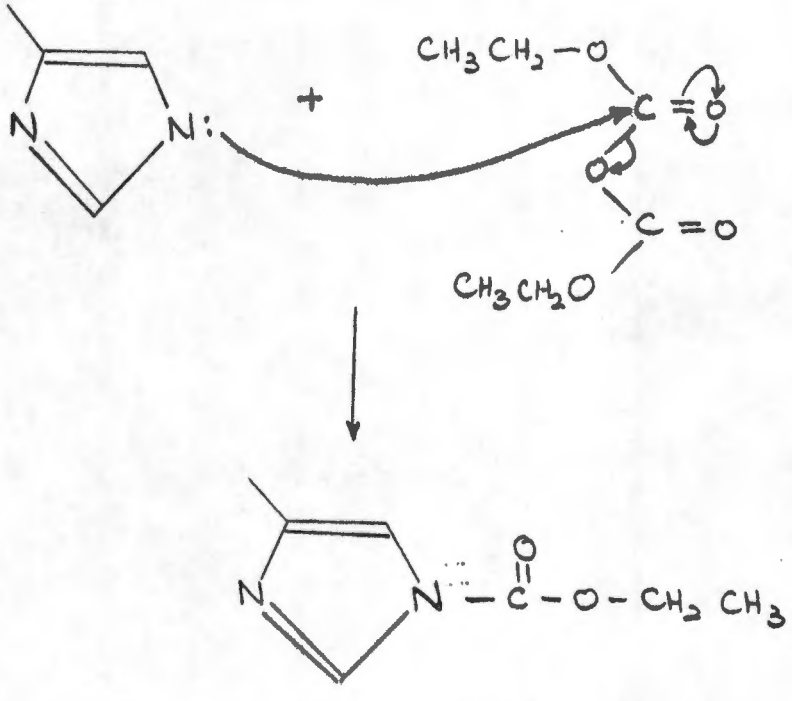

Ethoxy formyl histidine

Regeneration of Histidine with NH_2OH

Histidine is an excellent leaving group. The reaction of ethoxyformyl histidine would be most effective at high pH values [pKa (NH_2OH) = 8).

1. NH_2OH adds on to the ethoxyformyl histidine creating an unstable transitionary state.

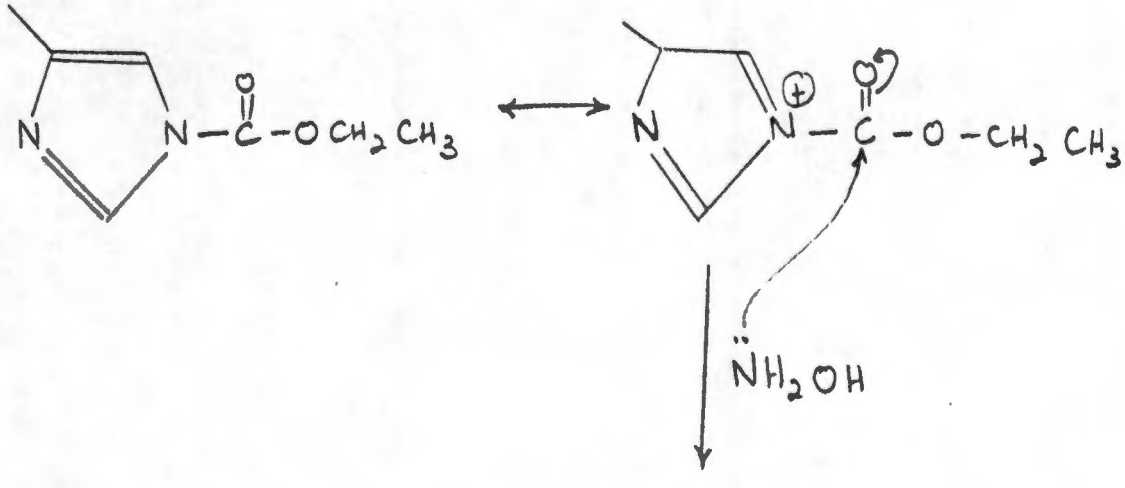

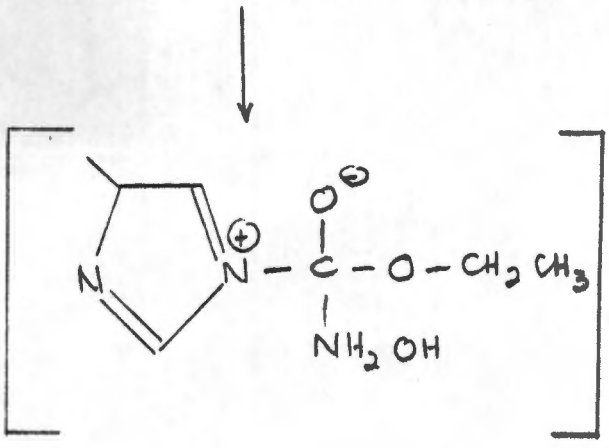

2.

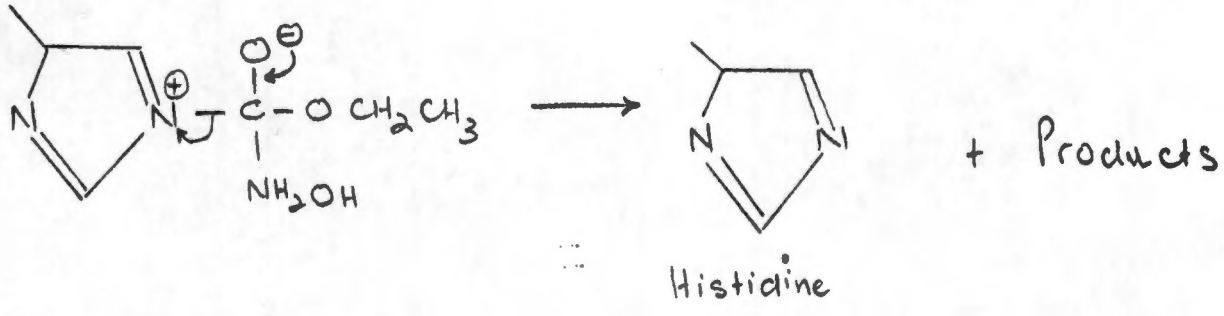

ADDENDUM III Crosslink Peptide with Zinc as modelled on DTMM.

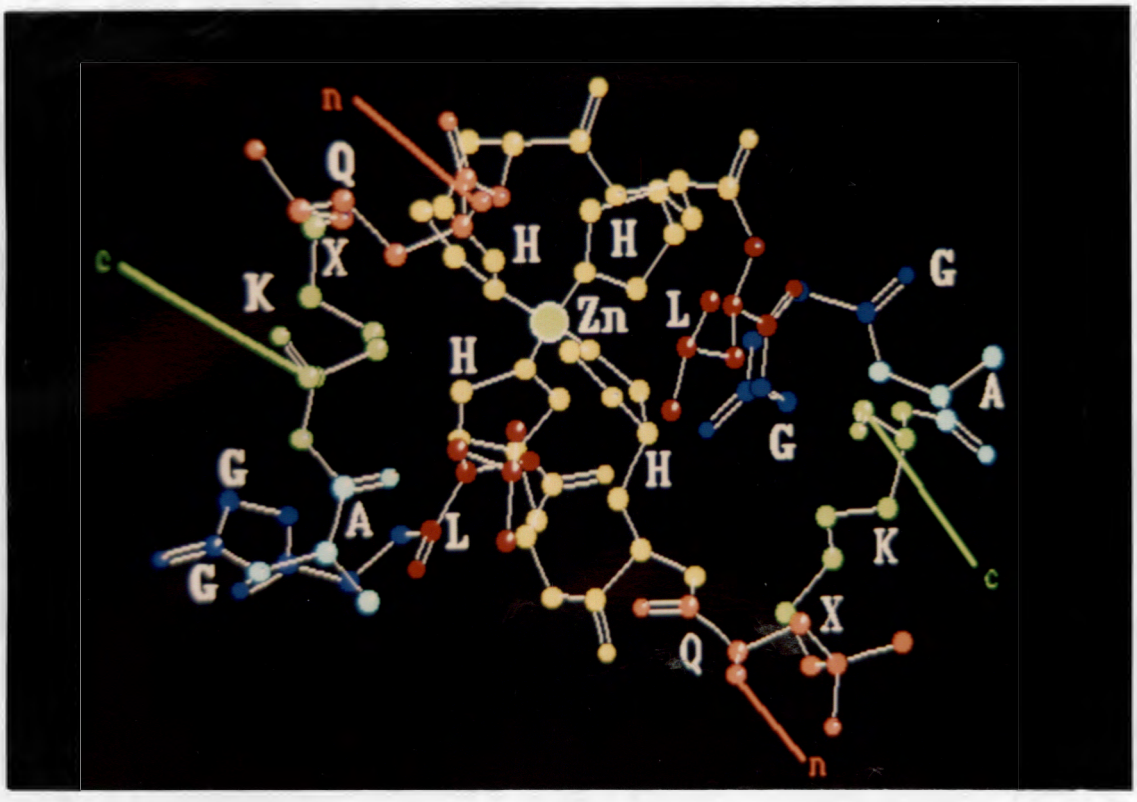

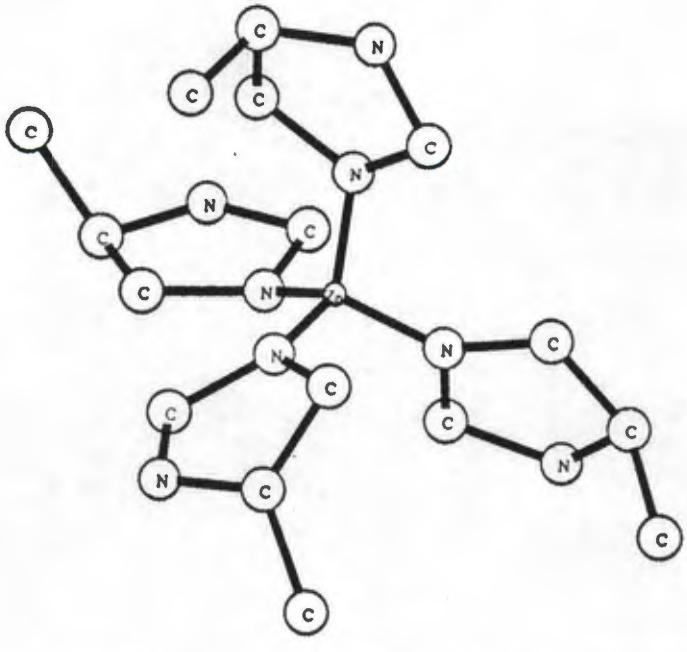

The co-ordination capsule of zinc(II) in the crosslink peptide. The zinc ion is liganded to four histidine residues in an almost perfect tetrahedral configuration.

ADDENDUM IV: Case Report of a Factor XIII deficiency

A seven year old female presented with abnormal bruising. There was umbilical bleeding at birth and probably intracranial bleeding thought to be the cause of a degree of mental retardation. Whole blood, plasma and serum samples from the patient were tested. Normal clotting times were observed, but the clot was soluble in 4M urea indicative of a Factor XIII deficiency (Lorand et al, 1980). To confirm the diagnosis, the clot was subject to digestion by plasmin in 0.1 M Tris, pH 7.4, 150 mM NaCl and 10 mM $CaCl_2$. The digest was analysed by SDS-PAGE (Figure infra).

The plasmic digest of the patient clot results in D-monomer and E-fragments with total absence of the characteristic D-dimer fragments. This indicates that Factor XIII catalysed crosslinking of the antiparallel γ-chains did not occur. SDS-PAGE of β-mercaptoethanol-treated plasmic digest samples revealed absence of the di-γ-chain, only the γ-chain was present, confirming the absence of Factor XIII activity.

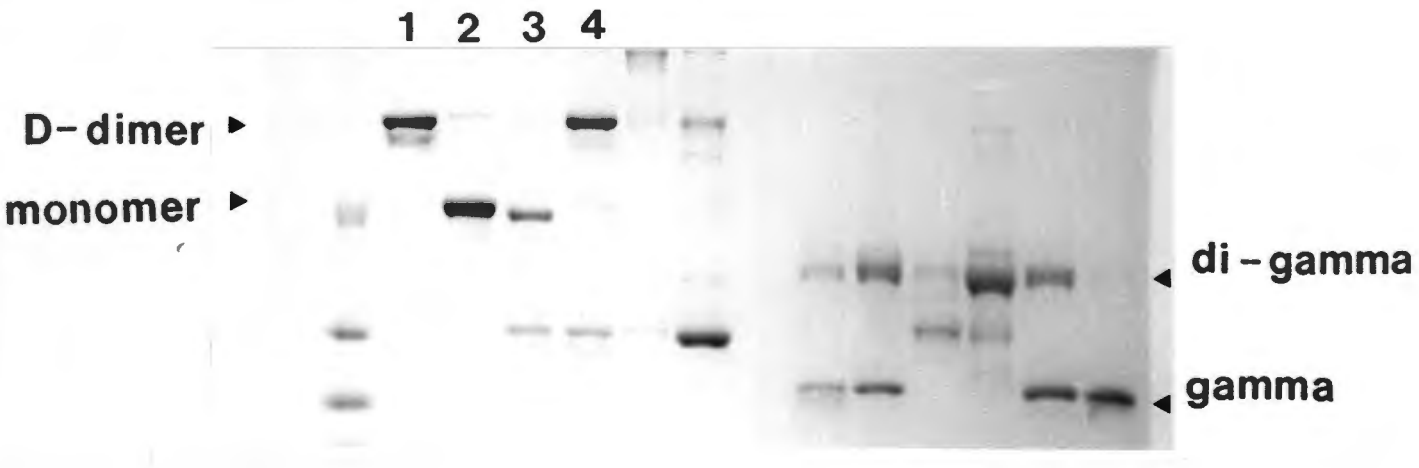

Figure addendumIV. 6-15%SDS-PAGE of plasmic digests of patient (lane 3) and normal(4) clots. Lanes 1 and 2 are standard D-dimer and D-monomer markers respectively.

BIBLIOGRAPHY

Achyuthan KE, Dobson JV & Greenberg CS (1986). Gly-Pro-Arg-Pro modifies the glutamine residues in the alpha- and gamma-chains of fibrinogen: inhibition of transglutaminase cross-linking.
Biochim. Biophys. Acta. 872, 261.

Achyuthan KE, Mary A & Greenberg CS (1988). The binding sites on fibrin(ogen) for guinea pig liver transglutaminase are similar to those in blood coagulation factor XIII.
J. Biol. Chem. 263, 14296.

Alkjaersig N & Fletcher AP (1983). Formation of soluble fibrin oligomers in purified systems and in plasma.
Biochem. J. 213, 17.

Alkjaersig N, Davies A & Fletcher A (1977). Fibrin and fibrinogen proteolysis products. Comparison between gel filtration and SDS polyacrylamide electrophoresis analysis.
Throm. Haemostas. 38, 524.

Apap-Bologna A, Webster A, Raitt F & Kemp G (1989). The influence of calcium ions on fibrinogen conformation.
Biochim. Biophys. Acta. 995, 70.

Bailey K, Bettelheim FR, Lorand L & Middlebrook WR (1951). Action of Thrombin in the clotting of fibrinogen.
Nature 167, 233.

Bajwa SS, Kirakossian H, Reddy KNN & Markland FS (1982). Thrombin-like and fibrinolytic enzymes in the venoms from the Gaboon viper (Bitis gabonica), Eastern cottonmouth moccasin (Agkistrodon P. Piscivarus) and Southern copperhead (Agkistrodon C. Contortrix) snakes.
Toxicon. 20, 427.

Bajwa SS, Markland FS & Russel FE (1980). Fibrinolytic enzymes in Western diamond back rattlesnake (Crotalus atrox) venom.
Toxicon. 18, 285.

Bajwa SS, Markland FS & Russel FE (1981). Fibrinolytic and fibrinogen clotting enzymes present in the venoms of western diamondback rattlesnake, Crotalus atrox, eastern diamondback rattlesnake, Crotalus adamanteus, and southern diamondback rattlesnake, Crotalus viridus helleri.
Toxicon. 19, 53.

Berg JM (1986a). Potential metal-binding domains in nucleic acid binding proteins.
Science 232, 485.

Berg, JM (1986b). More metal-binding fingers.
Nature 319, 264.

Berg JM (1988). Proposed structure for zinc-binding domains from transcription factor IIIA and related proteins.
Proc. Natl. Acad. Aci., USA. 85, 99.

Bertini I & Luchinat C (1984) High spin cobalt(II) as a probe for the investigation of metalloproteins. Adv.Inorg.Chemistry 6, 71.

Bjarnson JB & Tu AT (1978). Hemorrhagic toxins from Western diamondback rattlesnake (Crotalus atrox) venom. Isolation and characterisation of five toxins and role of zinc in hemorrhagic toxin e.
Biochemistry 17, 3395.

Bjarnson JB & Fox JW (1983). Proteolytic specificity and cobalt exchange of hemorrhagic toxin e, a zinc protease isolated from the venom of the Western diamondback rattlesnake (Crotalus atrox).
Biochemistry 22, 3770.

Blomback B, Hessel B, Hogg D & Therkildsen L (1978). A two-step fibrinogen-fibrin transition in blood coagulation.
Nature 275, 501.

Blow DM & Steitz TA (1970). X-ray diffraction studies on enzymes.
Ann. Rev. Biochem. 39, 78.

Board PG, Webb GC, McKee J & Ichinose A (1988). Localisation of the coagulation factor XIIIA subunit gene (F13A) to chromosome bands 6p24-p25.
Cytogenet. Cell. Genet. 48, 25.

Bohonus VL, Doolittle RF, Poutes M & Strong DD (1986). Complementary cDNA sequence of Lansprey fibrinogen beta-chain.
Biochemistry 25, 6521.

Bok RA & Mangel WF (1985). Quantitative characterization of the binding of plasminogen to intact fibrin clots, lysine-sepharose, and fibrin cleaved by plasmin.
Biochemistry 24, 3279.

Bottenus RE, Ichinose A & Davie EW (1990). Nucleotide sequence of the gene for the b subunit of human factor XIII.
Biochemistry 29, 11195.

Boyer MH, Schainoff JR & Ratnoff OD (1972). Acceleration of fibrin polymerisation by calcium ions.
Blood 39, 382.

Brand L & Witholt B (1967). Fluorescence measurements.
Meth. Enzymol. 11, 776.

Britton DW, Lawrie JS & Kemp GD (1982). The influence of calcium ions on the conformation of fragment D: The use of chemical crosslinking agents.
Thrombin. Res. 27, 167.

Budzynski AZ, Marder VJ & Shainoff JR (1974). Structure of plasmic degradation products of human fibrinogen.
J. Biol. Chem. 249, 2294.

Cantor CR & Schimmel PR (1980) in Biophysical Chemistry,Part II: Techniques for the study of biological structure and function, WH Freeman Co., San Francisco.

Cantor CR & Schimmel PR (1980) in Biophysical Chemistry, Part III: The behavior of biological macromolecules, WH Freeman CO., San Francisco.

Chang SK & Chung SI (1986). Cellular transglutaminase.
J. Biol. Chem. 261, 8112.

Chen R & Doolittle RF (1970). Isolation, characterisation and location of donor-acceptor unit from crosslinked fibrin.
Proc. Natl. Acad. Sci., USA. 66, 472.

Chesters JK & Will M (1981). Zinc transport proteins in plasma.
Br. J. Nutr. 46, 111.

Cierniewski CS, Kloczewiak M & Budzynski AZ (1986). Expression of primary polymerisation sites in the D-domain of human fibrinogen depends on intact conformation.
J. Biol. Chem. 261, 9116.

Civello DJ, Duong HL & Geren CR (1983). Isolation and characterisation of a hemorrhagic proteinase from timber rattlesnake venom.
Biochemistry 22, 749.

Cunningham BC, Bass S, Fuh G & Wells JA (1991). Zinc mediation of the binding of human growth hormone to the human prolactin receptor.
Science, 250, 1709.

Cunningham BC, Mulkerrin, MG & Wells, JA (1991). Dimerization of human growth hormone by zinc.
Science 253, 545.

Cunningham BC, Ultch M, de Vos AM, Mulkerrin MG, Clauser KR & Wells JA (1991). Dimerization of the extracellular domain of the human growth hormone receptor by a single hormone molecule.
Science 254, 821.

Dang CV, Shin CK, Bell WR, Nagaswami C & Weisel JW (1989). Fibrinogen sialic acid residues are low affinity calcium-binding sites that influence fibrin assembly.
J. Biol. Chem. 264, 15104.

Davies PJA, Murtaugh MP, Moore WT, Johnson GS & Lucas D (1985). Retinoic acid-induced expression of tissue transglutaminase in human promyelocytic leukemia (HL-60) cells.
J. Biol. Chem. 260, 5166.

De Cristofaro R, Landolfi R, De Candia E, Castagnola M, Di Cera E & Wyman J (1988). Allosteric equilibria in the binding of fibrinogen to platelets. Proc. Natl. Acad. Sci., USA. 85, 8473.

Dent AJ, Beyersmann D, Block C & Hasnain SS (1990). Two different zinc sites in Bovine 5-aminolevulinate dehydratase distinguished by extended X-ray absorption fine structure. Biochemistry, 29, 7822.

Di Minno G, Cerbone AM, Margaglione M, Cirrilo F, Vecchione G, Grandone E, et al (1990). Searching for the thrombogenic mechanism(s) of fibrinogen. Thromb. Res. Suppl. XI, 61.

Donovan JW & Mihalyi E (1985). Clotting of fibrinogen. I. Scanning calorimetric study of the effect of calcium. Biochemistry 24, 3434.

Doolittle RF & Laudano AP (1980). Synthetic peptide probes and the location of fibrin polymerisation sites. Protides. Biol. Fluids 28, 311.

Doolittle RF (1973). Fibrinogen and fibrin. Adv. Prot. Chem. 27, 1.

Doolittle RF (1975) in The Plasma Proteins ed Putman F, 2, 109, New York, Academic 2nd ed.

Doolittle RF (1984). Fibrinogen and fibrin. Ann. Rev. Biochem. 53, 195.

Doolittle RF, Cussmann KG, Cottrell BA, Friezner SJ, Hucko JT & Takagi T (1977a). Amino acid sequence studies on the alpha-chain of human fibrinogen. Characterisation of II cyanogen bromide fragments. Biochemistry 16, 1703.

Doolittle RF, Cassman KG, Cottrell BA, Friezner SJ & Takagi T (1977b). Amino acid sequence studies on the alpha chain of human fibrinogen. Covalent structure of the alpha-chain portion of fragment D. Biochemistry 16, 1710.

Doolittle RF, Cassman KG, Cottrell BA & Friezner SJ (1977c). Amino acid sequence studies on the alpha chain of human fibrinogen. Isolation and characterisation of two linked alpha-chain cyanogen bromide fragments from fully crosslinked fibrin. Biochemistry 16, 1715.

Doolittle RF, Cottrell BA, Strong D & Watt KWK (1979a). Preliminary report on the amino acid sequence of the alpha-chain of human fibrinogen. Throm. Res. 14, 787.

Doolittle RF, Watt KWK, Cottrell BA, Strong DD & Riley M (1979b). The amino acid sequence of alpha-chain of human fibrinogen. Nature 280, 464.

Dyr JE, Blomback B & Kornalik F (1983). The fibrinolytic and procoagulant activity of Southern copperhead venom enzymes.
Throm. Res. 30, 185.

Dyr JE, Blomback B, Hessel B & Kornalik F (1989). Conversion of fibrinogen to fibrin induced by preferential release of fibrinopeptide B.
Biochim. Biophys. Acta. 990, 18.

Eklund H & Branden C-I (1983) in Zinc Enzymes (Spiro TG ed) p. 123, Wiley-Interscience, New York.

Elms MJ, Bunce IH, Bundesen PG, Rylatt DB, Webber AJ, Masci PP & Whitaker AN (1986). Rapid detection of crosslinked fibrin degradation products in plasma using monoclonal antibody-coated latex particles.
Am. J. Clin. Pathol. 85, 360.

Endres GF & Scheraga HA (1972). Equilibria in the fibrinogen fibrin conversion IX. Effects of calcium ions on the reversible polymerisation of fibrin monomer.
Arch. Biochem. Biophys. 153, 266.

Evan HJ (1981). Cleavage of the A^{-}-chain of fibrinogen and the alpha-polymer of fibrin by the venom of spitting cobra (Naja nigricollis).
Biochim. Biophys. Acta. 660, 219.

Failla ML, van der Veerdank M, Morgan WT & Smith JC (1982). Characterisation of zinc-binding proteins of plasma in familial hyperzincemia.
J. Lab. Clin. Med. 100, 943.

Fairall L, Rhodes D & Klug A (1986). Mapping of the sites of protection on a 5S RNA gene by the Xenopus transcription factor XIII. A model for interaction.
J. Mol. Biol. 192, 577.

Farid TM & Tu AT (1989) Characterisation of Cerastobin, a thrombin-like enzyme from the venom of Cerastes vipera (Sahara sand piper).
Biochemistry 28, 371.

Fears R (1989). Binding of plasminogen activators to fibrin: characterisation and pharmacological consequences.
Biochem. J. 261, 313.

Fesus L, Thomazy V & Falus A (1987). Induction and activation of tissue transglutaminase during programmed cell-death.
FEBS Letters, 224, 104.

Fisher GL (1975). Function and haemostasis of copper and zinc in mammals in The Science of the total Environ. 4, 373.

Fortova H, Dyr JE & Suttner J (1990) Isolation of fibrinogen converting enzyme ficozyme from the venom of Bothrops asper by one step affinity chromatography on Blue Sepharose.
J. Chromat. 523, 312.

Fox JW, Campbell R, Beggerly L & Bjarnson JB (1986) Substrate specificities and inhibition of two hemorrhagic zinc proteases Ht-c and Ht-d from Crotalus atrox venom.
Eur.J.Biochem. 156, 65.

Francis CW, Marder VJ & Barlow GH (1980) Plasmin degradation of crosslinked fibrin.
J. Clin. Invest. 66, 1033.

Francis CW & Marder VJ (1982) A molecular model of plasmic degradation of crosslinked fibrin.
Sem. Thromb. Hemostas. 8, 25.

Francis CW, Keele, EM & Marder VJ (1984) Purification of three gamma-chains with different molecular weights from normal human plasma fibrinogen.
Biochim. Biophys. Acta. 797, 328.

Francis CW, Muller E, Henschen A, Simpson PJ & Marder VJ (1988) Carboxy-terminal amino acid sequences of two variant forms of the gamma chain of human plasma fibrinogen.
Proc. Natl. Acad. Sci. U.S.A. 85, 3358.

Frankel AD, Berg JM & Pabo CO (1987). Metal dependent folding of a single zinc finger from transcription factor IIIA.
Proc. Natl. Acad. Sci. USA, 84, 4841.

Fretto LJ, Ferguson EW, Steinman HM & McKee PA (1978). Localisation of the alpha-chain cross-linked acceptor sites of human fibrin.
J. Biol. Chem. 253, 2184.

Furlan M, Rupp C, Beck EA & Svendsoin L (1982). Effect of calcium and synthetic peptides on fibrin polymerisation.
Throm. Haemostas. 47, 118.

Fuster V, Badimon L, Badimon JJ and Chesebro (1992). Mechanisms of disease: The pathogenesis of coronary artery disease and the acute coronary syndromes. Parts one and two.
N. Eng. J. Med. 326, 242,310.

Gaffney PJ & Dobos P (1971). A structural aspect of human fibrinogen suggested by its plasmin degradation.
FEBS Letters 15, 13.

Gaffney PJ (1972). Localisation of carbohydrate in the subunits of human fibrinogen and its plasmin induced fragments.
Biochim. Biophys. Acta. 263, 453.

Gergely A (1981) Stereoselectivity in mixed zinc(II) histidinethreonine complex.
Inorg. Chim. Acta. 56, L75.

Greenberg CS, Devine DV & McCrae KM (1987). Measurement of plasma fibrin D-dimer levels with the use of a monoclonal antibody coupled to latex beads.
Am. J. Clin. Pathol. 87, 94.

Greenberg CS, Miraglia CC, Rickles FR & Shuman MA (1985). Cleavage of blood coagulation factor XIII and fibrinogen by thrombin during in vitro clotting.
J. Clin. Invest. 75, 1463.

Grundmann U, Amann E, Zettlmeissel G & Kupper HA (1986). Characterisation of cDNA coding for human factor XIIIa.
Proc. Natl. Acad. Sci. USA, 83, 8024.

Hall C & Slayter H (1959). The fibrinogen molecule: its size, shape and mode of polymerisation.
J. Biophys. Biochem. Cytol. 5, 11.

Harpel PC, Gordon BR & Parker TS (1989). Plasmin catalysed binding of lipoprotein (a) to immobilized fibrinogen and fibrin.
Proc. Natl. Acad. Sci. USA. 86, 3847.

Harris WR (1983). Thermodynamic binding constants of the zinc-human serum transferrin complex.
Biochemistry 22, 3920.

Hasegawa N & Sasaki S (1990). Location of the binding site "b" for lateral polymerisation of fibrin.
Thrombin. Res. 57, 183.

Haverkate F & Timan G (1977). Protective effect of calcium in the plasmin degradation of fibrinogen and fibrin fragments D.
Thromb. Res. 10, 803.

Hawiger J, Kloczewiak M, Bednarek MA & Timmons S (1989). Platelet receptor domains on the alpha chain of human fibrinogen: Structure - function analysis.
Biochemistry 28, 2909.

Hawiger J, Timmons S, Kloczewiak M, Strong DD & Doolittle RF (1982). Gamma and alpha chains of human fibrinogen possess sites reactive with human platelet receptors.
Proc. Natl. Acad. Sci. USA. 79, 2068.

Hawiger J, Timmons S, Strong DD, Cottrell BA, Riley M & Doolittle RF (1982). Identification of a region of human fibrinogen interacting with staphylococcal clumping factor.
Biochemistry 21, 1407.

Heene DL & Matthias FR (1973). Adsorption of fibrinogen derivatives on insolubilized fibrinogen and fibrin monomer.
Thromb. Res. 2, 137.

Henschen A, Lottspeich F, Kehl M & Saultan C (1983). Covalent structure of fibrinogen.
Ann. N.Y. Acad. Sci. 408, 28.

Higgins DL & Vehar GA (1987). Interaction of one-chain and two-chain tissue plasminogen activator with intact and plasmin-degraded fibrin.
Biochemistry 26, 7786.

Hoeprich Jr. PD & Doolittle RF (1983). Dimeric half molecules of human fibrinogen are joined through disulphide bonds in an antiparallel orientation.
Biochemistry 22, 2049.

Hoffman H & Bon C (1987a). Blood coagulation induced by the venom of Bothrops atrox. I. Identification, purification, and properties of a prothrombin activator.
Biochemistry 26, 772.

Hoffman H & Bon C (1987b). Blood coagulation induced by the venom of Bothrops atrox. 2. Identification, purification, and properties of two factor X activators.
Biochemistry 26, 780.

Holm B, Brosstad F, Kierulf P & Godal HC (1985). Polymerisation properties of two normally circulating fibrinogens, HMW and LMW. Evidence that the COOH-terminal end of the alpha-chain is of importants for fibrin polymerisation.
Thromb. Res. 39, 595.

Homma M & Tu T (1971). Morphology of local tissue damage in experimental snake envenomation.
Br. J. Exp. Pathol. 52, 528.

Horrocks WD, Ishky JN, Holmquist B & Thompson JS (1980) Structural and electronic mimics of the active site of cobalt(II) substituted zinc metalloenzymes.
J. Inorg. Biochem. 12, 131.

Horwitz BH, Varadi A & Scheraga HA (1984). Localisation of a fibrin gamma-chain polymerisation site within segment Thr-374 to Glu-396 of human fibrinogen.
Proc. Natl. Acad. Sci. USA, 81, 5980.

Huber P, Dalmon J, Coutois G, Laurent M, Assouline Z, & Marguerie G (1987). Characterization of the 5'flanking region of the human fibrinogen gene.
Nucleic Acids Res. 15, 1615.

Ichinose A & Davie EW (1988). Characterisation of the gene for a subunit of human factor XIII (plasma transglutaminase), a blood coagulation factor.
Proc. Natl. Acad. Sci. USA 85, 5829.

Ichinose A, Bottenus RE & Davie EW (1990). Structure of transglutaminases. J. Biol. Chem. 265, 13411.

Ichinose A, McMullen BA, Fujikawa K & Davie EW (1986). Amino acid sequence of the b subunit of human factor XIII, a protein composed of ten repetitive segments. Biochemistry 25, 4633.

Ikura K, Nasu T, Yokota H, Tsuchiya Y, Sasaki R & Chiba H (1988). Amino acid sequence of guinea pig liver transglutaminase from its cDNA sequence. Biochemistry 27, 2898.

Isaacs BS, Brew SA & Ingham KC (1989). Reversible unfolding of the gelatin-binding domain of fibronectin: Structure stability in relation to function. Biochemistry 28, 842.

Jakubowski HV & Owens WG (1989). Macromolecular specificity determinants on thrombin for fibrinogen and thrombomodulin. J. Biol. Chem. 264, 11117.

Jefferson JR, Hunt JB & Ginsbury A (1990). Zinc interactions with regulatory dimers from E.coli. Aspartate transcarbomoylase. Biochemistry 29, 6687.

Kanaide H, Uranishi T & Nakamura M (1982). Effects of divalent cations on the conversion of fibrinogen to fibrin and fibrin polymersiation. Am. J. Hematol. 13, 229.

Kirby EP, Niewiarowski S, Stocker K, Kettner C, Shaw E & Brudzynski TM (1979). Thrombocytin, a serine protease from Bothrops atrox. venom 1. Purification and characterisation of the enzyme. Biochemistry 18, 3564.

Kloczewiak M, Timmons S & Hawiger J (1982). Localization of a site interacting with human platelet receptor on carboxy-terminal segment of human fibrinogen gamma-chain. Biochem. Biophys. Res. Comm. 107, 181.

Kloczewiak M, Timmons S, Hawiger J (1987). Reactivity of chemically cross-linked fibrinogen and its fragment D toward the staphylococcal clumping receptor. Biochemistry 26, 6152.

Kloczewiak M, Timmons S, Lukas TJ & Hawiger J (1984). Platelet receptor recognition site on human fibrinogen. Synthesis and structure-function relati onship of peptides corresponding to the carboxy-terminal segment of the gamma-chain. Biochemistry 23, 1767.

Kloczewiak M, Timmons S, Bednarek MA, Sakon M & Hawiger J (1989) Platelet receptor recognition domain on the gamma chain of human fibrinogen and its synthetic peptide analogues. Biochemistry 28, 2915.

Klug A & Rhodes D (1987). 'Zinc fingers': a novel protein motif for nucleic acid recognition.
Trends. Biol. Sci. 12, 464.

Knox P, Crooks S & Rimmer CS (1986). Role of fibronectin in the migration of polymerisation sites in fibrinogen.
J. Cell. Biol. 102, 2318.

Koppert PW, Hoegee de Nobel E & Nieuwenhuizen W (1988). A monoclonal antibody-based enzyme assay for fibrin degradation products in plasma.
Throm. Haemostasis. 59, 310.

Koppert PW, Kuipers W, Nobel BH, Brommer EJP, Koopman J & Nieuwenhuizen W (1987). A quantitative immunoassay for primary fibrinogenolysis products in plasma.
Throm. Haemostas. 57, 25.

Kornalik F, Dyr JE, Vodrazka Z & Fortova H (1979). Fibrinogenolytic effect of ecarin a prothrombin converting enzyme.
Throm. Res. 15, 27.

Kowalski MA & Cierniewski CS (1982). The intrinsic fluorescence of human fibrinogen and its fragments D and E.
Thromb. Haemostas. 48, 21.

Kress LF & Paroski EA (1978). Enzymatic inactivation of human serine proteinase inhibitors by snake venom proteinases.
Biochem. Biophys. Res. Comm. 83, 649.

Kruzel M & Kress LF (1985). Separation of Crotalus atrox (Western diamondback rattlesnake) alpha proteinases from serine proteinase and hemorrhagic factor activities.
Anal. Biochem. 151, 471.

Kudryk BJ, Collen D, Woods KR & Blomback B (1974). Evidence for localisation of polymerisation sites in fibrinogen.
J. Biol. Chem. 249, 3322.

Kuwahara J & Coleman JE (1990). Role of the zinc(II) ion in the structure of the three-finger DNA binding domain of the Spl transcription factor.
Biochemistry, 29, 8627.

Labib RS, Azab MH & Farag NW (1981). Effects of Cerastes Cerastus (Egyptian sand piper) and Cerastus vipera (Sahara sand piper) snake venoms on blood coagulation: Separation of coagulant and anticoagulant factors and their correlation with arginine esterase and protease activities.
Toxicon. 19, 85.

Laemmli UK (1970). Cleavage of structural proteins during assembly of the head of bacteriophage T4.
Nature 227, 680.

Lakowicz JR (1985) in Principles of Fluorescence Spectroscopy, Plenum Press, New York.

Landano AP & Doolittle RF (1981). Influence of calcium ions on the binding of fibrin amino terminal peptides to fibrinogen.
Science 212, 457

Larsan GR, Henson K & Blue Y (1988). Variants of human tissue-type plasminogen activator.
J. Biol. Chem. 263, 1023.

Laudano AP, Cottrell BA & Doolittle RF (1983). Synthetic peptides modelled on fibrin polymerisation sites.
Annals N.Y. Acad. Sci. 408, 315.

Lawrence CH & Morris BJ (1981). Mechanism of activation of inactive renin in human plasma by Puff Adder venom.
Biochim. Biophys. Acta. 657, 13.

Lever ABP (1984) in Inorganic Electronic Spectroscopy (2nd ed) Elsevier, Amsterdam.

Levesque J, Hatzfeld J & Hatzfeld A (1990). A mitogenic fibrinogen receptor that differs from glycoprotein IIb-IIIa.
J. Biol. Chem. 265, 328.

Lewis BA, Freyssinet J & Holbrook JJ (1978). An equilibrium study of metal ion binding to human plasma coagulation factor XIII.
Biochem. J. 169, 397.

Lewis SD, Janus TJ, Lorand L & Shafer JA (1985). Regulation of formation of factor XIIIa by its fibrin substrates.
Biochemistry 24, 6772.

Lindsey GG, Brown G & Purves LR (1978a). Isolation of the crosslink peptide of fibrin.
Thrombosis. Res. 12, 467.

Lindsey GG, Brown G & Purves LR (1978b). Calcium binding to human fibrinogen - localisation of two calcium binding sites.
Thromb. Res. 13, 345.

Lindsey GG, Brown G, Merrifield EH & Purves LR (1979). The carbohydrate prosthetic groups of rat fibrinogen plasmic fragment E.
Biochim. Biophys. Acta. 577, 110.

Lorand L, Credo RB & Janus TJ (1981). Factor XIII (fibrin stabilising factor).
Meth. Enz. 80, 333.

Lorand L, Losowsky MS, Miloszewski KJM (1980). Human factor XIII: Fibrin stabilising factor.
Prog. Hemost. Thromb. 5, 245.

Lottenberg R, Christensen U, Jackson CM & Coleman PL (1981). Assay of coagulation proteases using peptide chromogenic and fluorogenic substrates.
Meth. Enz. 80, 341.

Lottspeich F, & Henschen A (1977). Amino acid sequence of human fibrinogen. Preliminary note on the completion of the gamma-chain sequence.
Hoppe-Seyler Z. Physiol. Chem. 358, 935.

Lucas MA, Fretto LJ & McKee PA (1983). The binding of human plasminogen to fibrin and fibrinogen.
J. Biol. Chem. 258, 4249.

Lucas MA, Straight DL, Fretto LJ & McKee PA (1983). The effects of fibrinogen and its cleavage products on the kinetics of plasminogen activation by urokinase and subsequent plasmin activity.
J. Biol. Chem. 258, 12171.

Maeda N, Seike M, Kume S, Takaku T & Shiga T (1987). Fibrinogen-induced erythrocyte aggregation: erythrocyte-binding site in the fibrinogen molecule.
Biochim. Biophys. Acta. 904, 81.

Mao SJT, Rechtin AE, Krstenansky JL & Jackson RL (1990). Characterisation of a monoclonal antibody specific to the amino terminus of the alpha-chain of human fibrin.
Thromb. Haemostas. 63, 445.

Marguerie G, Chagniel G & Suscillon M (1977). The binding of calcium to bovine fibrinogen.
Biochim. Biophys. Acta. 490, 94.

Marguerie G (1977). The binding of calcium to fibrinogen: Some structural features.
Biochim. Biophys. Acta. 494, 172.

Martell AE & Smith RM (1974) in Critical Stability Constants. Vol 1: Amino Acids, Plenum Press, New York.

Martin MT, Holmquist B & Riordan JF (1989) Effects of mechanism-based reversible inhibitors on the metal environment of cobalt(II)-carboxypeptidase A: An electronic spectral study.
J.Inorg.Biochem. 36, 27.

Martinez J, Rich E & Barsignian C (1989). Transglutaminase-mediated crosslinking of fibrinogen by human umbilical vein endothelial cells.
J. Biol. Chem. 264, 20502.

Marunyama M, Kamiguti AS, Cardoso JLC, Sano-Martins IS, Chudzinski AM, Santoro ML, Marena P, Tomy SC, Antonio LC, Mihara H & Kelen EMA (1990). Studies on blood coagulation and fibrinolysis in patients bitten by Bothrops jararaca.
Thromb. Haemostas. 63, 449.

Marx G (1988). Zinc binding to fibrinogen and fibrin.
Arch. Biochem. Biophys. 266, 285.

May PM & Murray K (1988). The use of glass electrodes for the determination of formation constants-III. Optimization of titration data: the ESTA library of computer programs.
Talanta 35, 825.

Mayo KH, Burke C, Lindon JN & Kloczewiak M (1990). 'H NMR sequential assignments and secondary structure analysis of human fibrinogen gamma-chain C-terminal residues 385-411.
Biochemistry 29, 3277.

McDonagh J (1981). Fibronectin. A molecular glue.
Arch. Pathol. Lab. Med. 105, 393.

Mebs D & Panholzer F (1982). Isolation of a hemorrhagic principle from Bitis arietans (Puff Adder) snake venom.
Toxicon. 20, 512.

Melchior WB & Fahrney D (1970). Ethoxyformylation of Proteins. Reaction of ethoxyformic anhydride with alpha-chymotrypsin, pepsin, and pancreatic ribonuclease at pH 4.
Biochemistry 9, 251.

Monzingo AF & Matthews BW (1982). Structure of a mercaptan-thermolysin complex illustrates modes of inhibition of zinc proteases by substrate-analogue mercaptans.
Biochemistry 21, 3390.

Moran JB & Geren CR (1981). Characterization of a fibrinogenase from northern copperhead (Agkistrodon contortrix mokasen) venom.
Biochim. Biophys. Acta. 659, 161.

Morita T & Iwanaga S (1978). Purification and properties of prothrombin activator from the venom of Echis carinatus.
J. Biochem. 83, 559.

Morris BJ & Lawrence CH (1980). Activation of inactive renin during the selective destruction of proteinase inhibitors in human plasma by a metalloproteinase in Bitis arietans venom.
Biochim. Biophys. Acta. 612, 137.

Morris BJ, Lawrence CH, Cantanzaro DF (1980). Activation of plasma prekallikrein and inactive renin by Puff Adder venom.
Clin. Exp. Pharmacol.Physiol. 7, 563.

Mosher DF (1980). Fibronectin.
Prog. Hemostas. Thromb. 5, 111.

Mossesson MW, Di Orio JP, Muller MF, Shainoff JR, Siebenlist JR, Amrani DL, Homanberg GA, Soria C & Samama M (1987). Studies on the ultrastructure of fibrin lacking fibrinopeptide B (B-fibrin).
Blood 69, 1073.

Mossesson MW, Finlayson JS, Umfleet RA & Galanakis D (1972). Human fibrinogen heterogeneities.
J. Biol. Chem. 247, 5210.

Mossesson MW, Homandberg GA & Amrani DL (1984). Human platelet fibrinogen gamma chain structure.
Blood, 63, 990.

Mossesson MW, Siebenlist KR, Amrani DL, & Di Orio JP (1989). Identification of covalently linked trimeric & tetrameric D domains in crosslinked fibrin.
Proc. Natl. Acad. Sci. USA. 86, 1113.

Muszbek L & Hauck M (1979). Fragmentation of actin by thrombin-like snake venom proteases.
Biochem. Biophys. Acta. 577, 34.

Nickerson JM & Fuller GM (1981). Modification of fibrinogen chains during synthesis: Glycosylation of BB and gamma-chains.
Biochemistry 20, 2818.

Nietfield W, El-Baradi T, Mentzel H, Pieter T, Koster M, Poting A & Knochel W (1989). Second-order repeats in Xenopus laevis finger proteins.
J. Mol. Biol. 208, 639.

Nikai T, Kito R, Mori N, Sugihara H & Tu AT (1983). Isolation and characterization of fibrinogenase from Western diamondback rattlesnake venom and its comparison to the thrombin-like enzyme, Crotalase.
Comp. Biochem. Physiol. 76B, 679.

Nahas L, Kamiguti AS & Barros MAR (1979). Thrombin-like and factor-X-activator components of Bothrops snake venoms.
Thrombos. Haemostas. 41, 314.

Norrman B, Wallen P & Ranby M (1985) Fibrinolysis mediated by tissue plasminogen activator.
Eur.J.Biochem. 149, 193.

Okada M, Blomback B, Chang M & Horowitz B (1985). Fibronectin and fibrin gel structure.
J. Biol. Chem. 260, 1811.

Okude M & Iwanaga S (1971). Carboxy-terminal residues of mammalian fibrinogen and fibrin.
Biochim. Biophys. Acta. 251, 185.

Olexa SA & Budzynski AZ (1980). Evidence for four different polymerisation sites involved in human fibrin formation.
Proc. Natl. Acad. Sci. USA. 77, 1374.

Olexa SA & Budzynski AZ (1981). Localisation of a fibrin polymerisation site.
J. Biol. Chem. 256, 3544.

Ouyang C & Huang T (1979). Alpha and beta fibrinogenases from Trimeresurus gramineus snake venom.
Biochim. Biophys. Acta. 571, 270.

Ouyang C, Teng C & Chen Y (1979). Properties of fibrinogen degradation products produced by alpha- and beta-fibrinogenases of Trimeresurus murosquamatus snake venom.
Toxicon 17, 121.

Pandya BV & Budzynski AZ (1984). Anticoagulant proteases from Western diamondback rattlesnake (Crotalus atrox.) venom.
Biochemistry 23, 460.

Pandya BV, Cierniewski CS & Budzynski AZ (1985). Conservation of human conformation after cleavage of B-beta chain NH_2 terminus.
J. Biol. Chem. 260, 2994.

Pandya BV, Gabriel JL, O'Brien J & Budzynski AZ (1991). Polymerisation site in the beta-chain of fibrin: mapping of the beta 1-55 sequence.
Biochemistry 30, 162.

Pandya BV, Rubin RN, Olexa SA & Budzynski AZ (1983). Unique degradation of human fibrinogen by proteases from Western diamondback rattlesnake (Crotalus atrox) venom.
Toxicon. 21, 515.

Parisi AF & Vallee BL (1970). Isolation of a zinc-alpha2-macroglobulin from human serum.
Biochemistry 9, 2421.

Pearlstein E, Gold LI & Garcia-Pardo A (1980). Fibronectin: A review of its structure and biological activity.
Mol. Cell. Biochem. 29, 103.

Penefsky HS (1977). Reversible binding of phosphate by beef heart mitochondrial adenosine triphosphate.
J. Biol. Chem. 252, 2891.

Pepper DS, Gaffney PJ & Blume HD (1974). The distribution of carbohydrate in the plasmin resistant core fragments (D,E) of human fibrinogen.
Biochim. Biophys. Acta. 365, 203.

Phillips DR & Baughan AK (1983). Fibrinogen binding to human platelet plasma membranes.
J. Biol. Chem. 258, 10240.

Pizzo SV, Schwartz ML, Hill RL & McKee RA (1972). The effect of plasmin on the subunit structure of human fibrinogen.
J. Biol. Chem. 247, 636.

Plow EF & Edgington TS (1982). Surface markers of fibrinogen and its physiologic derivatives revealed by antibody probes.
Sem. Thromb. Haemostas. 8, 36.

Prince RH (1979). Adv. Inorg. Chem. Radiochem. 22, 349.

Purves L, Purves M & Brandt W (1987). Cleavage of fibrin-derived D-dimer into monomers by endopeptidase from Puff Adder (Bitis arietans) acting at crosslinked sites of the gamma-chain. Sequence of carboxy-terminal cyanogen bromide gamma-chain fragments.
Biochemistry 26, 4640.

Purves LR & Lindsey GG (1978b). Role of calcium in the structure and interaction of fibrinogen.
S. Afr. J. Sci. 74, 202.

Purves LR, Lindsey GG & Franks JJ (1980). Sites of D-domain interaction in fibrin-derived D-dimer.
Biochemistry 19, 4051.

Purves LR, Lindsey GG, Brown G & Franks J (1978a). Stabilization of the plasmin digestion products of fibrinogen and fibrin by calcium ions.
Throm. Res. 12, 473.

Purves LR, Purves M, Hickman R, Jones G & Brossy JJ (1984). The role of fibronectin.
S. Afr. J. Sci. 80, 469.

Purves LR, Purves M, Lindsey GG & Linton NJ (1986). Specific cleavage of fibrin-derived D-dimer by a metalloproteinase isolation from venom of the Puff Adder (Bitis arietans)
S. Afr. J. Sci. 82, 30.

Purves M & Purves LR (1989). Specific fibrinolytic enzyme from venom acting at the fibrin-specific gamma-chain crosslink site: Fibrinogen chain specificity and presence in various snake species.
S. Afr. J. Sci. 85, 519.

Ranby M (1982). Studies on the kinetics of plasminogen activation by tissue plasminogen activator.
Biochim. Biophys. Acta. 704, 461.

Rixon MW, Chung DW & Davie EW (1985). Nucleotide sequence of the gene for the gamma chain of human fibrinogen.
Biochemistry 24, 2077.

Rogers TB, Gold RA & Feeney RE (1977). Ethoxyformylation and photo-oxidation of histidines in Transferrins.
Biochemistry 16, 2299.

Russel FE (1980) in Snake venom poisoning. J.B. Lippincot Co.

Sakata Y, & Aoki N (1982). Significance of crosslinking of alpha$_2$-plasmin inhibitor to fibrin in inhibition of fibrinolysis and in hemostasis.
J. Clin. Invest. 69, 536.

Schielen WJG, Adams HPHM, van Leuven K, Voskuilen M, Tesser GI & Nieuwenhuizen W (1991). The sequence gamma-(312-324) is a fibrin-specific epitope.
Blood 77, 2169.

Schwartz ML, Pizzo SV, Hill RL & McKee PA (1971). The subunit structures of human plasma and platelet factor XIII (fibrin-stabilising factor).
J. Biol. Chem. 246, 5851.

Schwartz ML, Pizzo SV, Hill RL & McKee PA (1973). Human factor XIII from plasma and platelets.
J. Biol. Chem. 248, 1395.

Scully MF & Kakker VV (1982). Structural features of fibrinogen associated with binding to chelated zinc.
Biochim. Biophys. Acta. 700, 130.

Selmayr E, Mahn I & Muller-Berghaus G (1985). Crosslinking of soluble fibrin and fibrinogen.
Thromb. Res. 39, 467.

Shainoff JR, Dardik BN (1979). Fibrinopeptide B aggregation of fibrinogen.
Science 204, 200.

Sharp JJ, Cassman KG & Doolittle RF (1972). Amino acid sequence of the carboxyterminal cyanogen bromide fragment from bovine and human fibrinogen gamma-chains.
FEBS Letters 25, 334.

Shimizu A, Saito Y & Inada Y (1986). Distinctive role of histidine-16 of the B-beta chain of fibrinogen in the end-to-end association of fibrin.
Proc. Natl. Acad. Sci. USA 83, 591.

Signorini M, Chiozzi P & Bergamini CM (1989). Interaction of erythrocyte transglutaminase with calcium ions.
Biochemistry International 19, 1205.

Smith GF (1980). Fibrinogen-fibrin conversion.
Biochem. J. 185, 1.

South TL, Blake PR, Sowder RC, Arthur LO, Henderson LE & Summers MF (1990). The nucleocapsid protein isolated from HIV-1 particles binds zinc and forms retroviral type zinc fingers.
Biochemistry 29, 7786.

Southan C, Thompson E, Panico M, Etienne T, Morris HR & Lane DA (1985). Characterisation of peptides cleaved by plasmin from the C-terminal polymerisation domain of human fibrinogen.
J. Biol. Chem. 260, 13095.

Spector T (1978). Refinement of the Commassie Blue method of protein quantitation.
Anal. Biochem. 86, 142.

Streitwiezer Jnr, A & Heathcock CH (1981) in Introduction to Organic Chemistry, MacMillan Public. Co., New York.

Strong DD, Laudano AP, Hawiger J & Doolittle RF (1982). Isolation, characterisation and synthesis of peptides from human fibrinogen that blocks the staphylococcal clumping reaction and contribution of a synthetic clumping particle.
Biochemistry 21, 1414.

Takada A, Urano T & Takada Y (1990). The regulation of the activation of the fibrinolysis system.
Adv. Exp. Biol. 281, 209.

Takagi T & Doolittle RF (1975). Amino acid sequence studies on the alpha chain of human fibrinogen. Localisation of four plasmic attack points and a covalent cross-linking agent.
Biochemistry 14, 5149.

Takahashi N, Takahashi Y & Putnam FW (1986). Primary structure of blood coagulation factor XIIIa (fibrinoligase, transglutaminase) from human placenta.
Proc. Natl. Acad. Sci. USA. 83, 8019.

Teng C, Onyang C & Lin S (1985). Species difference in the fibrinogenolytic effects of alpha- and beta-fibrinogenases from Timerescurus murosquamatus snake venom.
Toxicon. 23, 777.

Timmons S, Bednarek MA, Kloczewiak M & Hawiger J (1989). Antiplatelet 'hybrid' peptides analogous to receptor recognition domains of gamma and alpha chains of human fibrinogen.
Biochemistry 28, 2919.

Turner PM & Lorand L (1989). Complexation of fibronectin with tissue transglutaminase.
Biochemistry 28, 628.

Underwood EJ (1971) in Trace elements in human and animal nutrition. Academic Press, New York.

Vallee BL & Auld DS (1990a). Active site ligands and activated H_2O of zinc enzymes.
Proc. Natl. Acad. Sci. USA 87, 220.

Vallee BL & Auld DS (1990b). Zinc coordination, function and structure of zinc enzymes and other proteins.
Biochemistry 29, 5647.

van der Walt SJ & Joubert FJ (1971). Studies on Puff Adder (Bitis arietans) venom I. Purification and properties of Protease A.
Toxicon. 9, 153.

van der Walt SJ (1972). Studies on Puff Adder (Bitis arietans) venom, IV Association of protease A.
Hoppe-Seyler Z. Physiol. Chem. 353, 1217.

Varadi A & Patthy L (1983). Location of plasminogen-binding site in human fibrin(ogen).
Biochemistry 22, 2440.

Varadi A & Scheraga HA (1986). Localisation of segments essential for polymerisation and for calcium binding in the gamma chain of human fibrinogen.
Biochemistry 25, 519.

Walker FJ, Owen WG, Esman CT (1980). Characterisation of the prothrombin activator from the venom of Oxyuranus scutellus scutellus (Taipan venom).
Biochemistry 19, 1020.

Weast RC (ed) (1987) in Handbook of Chemistry and Physics, 67th ed., CRC Press, Batan Rouge, Florida.

Webb GC, Coggan M, Ichinose A & Board PG (1989). Localisation of the coagulation XIII B subunit gene (F13B) to chromosome bands 1q 31-32.1 and restriction fragment length polymorphism at the locus.
Hum. Genet. 81, 157.

Weis MA, Mason KA, Dahl CE & Keutmann HT (1990). Alternating zinc-finger motifs in the male-associated protein ZFY.
Biochemistry 29, 5660.

Whitaker AN, McFarlane JR, Rowe EA, Lee K & Masci PP (1985). Measurement of autoantibodies against fibrinogen and fibrin degradation products by enzyme linked immunoassay.
Thromb. Haemostas. 80,

Wiman B & Collen D (1978). Molecular mechanism of physiological fibrinolysis.
Nature. 272, 549.

Wojta J, Beckmann R, Turcu L, Wagner OF, van Zonneveld A & Binder BR (1989). Functional characterisation of monoclonal antibodies directed against fibrin binding domains of tissue-type plasminogen activator.
J. Biol. Chem. 264, 7957.

Wolfenstein-Todel C & Mossesson MW (1981). Carboxy-terminal amino acid sequence of human fibrinogen gamma-chain variant (gamma').
Biochemistry 20, 6146.

Wolfenstein-Todel C & Mossesson MW (1980). Human plasma fibrinogen heterogeneity: Evidence for an extended carboxy-terminal sequence in a normal gamma chain variant (gamma').
Proc. Natl. Acad. Sci. USA, 77, 5069.